

Vol. 03 No. 02 2025



**RiESTech**

**JOURNAL**  
RECENT IN ENGINEERING  
SCIENCE AND TECHNOLOGY



E- ISSN : 2985-8321

P -ISSN : 2985-704X



# Recent in Engineering Science and Technology (RiESTech)

Volume 3 No 2 April 2025

## FOCUS AND SCOPE

### RIESTECH

Recent in Engineering Science and Technology (**RiESTech**): ISSN: 2985-704X (*print*), ISSN: 2985-8321 (*online*) a peer-reviewed quarterly engineering journal, publishes theoretical and experimental high-quality papers to promote engineering and technology's theory and practice. In addition to peer-reviewed original research papers, the Editorial Board welcomes original research reports, state-of-the-art reviews, and communications in the broadly defined field of recent engineering science and technology. **RiESTech** covers topics contributing to a better understanding of engineering, material science, computer science, environmental science, and their applications. **RiESTech** is concerned with scientific research on mechanical and civil engineering, Electrical/Electronics and Computer Engineering, and Metallurgical and Materials Engineering with specific analytical techniques and/or computational methods.

The frequency of RiESTech publications is four times a year namely in January, April, July, and October. The scope of RiESTech includes a wide spectrum of subjects namely:

Mechanical and Civil Engineering (Automotive Technologies; Construction Materials; Design and Manufacturing; Dynamics and Control; Energy Generation, Utilization, Conversion, and Storage; Fluid Mechanics and Hydraulics; Heat and Mass Transfer; Micro-Nano Sciences; Renewable and Sustainable Energy Technologies; Robotics and Mechatronics; Solid Mechanics and Structure; Thermal Sciences)

Electrical/Electronics and Computer Engineering (Instrumentation; Coding, Cryptography, and Information Protection; Communications, Networks, Mobile Computing, and Distributed Systems; Compilers and Operating Systems; Parallel Processing, and Dependability; Computer Vision and Robotics; Control Theory; Electromagnetic Waves, Microwave Techniques and Antennas; Embedded Systems; Integrated Circuits, VLSI Design, Testing, and CAD; Microelectromechanical Systems; Microelectronics, and Electronic Devices and Circuits; Power, Energy and Energy Conversion Systems; Signal, Image, and Speech Processing; Machine Learning and Data Science)

Metallurgical and Materials Engineering (Advanced Materials Science; Ceramic and Inorganic Materials; Electronic-Magnetic Materials; Energy and Environment; Materials Characterization; Metallurgy Extractive; Polymers and Nanocomposites)

Environmental Science and Engineering (Waste Management, Climate Change, Zero Waste, Environmental Disaster Management, Circular Economy, Sustainable Development, Environmental Security, Environmental Management, Environmental Ecology, Conservation of Natural Resources And Environment, Environmental Impact Analysis, Planning and Environmental Administration, Environmental Health, Environmental Pollution, Environmental Accounting, and Environmental Information Systems)

# Recent in Engineering Science and Technology (RiESTech)

Volume 3 No 2 April 2025

## EDITOR TEAM

### *Editor in Chief*

Prof. Dr. Ir. Johny Wahyuadi M. Soedarsono, DEA

### *Managing Editor*

Iwan Susanto, Ph.D

Dr. Vika Rizkia

### *Editorial Board*

Prof. Dr. Drs. Agus Edi Pramono. S.T., M.Si, Politeknik Negeri Jakarta, Indonesia

Prof. Dr. Ir. Dwi Rahmalina MT, Universitas Pancasila, Indonesia

Prof. Ing-Song Yu, National Dong Hwa University, Taiwan

Prof. Chao-Yu Lee, National Formosa University, Taiwan

Prof. Ching-An Huang, Chang Gung University, Taiwan

Prof. Fabrice Gourbilleau, CIMAP CNRS/CEA/ENSICAEN/  
Université de Caen Normandie, France

Dr. Ir. Muhammad Amin, ST, MT, IPM, Universitas Samudra, Kota Langsa, Indonesia

Dr. Maykel Manawan, Universitas Pertahanan, Indonesia

Dr. Eng. Radon Dhelika, Universitas Indonesia

Dr. Ing. Haryanti Samekto, The University of Stuttgart, Germany (Alumni)

Dr. Ing. H. Agus Suhartono, BRIN, Indonesia

Yudhi Ariadi, Ph.D, Coventry University London, United Kingdom

Dien Taufan Lessy, S.ST, M.Sc Institute of Digital Signal Processing,  
Universiät Duisburg Essen

### *Peer-Reviewers*

Dr. Rachmat Adhi Wibowo, M.Sc., AIT Austrian Institute of Technology Center for Energy  
Energy Conversion and Hydrogen, Giefinggasse 2, 1210 Vienna, Austria

Dhayanantha Prabu Jaihindh, Ph.D Academia Sinica, Institute of Atomic and  
Molecular Sciences, Taiwan

Dr. rer nat Eko Budiyanto, Max-Planck-Institut für Kohlenforschung, Germany

Sk Jahir Abbas, Ph.D, Shanghai Jiao Tong University School of Medicine, Shanghai, China

Wandi Wahyudi, Ph.D, Uppsala University, Sweden

Dr. Agus Budi Prasetyo, Pusat Riset Metalurgi, BRIN, Indonesia

Atul Verma, Ph.D., National Dong Hwa University, Shoufeng, Taiwan

Haolia Rahman, Ph.D, Politeknik Negeri Jakarta, Indonesia

Andy Tirta, S.T., M.Eng., Ph.D., Universitas Darma Persada, Indonesia

Dr. Vincent Irawan, Eindhoven University of Technology, Netherlands

Muhammad Hilmy Alfaruqi, S.T., M.Eng., Ph.D. Chonnam National University, South Korea

***Layout and Typesetting:***

Imam Sapto Nugroho, Universitas Indonesia (Alumni), Indonesia

Kamil Raihan Permana, Universitas Indonesia, Indonesia

Raihan Trinanda Agsya, Politeknik Negeri Jakarta, Indonesia

**PUBLISHER**

**PT MENCERDASKAN BANGSA INDONESIA (MBI)**

**Address : 4th Floor Gedung STC Senayan Room 31-34, Jl. Asia Afrika Pintu IX,  
Jakarta 10270, Indonesia.**

# **Recent in Engineering Science and Technology (RiESTech)**

**Volume 3 No 2 April 2025**

## **PREFACE**

**Journal RiESTech** (p-ISSN: 2985-704X (print), e-ISSN: 2985-8321 (online); is a peer review journal published by PT Mencerdaskan Bangsa Indonesia. The RiESTech journal is published four times a year in January, April, July, and October. This journal provides direct open access to its content on the principle that making research freely available to the public supports a greater global exchange of knowledge within the engineering field. This journal aims to provide a place for academics, researchers, and practitioners to publish original research articles or review articles. The scope of articles published in this journal relates to various topics in the field of outcomes of research activities.

The RiESTech journal publishes papers strictly following the RiESTech guidelines and templates for manuscript preparation. All submitted manuscripts will go through a double-blind peer review process. The paper is read by members of the editor (according to the area of specialization) and will be screened by the Managing Editor to meet the criteria required for RiESTech publication. Manuscripts will be sent to two reviewers based on their historical experience in reviewing manuscripts or based on their areas of specialization. RiESTech has review forms to keep the same item reviewed by two reviewers. Then the editorial board makes a decision on the comments or suggestions of the reviewers.

Reviewers provide an assessment of originality, clarity of presentation, contribution to the field/science. This journal publishes research articles, review articles/literature reviews, case reports and concept/policy articles, in all fields of Computer Science, Informatics Engineering, Multimedia, Arts. The article to be published is an original work and has never been published. Incoming articles will be reviewed by the reviewer team.

The Editorial Board will try to continue to improve the quality of the journal so that it can become an important reference in the development of engineering sciences. The greatest appreciation and gratitude to Mitra Bestari along with members of the Editorial Board and all parties involved in the publication of this journal. Complete writing instructions are displayed on the portal of this journal.

Regards,  
Chief Editor

# Recent in Engineering Science and Technology (RiESTech)

Volume 3 No 2 April 2025

## Contents

Focus and Scope	ii
Editor Team	iii
Preface	v
Contents	vi

## Articles

- ***Uneven Doping of Metal Powder in Carbon Polymer Composites Affects Electrical Conductivity Properties***  
Agus Edy Pramono; Iman Setyadi, Aminudin Zuhri, Anissa Puspa Dewi, Nanik Indayaningsih  
1 - 14
- ***The Effects of Soil Resistivity on The Corrosion Resistance of Carbon Steel***  
Syanatha Putri Salsabila, Rini Riastuti  
15 - 34
- ***The Analysis of the Effect of RIB Width and Channel Depth Design Modifications on CFD-Based Parallel Type Bipolar Plates for the Application of Proton Exchange Membrane Fuel Cell Stack Singles***  
Mochammad Tendi Noer Ramadhan, Amar Banu Mukhlisin, Belyamin, Radhi Maldzi, Abdul Azis Abdillah  
35 - 48
- ***Mobile Ad-Hoc Network (MANET) Method: Some Trends and Open Issues***  
Dwi Wijonarko, Samsul Arifin, Muhammad Faisal, Muhammad Nabil Pratama, Okta Nindita Priambodo, Edwin Setiawan Nugraha  
49 – 74
- ***Feasibility Study on One Shot Vapor Compression Systems for Gas Storage Applications Using R-32 in Residential Air Conditioning***  
Anisa Ramadhani, Haolia Rahman, Fauzan, Paulus Sukusno  
75 - 82



Article

# Uneven Doping of Metal Powder in Carbon Polymer Composites Affects Electrical Conductivity Properties

Agus Edy Pramono<sup>1,\*</sup>, Iman Setyadi<sup>1</sup>, Aminudin Zuhri<sup>1</sup>, Anissa Puspa Dewi<sup>1</sup>, Iwan Susanto<sup>1</sup>,  
Tatun Hayatun Nufus<sup>1</sup>, Nanik Indayaningsih<sup>2</sup>

<sup>1</sup> Magister Program in Applied Manufacturing Technology Engineering, Politeknik Negeri Jakarta, Jl. Prof. Dr. G.A. Siwabessy, Kampus UI, Depok 16425, Jawa Barat, Indonesia.

<sup>2</sup> Research Centre for Physics-National Research and Innovation Agency, Puspiptek Area, Gd. 440-442, South Tangerang, Banten 15310, Indonesia.

\* Correspondence: agus.edypramono@mesin.pnj.ac.id

**Abstract:** This paper compares the electrical conductivity of LLDPE (Linear Low-Density Polyethylene)-carbon composite materials, LLDPE-carbon-aluminum composites, and LLDPE-carbon-copper composites. Doping with aluminum (Al) and copper (Cu) metal powders influences electrical conductivity in carbon-based polymer composite materials. Adding metal powders as secondary fillers to a mixture of conductive carbon powders and LLDPE can decrease electrical conductivity. This is due to the agglomeration or clustering of metal powders within the polymer matrix, which disrupts conductive pathways and diminishes the efficiency of electrical charge transfer. The impact of filler type and quantity on electrical conductivity in composite materials was examined, and the findings revealed that factors such as the filler's amount, shape, and dispersal significantly affect the composite's electrical resistance properties. Increasing the amount of metal powder filler raises the composite's viscosity, reducing adhesion between the metal and polymer fillers while promoting metal-to-metal contacts.

**Keywords:** Copper powder doping; Aluminum powder doping; Polymer composite; Electrical conductivity; LLDPE-carbon composite.

**Citation:** Pramono, A. E., Setyadi, I., Zuhri, A., Dewi, A. P., Suswanto, I., Nufus, T. H., Indayaningsih, N. (2025). Uneven Doping of Metal Powder in Carbon Polymer Composites Affects Electrical Conductivity Properties. *Recent in Engineering Science and Technology*, 3(02), 1–14. Retrieved from <https://www.mbi-journals.com/index.php/riestech/article/view/95>

Academic Editor: Vika Rizkia

Received: 31 January 2025

Accepted: 16 April 2025

Published: 30 April 2025

**Publisher's Note:** MBI stays neutral with regard to jurisdictional claims in published maps and institutional affiliations.



**Copyright:** © 2025 by the authors. Licensee MBI, Jakarta, Indonesia. This article is an open access article distributed under MBI license (<https://mbi-journals.com/licenses/by/4.0/>).

## 1. Introduction

This study reveals evidence that the addition of aluminum or copper metal increases the electrical conductivity of Linear Low-Density Polyethylene (LLDPE) polymer composites, but not significantly compared to electrically conductive carbon fillers.

This study focuses on developing conductive polymer composite (CPC) materials made from a blend of conductive organic carbon fillers as the primary filler and metal powders as the secondary filler (doping), integrated into a thermoplastic polymer matrix of LLDPE. The resulting hybrid composite combines three components to create a carbon-based material with enhanced mechanical properties and sufficient electrical conductivity to function as a raw material in electrical distribution systems. The hybrid composition improves the performance of both the fillers and the polymer matrix.

A few years ago, electrically conductive polymer-carbon composites were extensively researched. To improve the electrical conductivity properties of the polymer composite, some studies added metal powder mixed with conductive carbon powder.



Carbon fillers and metal powders enhance the composite's mechanical, functional, physical, chemical, and conductive properties, while LLDPE provides excellent thermoplastic performance. Incorporating 2% MWCNT (Multi-Walled Carbon Nanotubes) into the polymer-carbon black composite significantly improves the electrical conductivity of the carbon filler [1]. A hybrid carbon polymer composite consisting of LLDPE (92%), Polypyrrole/PPY (2%), and Graphene Nanoplatelet/GnP filler (6%) exhibits superior mechanical properties compared to a two-component LLDPE-GnP composite [2]. Hybrid composites are essentially modifications of two-component conductive polymer composites (CPCs). CPC materials can be fabricated by engineering thermoplastic polymers as the binding matrix mixed with conductive carbon fillers [3]. At a certain composition level, conductive carbon fillers are interconnected through interfacial bonding between carbon particles, forming a network of conductive channels through which electrons can flow, creating an electrical current [4]. Electrically conductive carbon allotropes are commonly used as fillers, yielding varying results. Carbon Black (CB) filler at loadings of 5%, 10%, 15%, and 20% within an LLDPE matrix enhances the surface hardness of the CB/LLDPE composite. However, tensile strength declines when filler loading exceeds 5% due to particle agglomeration, which impairs the transfer and distribution of tensile stress from the polymer chains to the clustered CB particles. Similarly, due to percolation effects, electrical conductivity decreases beyond 5% filler loading [5]. CNT (Carbon Nanotube) serves as a conductive filler in carbon polymer composites. SWCNT (Single-Walled Carbon Nanotube) with its single-layered structure has direct interaction with the polymer matrix, enhancing the mechanical properties and electrical conductivity of the composite [6]. MWCNT (Multiwalled Carbon Nanotube) is formed by several SWCNTs arranged in a complex matrix. This structure provides higher mechanical strength compared to SWCNTs. MWCNTs exhibit good resistance to pressure and strain, contributing to high load-bearing strength [7]. Graphite is used as a conductive filler in combination with various types of thermoplastic polymers such as ABS, PP, PE, and PET. This results in carbon polymer specimens with conductivity ranging from 0.71 to 5.0 S/cm at the temperatures used in the 3D printing filament manufacturing process [8]. The polymers used as matrices are quite effective in forming conductive channels, especially for non-polar polymers such as Polypropylene (PP), Polyethylene (PE), and Polyvinyl Chloride (PVC) [9]. This article explores the creation of cost-effective thermoplastic composite filaments for 3D printing. These filaments employ polypropylene (PP) as the polymer matrix and carbon black (CB) as the conductive filler. The composite demonstrates stable electrical properties and has been successfully utilized in 3D-printed applications such as plastic thermometers and flexible sensors [10]. In a related study, a Polycaprolactone (PCL) polymer matrix was successfully converted into an electrically conductive composite by incorporating 15% carbon black (CB) filler, which was subsequently processed using a 3D printing (3DP) machine. The PCL/CB composite was utilized to produce flexible sensors and 3D-printed gloves as demonstration applications. However, filler loadings exceeding 15% were found to hinder the 3D printing process, posing challenges in achieving consistent results [11]. This article

examines polymer composites made from carbon black particles derived from apple wood shells. Higher carbonization temperatures and filler content improve the carbon content, tensile strength, and flexural strength of the composites. Scanning electron microscopy (SEM) analyzes the filler-matrix bonding [12]. This article examines polymer composites with nickel and copper fillers, offering metal-like electrical and plastic-like mechanical properties. Electrical conductivity follows percolation theory, while thermal conductivity is unaffected. Particle shape and packing factor are key to concentration dependence [13]. This study examines three types of fillers (Al, Fe, Cu) with varying particle shapes and sizes in HDPE. The relationship between filler percentage and the composite's tensile properties and electrical resistivity is explored. Tensile properties are influenced by filler shape, adhesion, and loading, while electrical resistivity depends on filler shape and amount. Young's modulus increases with higher filler content, following the typical trend in polymer composites [14]. The use of organic materials for conductive carbon has gained attention due to sustainability concerns. However, achieving optimal conductivity often requires high filler content, which can reduce toughness. Percolation theory shows that higher conductivity can be achieved by increasing filler quantity and improving its distribution [15]. A study with a 70/30 polymer/carbon composition achieved a conductivity of 9.09 S/m using carbon from palm fruit bunches. SEM revealed uniform carbon pore distribution in the longitudinal layers, with higher filler concentration in the lower vertical layers [16]. This research develops conductive polymers (CPs) by blending nylon with activated carbon. Electrical conductivity and activation energy were measured at different activated carbon mass fractions. Results showed conductivity increased from  $5.62 \times 10^{-9} \pm 1.89 \times 10^{-10}$  S/cm in pure nylon to  $2.51 \times 10^{-8} \pm 2.87 \times 10^{-10}$  S/cm with 8% activated carbon. Activation energy decreased as the carbon fraction increased [17]. This study characterizes PAni/carbon composites from candlenut shells as capacitor electrodes. Activated carbon was synthesized at various temperatures (300°C, 400°C, 500°C, and 600°C). Higher activation temperatures improved the composite's electrical conductivity, reaching a maximum of  $5.7 \times 10^{-3}$  S/m. The composite activated at 600°C had more and deeper pores, with the highest measured capacitance at 10.52  $\mu$ F [18]. Conductive polymer composites (CPCs) are being developed to enhance electrical conductivity and mechanical properties. Metal powders are used as conductive fillers in CPCs. This research examines the melt flow rate (MFR) of an aluminum (Al) and ABS polymer composite with a 10% weight loading of Al filler. The results indicate an increase in MFR. This research holds potential for the production of lightweight and customizable conductive structures [19], improving the impact resistance [20]. At certain concentrations, it can reach a low percolation threshold to obtain a conductive material [21]. In PP-based conductive polymer composites (CPC) with carbon filler, copper enhances mechanical properties. Research using compounding, remixing, hot blending, and hot-pressing processes showed that adding copper with a conductivity of  $5.80 \times 10^5$  S/cm to the PP/C composite improved both conductivity and mechanical properties. Copper increased the composite's density, reduced porosity, and enhanced tensile strength, flexural strength, tensile modulus, flexural modulus, and elongation [22]. LLDPE polymer was used in this study

because it is a suitable material for conducting polymer composites (CPC) due to its ease of processing at its recrystallization temperature and its non-polar nature [9,23]. Several studies have shown that LLDPE-based conductive polymer composites (CPC) incorporating nano-sized carbon allotropes can achieve very low percolation thresholds [6,8,24]. Significant advancements have been made in developing polymers with great potential as alternative materials across industries. For example, Polyetheretherketone (PEEK) can be used to create conductive polymer composites (CPC) with excellent mechanical properties, particularly in fatigue resistance and impact strength [25]. PEEK is a polymer with a very high processing temperature. Currently, there is no known development of composite materials using electrically conductive carbon fillers from organic materials in PEEK polymer. However, several composite materials have been introduced as industrial materials, fabricated and processed from various components or hybrids, with binders made from low-melting-point metal materials [26]. The research shows that the prototype Extruder Head effectively stabilizes composite density. Higher density resulted in a notable increase in electrical conductivity. These findings highlight the successful development of a CPC material with improved conductivity, making it ideal for high-carbon-loading composites [27]. The purpose of this study was to study the characteristics of physical properties and electrically conductive properties of composites fabricated from organic carbon materials (rice husks) and LLDPE [28]. This paper explores the electrical and mechanical properties of filament materials made from biomass-derived carbon particles in an LLDPE matrix. Filaments, slender threads or fibers, are used in various fields such as textiles, plastic manufacturing, and more, including 3D printing. The study aims to develop composites with electrically conductive carbon and LLDPE polymer to enhance electrical conductivity [29]. This article discusses the engineering of composite materials made from a mix of conductive organic carbon filler and LLDPE polymer. Conductive micro carbon from rice husks was incorporated into an LLDPE matrix using hot compaction. The composite varied in filler composition with carbon loadings of 50%, 45%, and 40%, and mesh sizes of #150, #200, and #250 [30].

This article presents an experiment on fabricating composite materials using LLDPE polymer as the binding matrix, enabling the formation process to occur at a low temperature for easy shaping. Electrically conductive carbon from abundant organic materials served as the primary filler, while aluminum (Al) and copper (Cu) metal powders were used as secondary fillers to create a hybrid composite.

## **2. Materials and Experiment Methods**

### **Carbonization**

Conductive carbon is made from rice husk filler through carbonization at 950°C, with a heating rate of 2°C per minute. The material is held at this temperature for 4 hours, then cooled naturally. The resulting conductive carbon is milled and sieved to obtain carbon particles with a mesh size of #200 (about 74 µm).

### Metal powder filler

This study uses copper (Cu) and aluminum (Al) powders as conductive fillers, known for their high conductivity and use in electrical equipment manufacturing. The Cu powder has 99.90% purity, a mesh size of #200 (about 74  $\mu\text{m}$ ), a conductivity of  $5.96 \times 10^7$  S/m, and a density of 8.96 g/cm<sup>3</sup>. The Al powder has 96.00% purity, a mesh size of #300 (about 44  $\mu\text{m}$ ), a conductivity of  $3.5 \times 10^7$  S/m, and a density of 2.70 g/cm<sup>3</sup>, used in power distribution.

### Thermoplastic LLDPE

The plastic resin used in this research is LLDPE (Linear Low-Density Polyethylene), specifically the ETILINAS LL3840UA grade. It has a white base color and a mesh size of #40 (approximately 400  $\mu\text{m}$ ). The resin's relative density to water ranges from 0.91 to 0.98, and its MFR (Melt Flow Rate) is 4 g/10 min. The polymer melts at 124°C, with crystallization occurring at 111°C.

### Hot compaction

Heat compaction is carried out by a manual hydraulic machine with a power of 400 bar. The heat printing process is carried out at a pressure of gradually up to 100 bar while being heated on a controlled electric heater.

The composite samples were fabricated using a high-precision digital scale with weight fraction composition ratios. Five specimens were prepared for each ratio.

Table 1 shows the composition of LLDPE carbon composites without the addition of metal powder.

**Table 1.** Composition of carbon-LLDPE

Sample Code	HOA	HOB	HOC
LLDPE, % w	50	55	60
Carbon, % w	50	45	40
Metal doping, %w	0	0	0

Table 2 shows the composition of carbon-LLDPE composites with the addition of aluminum powder, and the composition of aluminum powders with LLDPE, with carbon.

Table 3 shows the composite composition of carbon-LLDPE with the addition of copper powder, and the composition of copper powder and LLDPE, with carbon.

Mixing all ingredients is done manually, compressing the heat gradually, and pressing at a gradual pressure. The pressure gradually reaches 100 bar and is lowered to 50 bar at an initial temperature of 90°C. The temperature of the compass is raised to 130°C and held for 20 minutes. The sample is degraded from the mold. The shape and dimensions of the electrical and physical properties of the test sample are 10 × 10 × 5 mm.

**Table 2.** Composition of Carbpn-LLDPE-Al powder

Sample code	HAA	HAB
LLDPE, %w	50	50
Carbon, %w	40	30
Al_powder, %w	10	20

*Table 3. Composition of Carbon-LLDPE-Cu powder*

Sample code	HCA	HCB
LLDPE, %w	50	50
Carbon, %w	40	30
Cu powder, %w	10	20

### SEM-EDS testing

Carbon element and microstructure testing were conducted using the Hitachi SU 3500 SEM machine at the National Research and Innovation Agency (BRIN) Physics Laboratory in Serpong, Indonesia. Microscopic imaging uses the Secondary Electron (SE) and Backscattered Electron (BSE) techniques.

### Electrical conductivity test

Electrical conductivity testing was conducted at the Physics Laboratory of the National Research and Innovation Agency (BRIN) in Serpong, Indonesia, following the ASTM D4496 standard. The four-point probe method used the Keithley Source Meter® 2450.

## 3. Results and Discussion

The composite specimens of only LLDPE and carbon, shown in Table 4, used homogeneous blends of LLDPE polymer and micro carbon filler from rice husk in ratios of 50:50, 55:45, and 60:40. These were used as a reference to measure the effect of adding metal powders to the carbon polymer composite.

The LLDPE-carbon composite specimens will be compared to the characterization of specimens using metal powder fillers as a substitute for conductive carbon. The specimens with aluminum powder fillers are coded as HAA, HAB, HAC, and HAD, while the specimens with copper powder fillers are coded as HCA, HCB, HCC, and HCD.

The specimens HOB and HOC also consist of a homogeneous mixture of LLDPE as the binding matrix and microcarbon conductive filler from rice husk but in different

ratios. The code HOB is used for the composite with a composition of LLDPE: C (55:45), and the code HOC is used for the composite with a composition of LLDPE: C (60:40), referring to the codification in Table 4.

The results of electrical conductivity testing for conductive carbon loading are in Figure 1. Higher carbon content led to higher conductivity. The HOA composite with a 50:50 LLDPE: C ratio achieved the highest conductivity of  $9.43\text{E-}04$  S/cm. The HOC composite with a 60:40 LLDPE: C ratio had the lowest conductivity of  $1.35\text{E-}04$  S/cm. Lower carbon composition reduces the formation of conductive pathways, hindering electron flow within the composite.

**Table 4.** Sample code and composition ratio

Sample Code	HOA	HOB	HOC
LLDPE, % w	50	55	60
Carbon, % w	50	45	40
Metal doping, %w	0	0	0
Electrical Conductivities, S/cm	$9.43\text{E-}04$	$3.47\text{E-}04$	$1.35\text{E-}04$

The electrical conductivity performance can be supported by the conductive carbon reinforcement composition. Research shows that using a combination of several carbon allotropes in hybrid composites significantly enhances conductivity [22]. The very low conductivity is due to the high LLDPE matrix composition. Its insulating properties cause it to effectively insulate the carbon filler, hindering electricity flow in the HOC specimen. This is further supported by using PP as a polymer in hybrid composites without metal fillers [31]. The addition of carbon reinforcements successfully increased the electrical conductivity value of the hybrid composite based on PP polymer [22].

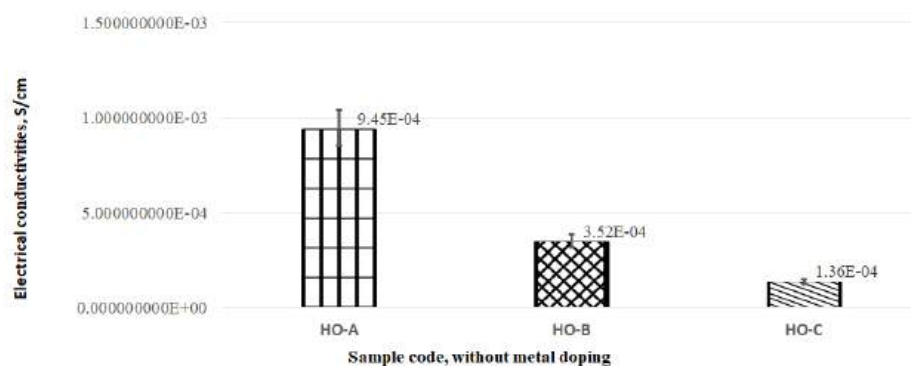


**Figure 1.** Electrical conductivity of LLDPE-carbon composite

During the initial mixing and compaction, conductive carbon particles aggregate within the polymer powder voids due to their smaller quantity and similar size to the voids. With increased heat, these particles absorb the molten polymer, forming a thin layer



on their surfaces. The densely packed carbon clusters absorb the polymer layer initially and diffuse into the polymer as the molten polymer equilibrium changes.

Under certain conditions, carbon particles aggregate in the polymer voids, forming conductive channels that enhance the material's electrical conductivity. These interconnected carbon aggregates create pathways for electron flow. More conductive channels result in higher conductivity.

### Electrical conductivity of metal filler LLDPE-carbon composite

To increase electrical, metal powders are added to the LLDPE/C carbon-polymer composite. This is done by replacing microcarbon weight with an equal weight of metal fillers like aluminum and copper powders, as metals are good conductors.

In the HAA specimen, 40% microcarbon and 10% aluminum powder by weight are used, matching the 50% total filler weight in the HOA specimen. This substitution is used to observe its effect on the hybrid composite's electrical conductivity.

Figure 2 shows the electrical conductivity graphs for LLDPE/C-Al and LLDPE/C-Cu hybrid composites. Substituting 10% conductive carbon with aluminum (HAA) and copper (HCA) did not improve conductivity compared to the HOA specimen without metal powder.

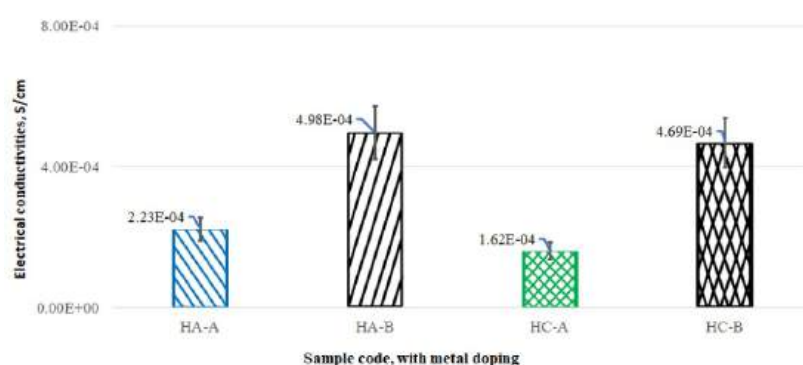


**Figure 2.** Electrical conductivity of hybrid composite

The distribution of metal fillers in HAA and HCA did not form sufficient conductive channels. The HOA specimen with microcarbon filler mesh #200 ( $\pm 74 \mu\text{m}$ ) achieved  $9.43\text{E-}04 \text{ S/cm}$ , while HAA (LLDPE/C-Al 10%) and HAB (LDPE/C-Al 20%) achieved  $0.000223 \text{ S/cm}$  and  $0.000498\text{S/cm}$ , respectively, as showed at Table 5.

**Table 5.** Composition ratio LLDPE-carbon-Al

Sample code	HAA	HAB
LLDPE, %w	50	50
Carbon, %w	40	30

Al powder, %w	10	20
Electrical Conductivities, S/cm	2.23E-04	4.98E-04

A 20% by-weight substitution of micro carbon in hybrid composites increases electrical conductivity, as seen in HAB and HCB specimens, as shown in Figure 2, and Table 5 and 6. However, adding too much metal powder to the LDPE/C carbon polymer composite can decrease conductivity, likely due to metal powder agglomeration within the polymer matrix. Compare the data in Figures 1 and 2, specifically between the HOA (no doping metal), HAA (Al doping metal), and HCA (Cu doping metal) samples.

**Table 6.** Composition ratio LLDPE-carbon-Cu

Sample code	HCA	HCB
LLDPE, %w	50	50
Carbon, %w	40	30
Cu powder, %w	10	20
Electrical Conductivities, S/cm	1.62E-04	4.69E-04

Adding metal powder Al and Cu to the LLDPE/C carbon polymer composite affects its flow behavior. Metal powders have higher densities than carbon and LLDPE, increasing melt viscosity and reducing the flowability or rheology of LLDPE. This high viscosity can lead to particle agglomeration within the polymer matrix. Metal powder particles, along with microcarbon, act as nuclei for forming conductive pathways. If pressure and thermal energy are insufficient, conductive pathways may not increase during compaction and heating.

Uneven dispersion of conductive filler particles disrupts electrical pathways and reduces charge transfer efficiency in the polymer matrix. Metal powder agglomeration decreases contact between metal and carbon powders, lowering conductivity. Additionally, agglomeration can reduce the composite's density, further decreasing conductivity.

#### **Microstructure dispersion of metal filler LLDPE-carbon composite**

The explanation of the SEM test results directly points to the feature points that are suspected to be carbon filler or porosity (voids) or cracks, or LLDPE matrix. Porosity or voids are indicated by very dark images, compared to carbon fillers, and cracks are indicated by irregularly elongated groove images, and usually occur at the interface between the matrix and carbon filler.

In Figure 3, SEM images of the HOA specimen (LLDPE/C) show micro carbon particles from rice husk bound by a polymer layer (LLDPE), forming micro carbon

channels in the matrix. These closely packed conductive channels facilitate electron transfer, resulting in a conductivity of  $9.43\text{E-}04\text{ S/m}$ .

In Figure 3, the SEM test results also show that a metal intrusion has been detected. This intrusion is an impurity in the LLDPE-carbon composite. The detected metal was accidentally included in the composite mixture.

In Figure 3, there is a difference in the contrast of appearance between the carbon filler and the LLDPE matrix. The carbon filler looks darker than the plastic matrix in the SEM image.

LLDPE-carbon and metal aluminum composites are shown in Figure 4 with the HAA sample code. Figures 4 and 5 show SEM images comparing the microstructure of HAA (LLDPE/C-Al) and HCA (LLDPE/C-Cu) specimens, each with a 10% by-weight metal powder loading. The comparison reveals that these composites are more porous than the HOA (LLDPE/C) specimen. In the HAA (LLDPE/C-Al; 50/40/10) and HCA (LLDPE/C-Cu; 50/40/10) specimens, adding 10% metal powder results in relatively good dispersion of metal particles. However, this dispersion does not fully replace the lost conductive microcarbon network. Consequently, the conductivity values of HAA ( $1.06\text{E-}04\text{ S/cm}$ ) and HCA ( $1.33\text{E-}04\text{ S/cm}$ ) are significantly lower than HOA ( $9.43\text{E-}04\text{ S/cm}$ ), which has no metal filler.

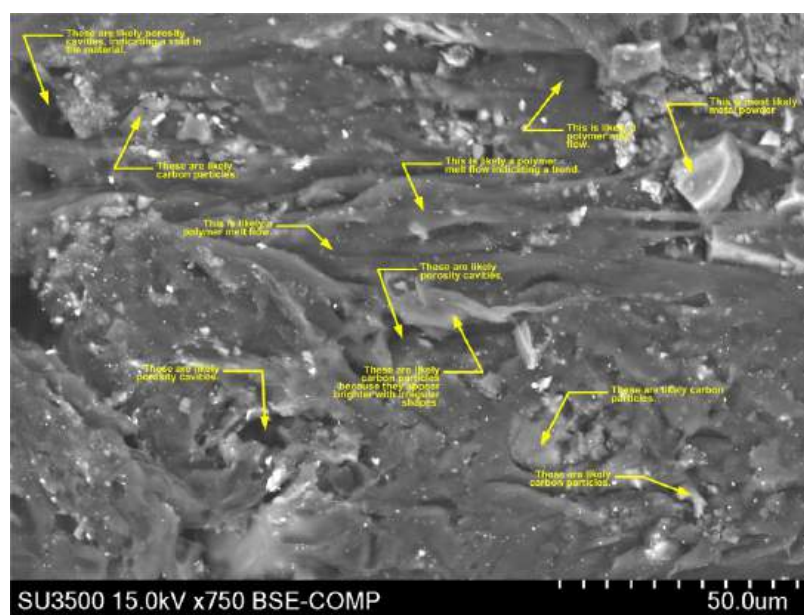


**Figure 3.** SEM of HOA composite (LLDPE/C)

The composite's conductivity depends on the amount of conductive filler particles, with higher metal content providing a larger surface area per unit volume. This larger surface area improves metal-to-metal contacts and electrical conductivity. With a 20% filler loading, the HAB ( $1.82\text{E-}04\text{ S/cm}$ ) and HCB ( $3.54\text{E-}04\text{ S/cm}$ ) specimens show the highest conductivity values among the tested compositions. The HCB's conductivity is approximately one-third of the HOA's ( $9.43\text{E-}04\text{ S/cm}$ ). These results support the hypothesis that a larger surface area-to-volume ratio of the filler influences conductive

channel formation. The HOA specimen has a larger surface area-to-volume ratio for the filler, considering particle size and filler density. In contrast, the HCB specimen, with a 20% copper filler loading, shows higher conductivity than the HCA specimen.

In the LLDPE/C-Al hybrid composite, the aluminum (Al) element shows a decrease in weight percentage at selected points, likely due to poor aggregation with other Al metals or carbon, leading to Al-Polymer-Carbon agglomeration. For the hybrid composite with copper (Cu) filler, the Cu element's weight percentage increases. The decrease in electrical conductivity is suspected to be due to unevenly dispersed conductive aggregates. The overall conductivity value drops significantly due to numerous agglomerated areas with higher resistance.

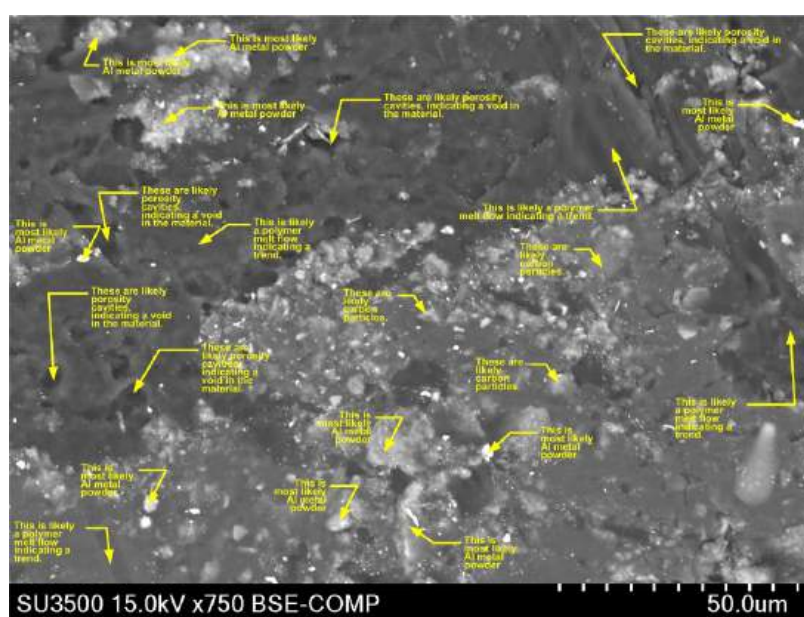


Figure 4. SEM of HAA composite (LLDPE/C-Al)

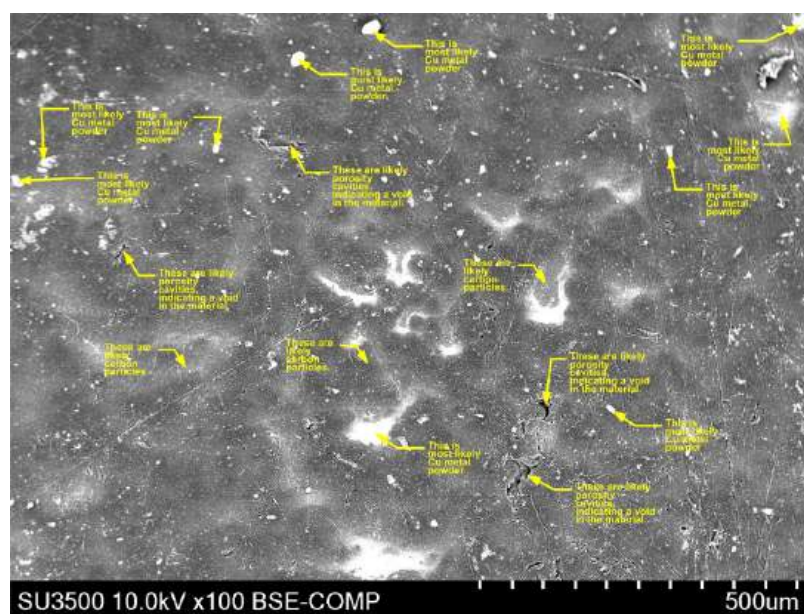


Figure 5. SEM of HCA composite (LLDPE/C-Cu)

SEM analysis of LLDPE/C-Al and LLDPE/C-Cu specimens indicates the occurrence of oxidation on the metal particles within the composite, leading to material degradation on the metal surfaces and resulting in increased contact resistance between metal fillers or between metal fillers and carbon. In carbon polymer composites, metal particles are dispersed throughout the carbon matrix. Exposure to oxygen and other reactive elements leads to oxidation, forming metal oxides like CuO on copper and Al<sub>2</sub>O<sub>3</sub> on aluminum. Oxidation causes metals to lose electrical conductivity, as metal atoms lose electrons and become ions. Metal oxides on particle surfaces decrease conductivity by impeding electron movement and increasing surface roughness, affecting interfacial properties. Copper is more reactive with oxygen than aluminum, making it more prone to oxidation.

In applications where the electrical conductivity of carbon polymer composites is important, steps need to be taken to prevent or minimize the effects of oxidation on the metal particles, such as using antioxidants in the carbon-metal composite mixture [22] or storing the specimens under vacuum conditions [14] to minimize oxygen exposure.

Another factor that contributes to the decrease in electrical conductivity in composites is the high concentration of metal fillers. It becomes more difficult for the metal fillers to disperse effectively in the composite.

A study by Nurazreena et al. (2006) found that Metal-Filled HDPE Composites with 30% aluminum filler had lower electrical conductivity than those with 10%. Conductivity is influenced by the amount and dispersion of conductive fillers and their shape. Regular-shaped fillers tend to agglomerate, reducing adhesion between the metal filler and polymer. Irregular-shaped fillers, like flakes, provide better conductivity due to a larger interfacial contact area [32].

The significant decrease in electrical conductivity in LDPE/C-Al (HAC) and LDPE/C-Cu (HCC) composites with 20% to 30% metal filler loading indicates inverse percolation. This occurs when the conductive filler is not well dispersed or when non-conductive regions hinder conductive pathways, resulting in disrupted pathways and decreased conductivity. Inverse percolation often happens in composites where the filler agglomerates or is poorly dispersed, or when there is a significant mismatch in electrical properties between the filler and the polymer matrix. Further research is needed to determine the specific point of this phenomenon.

#### **4. Conclusion**

Adding metal powder generally increases electrical conductivity in carbon polymer composites by filling voids during formation. At low concentrations ( $\leq 10\%$ ), metal fillers disperse well, forming conductive channels. However, beyond 10% concentration, non-uniform dispersion and agglomeration occur, forming high-concentration aggregates that affect mechanical and electrical properties. Copper particles tend to agglomerate more than aluminum due to higher surface energy and reactivity, forming stronger bonds and aggregates. Additionally, copper's tendency to oxidize in air further contributes to agglomeration.

**Funding:** The research was funded through the Basic Research Scheme 2024. Contract number: Nomor: 368/PL3.A.10/PT.00.06/2024, April 25, 2024, Politeknik Negeri Jakarta.

**Acknowledgments:** The authors acknowledge the facilities, scientific and technical support from Advanced Characterization Laboratories, National Research and Innovation Agency through E-Layanan Sains, Badan Riset dan Inovasi Nasional (BRIN), Serpong, Indonesia.

**Conflicts of Interest:** “The authors declare no conflict of interest.”

## References

1. Burmistrov, I. *et al.* Improvement of carbon black based polymer composite electrical conductivity with additions of MWCNT. *Compos. Sci. Technol.* **129**, 79–85 (2016).
2. Oberoi, S., Mohan, V. B. & Bhattacharyya, D. Mechanical and Electrical Characteristics of 3D Printed Multi-material Polymer Composites. in *SAMPE Conference Proceeding* (2019).
3. Balberg, I. A comprehensive picture of the electrical phenomena in carbon black-polymer composites. *Carbon N. Y.* **40**, 139–143 (2002).
4. Chiarini, A. & Nitzschner, M. Disconnection and Entropic Repulsion for the Harmonic Crystal with Random Conductances. *Commun. Math. Phys.* **386**, 1685–1745 (2021).
5. Qahtani, N. Al, Ejji, M. Al, Ouederni, M., Almaadeed, M. A. & Madi, N. Effect Of Carbon Black Loading On Linear Low-Density Polyethylene Properties. *Int. J. Sci. Eng. Investig.* **10**, 1–22 (2021).
6. Abdelbary, A. Swelling and electrical properties of LLDPE reinforced by SWCNTs nanocomposites for radiation and sensors applications. *J. Thermoplast. Compos. Mater.* **35**, (2020).
7. Banerjee, J. & Dutta, K. Melt-mixed carbon nanotubes/polymer nanocomposites. *Polym. Compos.* **40**, 4473–4488 (2019).
8. Horst, D. J., Andrade, P. P. J., Duvoisin, C. A. & Vieira, R. D. A. Fabrication of Conductive Filaments for 3D-printing: Polymer Nanocomposites. *Biointerface Res. Appl. Chem.* **10**, 6577–6586 (2020).
9. Choi, H., Kim, M. S., Ahn, D., Yeo, S. Y. & Lee, S. Electrical percolation threshold of carbon black in a polymer matrix and its application to antistatic fibre. *Sci. Rep.* 1–12 (2019) doi:10.1038/s41598-019-42495-1.
10. Kwok, S. W. *et al.* Electrically conductive filament for 3D-printed circuits and sensors. *Appl. Mater. Today* **9**, 167–175 (2017).
11. Leigh, S. J., Bradley, R. J., Pursell, C. P., Billson, D. R. & Hutchins, D. A. A Simple , Low-Cost Conductive Composite Material for 3D Printing of Electronic Sensors. *PLoS One* **7**, 1–6 (2012).
12. Ojha, S., Acharya, S. K. & Raghavendra, G. Mechanical properties of natural carbon black reinforced polymer composites. *J. Appl. Polym. Sci.* **132**, 1–7 (2015).
13. Mamunya, Y. P., Davydenko, V. V., Pissis, P. & Lebedev, E. V. Electrical and thermal conductivity of polymers filled with metal powders. *Eur. Polym. J.* **38**, 1887–1897 (2002).
14. Nurazreena, Hussain, L. B., Ismail, H. & Mariatti, M. Metal filled high density polyethylene composites - Electrical and tensile properties. *J. Thermoplast. Compos. Mater.* **19**, 413–425 (2006).
15. Zare, Y., Rhee, K. Y. & Park, S. J. Advancement of the Power-Law Model and Its Percolation Exponent for the Electrical Conductivity of a Graphene-Containing System as a Component in the Biosensing of Breast Cancer. *Polymers (Basel)*. **14**, (2022).
16. Indayaningsih, N., Zulfia, A., Priadi, D. & ... Synthesis of Empty Fruit Bunches Carbon Polymer Composites As Gas Diffusion Layer for Electrode materials. *J. Sains Mater.* ... (2018).



17. Lovelila, B. *et al.* The Study of The Electrical Conductivity and Activation Energy on Conductive Polymer Materials. *Comput. Exp. Res. Mater. Renew. Energy* **4**, 71–79 (2021).
18. Nurdianti, D. & Astuti. Sintesis Komposit PAni / Karbon dari Tempurung Kemiri ( Aleurites moluccana ) Sebagai Elektroda Kapasitor. *J. Fis. Unand* **4**, 51–57 (2015).
19. Kumar, N., Jain, P. K., Tandon, P. & Pandey, P. M. Investigations on the melt flow behaviour of aluminium filled ABS polymer composite for the extrusion-based additive manufacturing process. *Int. J. Mater. Prod. Technol.* **59**, 194–211 (2019).
20. Anis, A. *et al.* Aluminum-filled amorphous-PET, a composite showing simultaneous increase in modulus and impact resistance. *Polymers (Basel)*. **12**, (2020).
21. Boudenne, A., Ibos, L., Fois, M., Majesté, J. C. & Géhin, E. Electrical and thermal behavior of polypropylene filled with copper particles. *Compos. Part A Appl. Sci. Manuf.* **36**, 1545–1554 (2005).
22. Zulfia, A., Abimanyu, T. & Dalam, V. Effect of Copper Addition on Mechanical Properties and Electrical Conductivity of PP/C-Cu Bipolar Plate Composites. *Makara J. Technol.* **15**, 101 (2013).
23. Ramkumar, P. L., Kulkarni, D. M. & Chaudhari, V. V. Parametric and mechanical characterization of linear low density polyethylene ( LLDPE ) using rotational moulding. *S<sup>-</sup>adhan<sup>-</sup>a* **39**, 625–635 (2014).
24. Jin-hua, T., Guo-qin, L., Huang, C. & Lin-jian, S. Mechanical Properties and Thermal Behaviour of LLDPE/MWNTs Nanocomposites. *Mater. Res.* **15**, 1050–1056 (2012).
25. Saleem, Anjum; Frommann, Lars; Iqbal, A. High Performance Thermoplastic Composites: Study on the Mechanical, Thermal, and Electrical Resistivity Properties of Carbon Fiber-Reinforced Polyetheretherketone and Polyethersulphone. *Polym. Compos.* **28**, 785–796 (2007).
26. Islam, A., Hansen, H. N. & Tang, P. T. Direct electroplating of plastic for advanced electrical applications. *CIRP Ann. - Manuf. Technol.* **66**, 209–212 (2017).
27. Zuhri, A., Pramono, A. E., Setyadi, I. & Indayaningsih, N. Effect of Rheological on the Physical and Electrical Properties of Extruded Micro Carbon-LLDPE Composites. **02**, (2024).
28. Pramono, A. E. *et al.* The investigation on the electrical and physical properties of conductive filaments prepared using polymer-carbon composites. *AIP Conf. Proc.* **3222**, (2024).
29. Pramono, A. E. *et al.* Jurnal Polimesin. *Polimesin* **22**, 410–415 (2024).
30. Zuhri, A., Pramono, A. E., Setyadi, I., Maksum, A. & Indayaningsih, N. Effect of microcarbon particle size and dispersion on the electrical conductivity of LLDPE-carbon composite. *J. Appl. Res. Technol.* **13**, 374–381 (2024).
31. Pramono, A. & Zulfia, A. Konduktifitas Listrik Komposit Polimer Polipropilena/Karbon Untuk Aplikasi Pelat Bipolar Fuel Cell. *Setrum Sist. Kendali-Tenaga-elektronika-telekomunikasi-komputer* **1**, 46 (2012).
32. Nurazreena, Hussain, L. B., Ismail, H. & Mariatti, M. Metal filled high density polyethylene composites - Electrical and tensile properties. *J. Thermoplast. Compos. Mater.* **19**, 413–425 (2006).

Article

# The Effects of Soil Resistivity on The Corrosion Resistance of Carbon Steel

Syanatha Putri Salsabila <sup>1,\*</sup>, Rini Riastuti <sup>1</sup>

<sup>1</sup> Department of Metallurgical and Materials Engineering, Universitas Indonesia, Depok 16424

\* Correspondence: syanathap@gmail.com

**Abstract:** Indonesia, as a tropical country with high humidity, faces corrosion challenges in the underground infrastructure of the oil and gas industry, causing significant economic losses. This study analyzed the effect of soil characteristics on the corrosion rate of carbon steel using the weight loss and linear polarization methods. The weight loss method was used to determine the corrosion rate based on the mass reduction of the sample, while the linear polarization method evaluated the corrosion kinetics through icorr and polarization resistance values. The results showed that soil characteristics, especially moisture and resistivity, had a significant effect on the corrosion rate. Pakis Karawang beach sand soil with pH 5.2, humidity 87%, and resistivity 59.03  $\Omega$ -cm had the highest corrosion rate of 42.57 mpy and the lowest polarization resistance of 11.16  $\Omega$ . In contrast, the UI Native Forest Ravine soil showed the lowest corrosion rate of 16.89 mpy with the highest polarization resistance of 2,820.11  $\Omega$ . These findings confirm that environmental factors, particularly soil type, should be considered in corrosion mitigation strategies to improve the resilience of underground infrastructure.

**Keywords:** Corrosion; Soil Moisture; Soil Resistivity; EIS Method; Soil Corrosion

**Citation:** Salsabila, S. P.; Riastuti, R. (2025). The Effects of Soil Resistivity on The Corrosion Resistance of Carbon Steel. *Recent in Engineering Science and Technology* 3(02), 15–34. Retrieved from <https://www.mbi-journals.com/index.php/riestech/article/view/100>

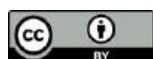
Academic Editor: Vika Rizkia

Received: 25 March 2025

Accepted: 28 April 2025

Published: 30 April 2025

**Publisher's Note:** MBI stays neutral with regard to jurisdictional claims in published maps and institutional affiliations.



**Copyright:** © 2025 by the authors. Licensee MBI, Jakarta, Indonesia. This article is an open access article distributed under MBI license (<https://mbi-journals.com/licenses/by/4.0/>).

## 1. Introduction

Indonesia as a tropical country has high levels of humidity and rainfall that affect soil conditions. This affects the systematics of industries that operate underground and depend on the environment, one of which is the oil and gas industry. The main challenge in this industry is failure or unexpected costs stemming from corrosion issues. The production process of this industry utilizes underground piping systems. Behind the ease of access, there are challenges that are difficult to avoid, one of which is contact with the underground environment [1,2]. The contact between the pipe material and its environment will trigger a process of degradation of the material's ability to operate according to its function, namely corrosion.

Corrosion is the process of deterioration of a metal material [3]. Corrosion in soil is a type of corrosion that is often the cause of failure of underground piping installation systems. Electrochemical corrosion of metals buried in soil with high humidity causes corrosion cells to form from paired anodes and cathodes [4].

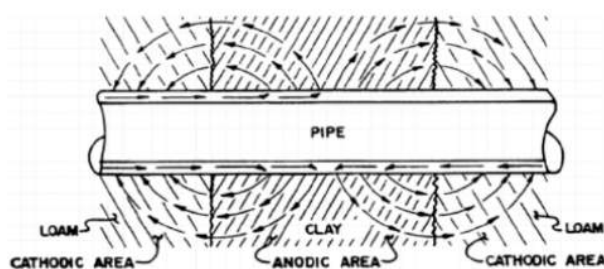


**Figure 1.** Ilustrasi mekanisme korosi pada pipa bawah tanah

Corrosion is influenced by soil aeration levels, acidity (soil pH), soil moisture, soil content, oxygen content and resistivity values. Soil moisture content represents the amount of water in the soil. High soil moisture can increase the corrosion rate of underground piping systems. Different soil types can affect the corrosiveness of the soil to the material being tested [5]. Acidity (soil pH) will affect the tendency for corrosion to occur or not [6]. The chemical composition contained in the soil has a significant effect on the soil resistivity value. And soil resistivity will affect the corrosion rate of materials exposed to the soil environment.

Failure or unexpected costs allocated to corrosion aspects can be reduced by 15-35% [7] by performing preventive methods so that corrosion does not occur, such as coating, inhibition, cathodic protection and other types of methods that are deemed appropriate. However, to determine the appropriate method, predictive analysis is needed related to corrosion that may occur, in this study a predictive analysis will be carried out related to the effect of soil on the corrosion resistance of carbon steel. Carbon steel is quite often used as the main material for making pipes. The choice of carbon steel as a pipe material is based on the suitability of the mechanical properties that can be produced, namely carbon steel has good plastic properties and will facilitate the manufacturing and machining process of pipe products [8]. Carbon steel also has a fairly good level of strength and is balanced with good toughness in absorbing energy.

Based on the background, this study aims to evaluate the relationship of soil moisture content to soil resistivity values, analyze how variations in soil resistivity affect the corrosion resistance of carbon steel and explore the relationship between variations in soil type to the composition and corrosion resistance of carbon steel under different environmental conditions. It is hoped that the findings of this research will contribute to the development of effective corrosion mitigation strategies for underground piping infrastructure in tropical countries such as Indonesia.

## 2. Materials and Experiment Methods

### 2.1 Sample Preparation

Carbon steel was divided into two sizes:  $1 \times 2.5 \text{ cm}^2$  for the weight loss method and  $5 \times 5 \text{ cm}^2$  for Electrochemical Impedance Spectroscopy (EIS) and linear polarization testing. The steel surfaces were cleaned using sandpaper to SP2 [9], cleanliness level, washed with Alconox, dried, and then soaked in acetone before being buried in soil.

## 2.2 Soil Preparation

The soil will serve as the electrolyte medium in direct contact with the carbon steel material. The soils used are sourced from three different locations: the Department of Metallurgy and Materials Engineering, the UI Original Forest Ravine, and Pakis Karawang Beach Sand.

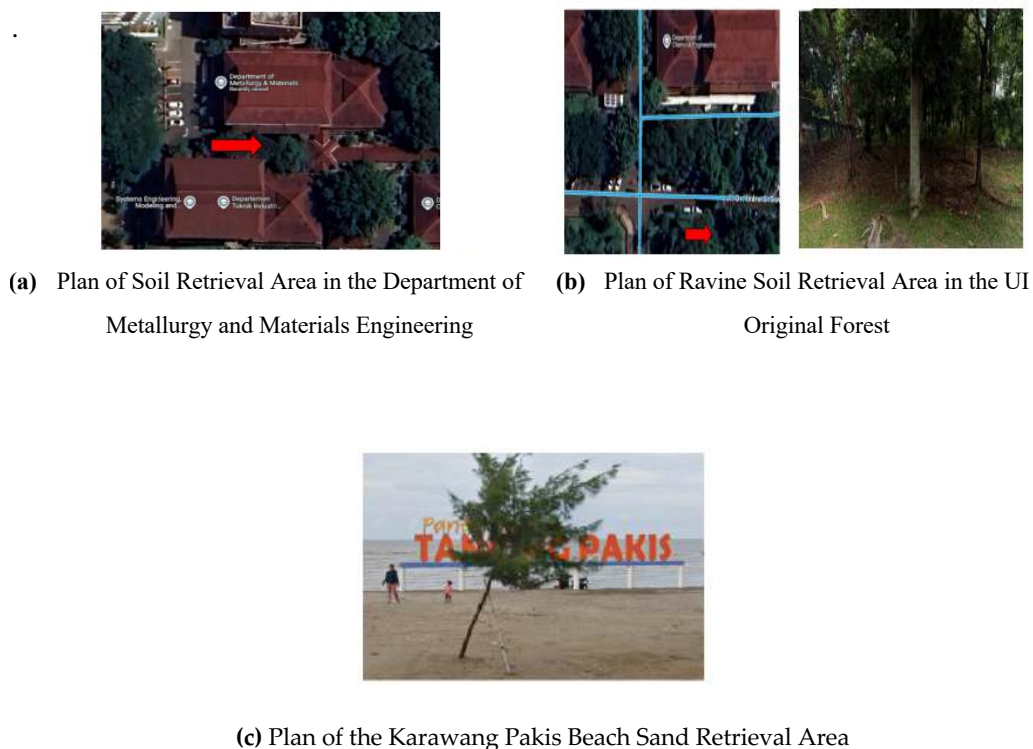


**Figure 2.** Plan of Soil Retrieval Area

The soil was tested before collection using a resistivity meter with the four-wenner pin method, then stored in a soil storing box in the laboratory. The parameters measured were moisture, pH, and temperature.

## 2.3 Testing Methods

- **Weight Loss Method:** Carbon steel samples ( $1 \times 2.5 \text{ cm}^2$ ) with a contact area of  $1 \times 1 \text{ cm}^2$  were immersed in soil ( $\geq 200 \text{ mL}$ ) for 7, 14, and 21 days. After immersion, the samples were weighed before and after sanding to determine the weight lost and calculate the corrosion rate using the ASTM G31-12a equation.
- **Linear Polarization Method:** Carbon steel samples ( $5 \times 5 \text{ cm}^2$ ) were placed in a flat cell containing soil as the electrolyte medium. The electrodes used included carbon steel (working electrode), carbon (counter electrode), and  $\text{Cu}/\text{CuSO}_4$  and  $\text{Ag}/\text{AgCl}$  (reference electrodes). After configuring the Nova Autolab device, the test began by measuring the Open Circuit Potential (OCP) for 900 seconds, followed by Linear Polarization within a potential range of  $-1\text{V}$  to  $1\text{V}$  at a scan rate of  $1 \text{ mV/s}$ . The results were analyzed using the Tafel Slope method to determine the corrosion kinetics.

- EIS Method: Carbon steel samples (5×5 cm<sup>2</sup>) were placed in a flat cell containing soil as the electrolyte medium. The electrodes used included carbon steel (working electrode), carbon (counter electrode), and Cu/CuSO<sub>4</sub> and Ag/AgCl (reference electrodes). After configuring the Nova Autolab device, the tests were conducted with a frequency range of 10<sup>-2</sup> to 10<sup>5</sup> Hz, where parameters such as scan rate and the number of reading points could be adjusted. The data obtained were analyzed to evaluate the impedance properties and corrosion mechanisms of carbon steel.

#### 2.4 Characterization Methods

- XRF (X-Ray Fluorescence): to analyze the elemental composition of soil samples. The sample is homogenized, divided into three containers, and then loaded into the XRF apparatus. X-rays are fired to excite atoms, producing fluorescent X-rays that are detected and analyzed based on their wavelength and intensity to determine the constituent elements and their concentration.
- OES (Optical Emission Spectroscopy): analyzes elements in steel samples that have been cleaned and sanded grit 80, 120, 240. The sample is placed on an OES electrode and given a spark shot, causing the atoms to be excited and emit light. The wavelength of the light is analyzed to identify the element, while its intensity determines the concentration.

### 3. Results and Discussion

#### 3.1 Material Characterization Results

##### 3.1.1 Carbon Steel OES Characterization Results

**Table 1.** Composition Results using OES Method

Fe	Mn	C	Cu	Si
99,590%	0,179%	0,046%	0,036%	0,025%
Al	Cr	Ni	As	P
0,025%	0,019%	0,018%	0,017%	0,012%
Trace Elements				
Fe.				

**Table 2.** Composition of Q235 Carbon Steel

C	Si	Mn	P	S
0,190%	0,105%	0,145%	0,020%	0,020%

Based on the results in Table 1, the Optical Emission Spectroscopy (OES) analysis shows that the carbon steel used has a carbon content (C) of 0.046%, classifying it as low-carbon steel. This carbon steel composition is similar to that of Q235 steel, as presented in Table 4.2, which is known for its good mechanical properties, particularly in terms of ductility and weldability [10].

### 3.1.2 Results of Soil Characterization Analysis

**Table 3.** Characterization data of soil variation

Soil Name	$\rho(\Omega/\text{cm})$	Soil Characteristics		
		Temperature (°C)	Humidity (%)	pH
Department of Metallurgical and Materials Engineering soil	4.577,17	29	65	6,6
Natural forest Universitas Indonesia's soil	21.772,70	26	51	5,9
Pakis Beach Karawang Sand	59,03	33	87	5,2

The soil of the Department of Metallurgical and Materials Engineering exhibits the second highest resistivity (4,577.17  $\Omega\text{-cm}$ ) and moisture content (65%). The soil in the UI Original Forest Ravine has the highest resistivity (21,772.70  $\Omega\text{-cm}$ ) and a more acidic pH (5.9), which contributes to better corrosion resistance. In contrast, Pakis Beach Karawang Sand has the lowest resistivity (59.03  $\Omega\text{-cm}$ ) and the highest moisture content (87%), making it the most corrosive environment for carbon steel.

These resistivity values align with existing literature regarding the relationship between moisture content and resistivity. Specifically, as moisture content increases, the resistivity value decreases, as higher water content in the soil facilitates the movement of ions, thus lowering the resistivity.



**Table 4.** Results of Soil Composition Using XRF Method

Compotition	Department of Met- allurgical and Mate- rials Engineering soil (ppm)	Natural forest Uni- versitas Indonesia's soil (ppm)	Pakis Beach Karawang Sand (ppm)
C	94.700,00	95.060,00	96.630,00
Si	19.059,57	18.260,07	15.136,64
Al	17.544,81	17.438,75	6.054,69
Fe	14.290,09	12.626,09	7.423,06
Ti	1.233,92	1.081,11	488,76
Ca	445,48	77,34	2.232,23
Mg	0	0	1.436,49
Mn	493,65	357,63	146,36
Ba	78,94	80,49	35,64
K	27,85	0	617,30
Ag	71,17	2,12	80,71
Na	0	0	123,70
V	45,19	41,85	18,65
Cu	40,20	9,60	23,25
Sn	30.53	17.20	23.31
Zn	38,17	14,28	8,02
Cr	14,06	9,59	17,51
P	0	0	40,30
Pb	13,90	1,43	8,76
Ni	14,05	4,44	4,37
Mo	4,63	3,06	2,61
S	0	0	47,35
Sb	0	0	20,92
Cd	0	0,75	6,15

In Table 4, the red-colored column will serve as a reference for considering several elemental compositions that show significant differences and influence soil variables as electrolyte media. The highest moisture content is observed in Pakis Beach Karawang Sand, while the lowest moisture content is found in the Natural Forest

Universitas Indonesia's soil. The calcium (Ca) content in the soil can form a barrier layer on the surface of carbon steel, inhibiting the diffusion of dissolved oxygen to the metal surface and thereby reducing the corrosion rate [11].

Pakis Beach Karawang Sand has a high content of sodium (Na, 123.70 ppm) and potassium (K, 617.30 ppm). Sodium can form NaCl, which increases soil conductivity and accelerates metal corrosion [12, 13]. Soil conductivity and acidity (pH) are influenced by the salt content, as well as aluminum (Al) and silicon (Si) levels. The lower Al and Si concentrations in Pakis Beach Karawang Sand contribute to a lower pH [14]. Iron (Fe) and carbon (C) elements in the soil play a role in maintaining pH stability, where Fe promotes corrosion by forming an acidic environment, while C helps neutralize acidity and reduce soil corrosivity [15, 16, 17].

### 3.2 Corrosion Resistance Test Results

#### 3.2.1 Weight Loss Method

**Table 5.** Corrosion Rate Value using Weight Loss Method Based on Burial Duration

Soil Name	Corrotrion Rate (mpy)		
	7 Days	14 Days	21 Days
Department of Metallurgical and Materials Engineering soil	15,81 mpy	17,66 mpy	20,52 mpy
Natural forest Universitas Indonesia's soil	14,57 mpy	15,36 mpy	16,89 mpy
Pakis Beach Karawang Sand	33,12 mpy	36,56 mpy	42,57 mpy

The weight loss method measures the corrosion rate by calculating the mass of material lost during the burial period. The test results indicate that the longer the burial time, the greater the mass loss, leading to an increase in the corrosion rate (measured in mils per year, mpy). The daily corrosion rate trend displayed linear values across all soil types tested, with the Natural Forest Universitas Indonesia's soil exhibiting the lowest corrosion rate and Pakis Beach Karawang Sand showing the highest. Soil characteristics, such as moisture content and resistivity, significantly affect the corrosion rate. Soils with higher moisture content and lower resistivity, such as Pakis Beach Karawang Sand, tend to be more corrosive.

### 3.2.2 Linear Polarization Method

**Table 6.** Error Value vs Icorr (Linear Polarization Test Results by Soil Type)

(a) Tafel Slope Data of Carbon Steel in Department of Metallurgical and Materials Engineering soil

Tafel Slope Data of Carbon Steel in Department of Metallurgical and Materials Engineering soil				
Components	Day 0	Day 7	Day 14	Day 21
Ecorr, Calc (mV)	-736.000	-673.350	-725.850	-635.620
icorr ( $\mu\text{A}/\text{m}^2$ )	0.00617	0.40611	0.47674	0.45319

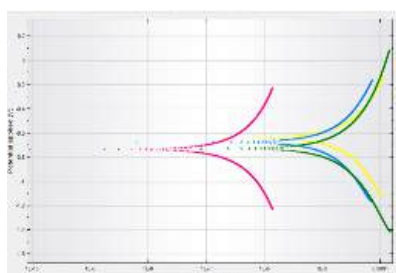
(b) Tafel Slope Data of Carbon Steel in Natural forest Universitas Indonesia's soil

Tafel Slope Data of Carbon Steel in Natural forest Universitas Indonesia's soil				
Components	Day 0	Day 7	Day 14	Day 21
Ecorr, Calc (mV)	-739.410	-734.500	-671.840	-720.220
icorr ( $\mu\text{A}/\text{m}^2$ )	0.28683	0.37888	0.17981	0.11903

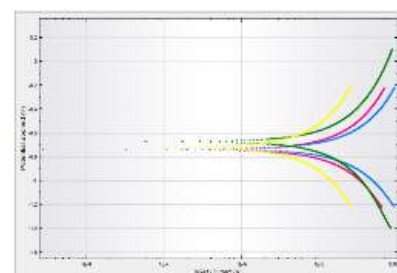
(c) Tafel Slope Data of Carbon Steel in Pakis Beach Karawang Sand

Tafel Slope Data of Carbon Steel in Pakis Beach Karawang Sand				
Components	Day 0	Day 7	Day 14	Day 21
Ecorr, Calc (mV)	-718.960	-747.790	-581.600	-728.260
icorr ( $\mu\text{A}/\text{m}^2$ )	2.2478	2.2362	3.2244	4.1246

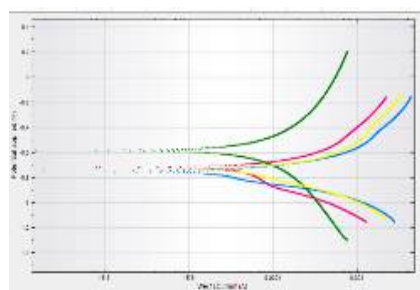
The highest corrosion current density (icorr) was observed for carbon steel buried in Pakis Beach Karawang Sand, reaching  $4.1246 \mu\text{A}/\text{cm}^2$ , indicating high corrosion activity. In contrast, the Natural Forest Universitas Indonesia's soil exhibited the lowest icorr value of  $0.11903 \mu\text{A}/\text{cm}^2$ , suggesting a less aggressive corrosion environment. Meanwhile, the Department Metallurgical and Materials Engineering soil had an icorr value of  $0.45319 \mu\text{A}/\text{cm}^2$ .



(a) Linear Polarization Test Results of Department Metallurgical and Materials Engineering soil (●) Day 0 (●) Day 7 (●) Day 14 (●) Day 21



(b) Linear Polarization Test Results of Natural forest Universitas Indonesia's soil (●) Day 0 (●) Day 7 (●) Day 14 (●) Day 21



(c) Linear Polarization Test Results of Pakis Beach Karawang Sand (●) Day 0 (●) Day 7 (●) Day 14 (●) Day 21

**Figure 3.** Linear Polarization Test Results by Soil Type

**Table 7.** Error Value vs Icorr (Linear Polarization Time Range Test Results)

(a) Day 0 Tafel Slope Data

Tafel Slope Data of			
Components	Pakis Beach Karawang Sand	Natural forest Universitas Indonesia's soil	Department Metallurgical and Materials Engineering soil
Ecorr, Calc (mV)	-718.960	-739.410	-736.000
icorr ( $\mu A/m^2$ )	2.2478	0.28683	0.0061759
Corrate (mm/yr)	0.02611	0.00333	0.00007

(b) Day 7 Tafel Slope Data

Tafel Slope Data of			
Components	Pakis Beach Karawang Sand	Natural forest Uni- versitas Indone- sia's soil	Department Metallurgical and Materials Engineer- ing soil
<b>Ecorr, Calc (<i>mV</i>)</b>	-747.790	-734.500	-673.350
<b>icorr (<math>\mu A/m^2</math>)</b>	2.2362	0.3788	0.4061
<b>Corrate (mm/yr)</b>	0.02598	0.00440	0.00471

(c) Day 14 Tafel Slope Data

Tafel Slope Data of			
Components	Pakis Beach Karawang Sand	Natural forest Universitas Indonesia's soil	Department Metallurgi- cal and Materials Engi- neering soil
<b>Ecorr, Calc (<i>mV</i>)</b>	-581.600 mV	-671.840 mV	-724.310 mV
<b>icorr (<math>\mu A/m^2</math>)</b>	3.2244 $\mu A/m^2$	0.1798 $\mu A/m^2$	0.4767 $\mu A/m^2$
<b>Corrate (mm/yr)</b>	0.00374	0.00208	0.00553

(d) Day 21 Tafel Slope Data

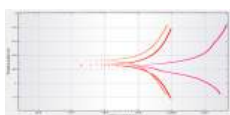
Tafel Slope Data of			
Components	Pakis Beach Karawang Sand	Natural forest Universitas Indonesia's soil	Department Metallurgical and Materials Engineer- ing soil
<b>Ecorr, Calc (<i>mV</i>)</b>	-718.960	-739.410	-736.000
<b>icorr (<math>\mu A/m^2</math>)</b>	2.2478	0.28683	0.0061759
<b>Corrate (mm/yr)</b>	0.02611	0.00333	0.00007

On day 0, carbon steel buried in Pakis Beach Karawang Sand exhibited the highest corrosion current density ( $i_{corr}$ ) of  $2.2478 \mu\text{A}/\text{m}^2$  and the greatest corrosion rate of  $0.0261 \text{ mm}/\text{year}$ , indicating a highly corrosive environment. In contrast, the Department Metallurgical and Materials Engineering soil showed the lowest  $i_{corr}$  value ( $0.0061759 \mu\text{A}/\text{m}^2$ ), suggesting minimal corrosion activity.

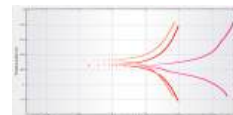
By day 7, the  $i_{corr}$  value for the Pakis Beach Karawang Sand remained the highest at  $2.2362 \mu\text{A}/\text{m}^2$ , while the Department Metallurgical and Materials Engineering soil experienced a notable increase in  $i_{corr}$  to  $0.4061 \mu\text{A}/\text{m}^2$ . Nevertheless, the highest corrosion rate was still observed in the Pakis Beach Karawang Sand ( $0.02598 \text{ mm}/\text{year}$ ).

On day 14, the  $i_{corr}$  of the Pakis Beach Karawang Sand increased significantly to  $3.2244 \mu\text{A}/\text{m}^2$ . Meanwhile, the  $i_{corr}$  of the Natural Forest Universitas Indonesia's soil decreased, likely due to the formation of a protective rust layer. Interestingly, the highest corrosion rate at this stage shifted to the Department Metallurgical and Materials Engineering soil, reaching  $0.00553 \text{ mm}/\text{year}$ .

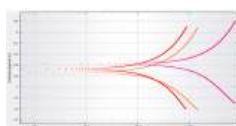
Finally, on day 21, the Pakis Beach Karawang Sand again recorded the highest  $i_{corr}$  and corrosion rate, with values of  $4.1246 \mu\text{A}/\text{m}^2$  and  $0.04792 \text{ mm}/\text{year}$ , respectively, confirming that it remained the most corrosive environment compared to the Natural Forest Universitas Indonesia's soil and the Department Metallurgical and Materials Engineering soil.



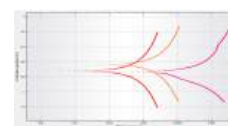
(a) Day 0 Linear Polarization Test Results, Pakis Beach Karawang Sand, Natural forest Universitas Indonesia's soil, and Department Metallurgical and Materials Engineering soil



(b) Day 7 Linear Polarization Test Results, Pakis Beach Karawang Sand, Natural forest Universitas Indonesia's soil, and Department Metallurgical and Materials Engineering soil



(c) Day 14 Linear Polarization Test Results, Pakis Beach Karawang Sand, Natural forest Universitas Indonesia's soil, and Department Metallurgical and Materials Engineering soil



(d) Day 21 Linear Polarization Test Results, Pakis Beach Karawang Sand, Natural forest Universitas Indonesia's soil, and Department Metallurgical and Materials Engineering soil

**Figure 4.** Linear Polarization Time Range Test Results



### 3.2.3 Electrochemical Impedance Spectroscopy Method (EIS)

**Table 7.** Day 0 EIS Testing Data and Results

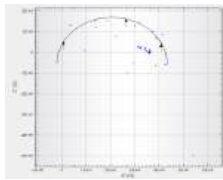
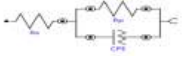
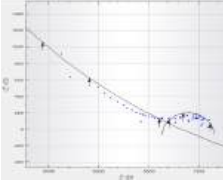
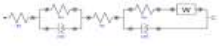
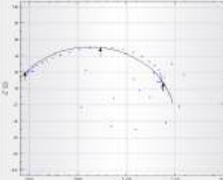
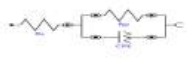
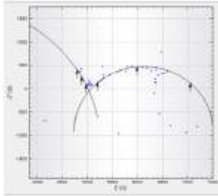
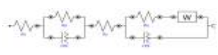
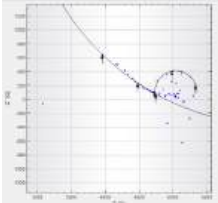
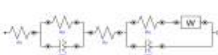
Soil Type	Electrochemical-fit Plot	Equivalent Circuit Model	EIS Data Values
Department Metallurgical and Materials Engineering soil			Chi-square ( $\chi^2$ ) = 7.3716  FIT 1 $R_s = -14.280 \text{ ohm}$ $R_p = 439.640,11 \text{ ohm}$ $CPE Y_0 = 39.1910 \text{ mF}$ $CPE N = 0.99718$
Natural forest Universitas Indonesia's soil			Chi-square ( $\chi^2$ ) = 0.01265  FIT 1 $R_s = 1.660 \text{ ohm}$ $R_p = 5.220,34 \text{ ohm}$ $CPE Y_0 = 9.930 \text{ mF}$ $CPE N = 0.99675$  FIT 2 $R_s = 6.604 \text{ ohm}$ $R_p = 501,94 \text{ ohm}$ $CPE Y_0 = 31.7080 \text{ mF}$ $CPE N = 0.99733$ $Y_0 W = 1.10 \text{ mho}$
Pakis Beach Karawang Sand			Chi-square ( $\chi^2$ ) = 0.0143  FIT 1 $R_s = 158,400 \text{ ohm}$ $R_p = 15.745,13 \text{ ohm}$ $CPE Y_0 = 14.269 \text{ mF}$ $CPE N = 0.9952$

Table 7 shows that differences in resistance mechanisms among the three soil types are indicated by variations in curve shapes, with the Natural Forest Universitas Indonesia's soil displaying two reaction mechanisms characterized by a double semicircle and the presence of a Warburg element. The polarization resistance ( $R_p$ ) values reflect the resistance of the electrolyte medium to corrosion, where the

Department Metallurgical and Materials Engineering soil exhibits the highest resistance, while the Natural Forest Universitas Indonesia's soil and Pakis Beach Karawang Sand are more susceptible to corrosion due to the presence of aggressive ions and their specific chemical compositions.

The constant phase element (CPE)  $Y_0$  values indicate the charge storage capacity of the electrode, with the Department Metallurgical and Materials Engineering soil showing the greatest capacity. In contrast, the Natural Forest Universitas Indonesia's soil and Pakis Beach Karawang Sand demonstrate more limited charge storage capacities, influenced by environmental factors and ion diffusion characteristics. It is also observed that there is a difference in the trends between the polarization method and the EIS test results in evaluating the corrosion resistance of the different soil types.

**Table 8.** Day 7 EIS Testing Data and Results

Soil Type	Electrochemical-fit Plot	Equivalent Circuit Model	EIS Data Values
Department Metallurgical and Materials Engineering soil			Chi-square ( $\chi^2$ ) = 0.4978  FIT 1 Rs = -634.57k ohm Rp = 5.640,00 ohm CPE Y0 = 1.035 mF CPE N = 0.99541  FIT 2 Rs = 5.070 ohm Rp = 2.090,00 ohm CPE Y0 = 11.176 mF CPE N = 0.99198 Y0 W = 0.9 mho
Natural forest Universitas Indonesia's soil			Chi-square ( $\chi^2$ ) = 0.38014  FIT 1 Rs = 4.900 ohm Rp = 3.190,00 ohm CPE Y0 = 187.210 mF CPE N = 0.99234  FIT 2 Rs = 4.74 k ohm Rp = 586,20 ohm

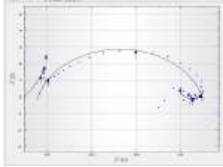
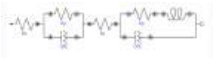
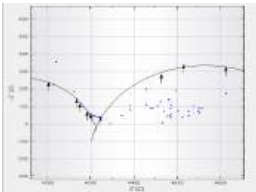
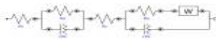
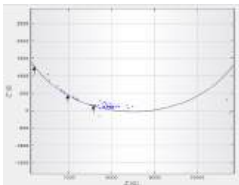
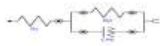
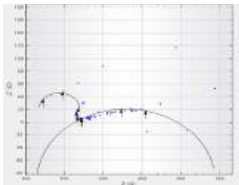
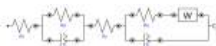
			CPE $Y_0$ = 365.120 mF CPE N = 0.99169 $Y_0 W$ = 90 mho
Pakis Beach Karawang Sand			Chi-square ( $\chi^2$ ) = 0.00340  FIT 1 $R_s$ = 73,054 ohm $R_p$ = 5,86 ohm CPE $Y_0$ = -55.8080 mF CPE N = 0.99776  FIT 2 $R_s$ = 79,580 ohm $R_p$ = 7,36 ohm CPE $Y_0$ = 30.482 mF CPE N = 0.99728 $L$ = 39.5 $\mu$ H

Table 8 shows that on the 7th day of testing, the corrosion mechanisms in all three soil types involved a combination of charge transfer and mass transfer processes, as indicated by the presence of double semicircles in the impedance curves. The polarization resistance ( $R_p$ ) values represent the resistance to electrochemical reactions, where the Natural Forest Universitas Indonesia's soil exhibits the lowest  $R_p$  value, suggesting that charge transfer and mass transfer processes occur more rapidly.

The Warburg and inductance values reflect differences in ion diffusion mechanisms among the soil types. The Department Metallurgical and Materials Engineering soil demonstrates easier ion diffusion, while the Natural Forest Universitas Indonesia's soil shows higher diffusion resistance. Meanwhile, the Pakis Beach Karawang Sand displays an ion inertia phenomenon that does not significantly impact the corrosion rate.

The highest constant phase element (CPE)  $Y_0$  value is found in the Natural Forest Universitas Indonesia's soil, indicating a higher level of reactivity or charge storage capacity compared to the Department Metallurgical and Materials Engineering soil and the Pakis Beach Karawang Sand. The phase-shift values (CPE n) close to 1 suggest that the capacitive behavior is near ideal. Additionally, the corrosion resistance test results on the 7th day show differing trends between the EIS and linear polarization methods in evaluating the corrosion resistance of the different soil types

**Table 9.** Day 14 EIS Testing Data and Results

Soil Type	Electrochemical-fit Plot	Equivalent Circuit Model	EIS Data Values
Department Metallurgical and Materials Engineering soil			<p>Chi-square (<math>\chi^2</math>) = 0.0572</p> <p>FIT 1</p> <p><math>R_s = 3.487,2 \text{ ohm}</math></p> <p><math>R_p = 730,20 \text{ ohm}</math></p> <p><math>CPE Y_0 = -2.24200 \text{ mF}</math></p> <p><math>CPE N = 0.9966</math></p> <p>FIT 2</p> <p><math>R_s = 4.230 \text{ ohm}</math></p> <p><math>R_p = 996,49 \text{ ohm}</math></p> <p><math>CPE Y_0 = 58.6240 \text{ mF}</math></p> <p><math>CPE N = 0.9957</math></p> <p><math>Y_0 W = 1.15 \times 10^{11} \text{ mho}</math></p> <p><math>Y_0 W = 0,00000842 \text{ Mho}</math></p>
Natural forest Universitas In-donesia's soil			<p>Chi-square (<math>\chi^2</math>) = 0.17635</p> <p>FIT 1</p> <p><math>R_s = 6.1250 \text{ ohm}</math></p> <p><math>R_p = 2.108,00 \text{ ohm}</math></p> <p><math>CPE Y_0 = 109 \text{ mF}</math></p> <p><math>CPE N = 0.99710</math></p>
Pakis Beach Karawang Sand			<p>Chi-square (<math>\chi^2</math>) = 1.5574</p> <p>FIT 1</p> <p><math>R_s = 131,550 \text{ ohm}</math></p> <p><math>R_p = 23,71 \text{ ohm}</math></p> <p><math>CPE Y_0 = 525.630 \text{ mF}</math></p> <p><math>CPE N = 0.98811</math></p> <p>FIT 2</p> <p><math>R_s = 162,090 \text{ ohm}</math></p> <p><math>R_p = 171,85 \text{ ohm}</math></p> <p><math>CPE Y_0 = 628.070 \text{ mF}</math></p>

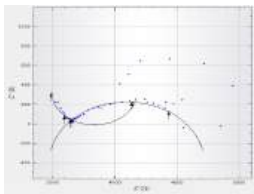
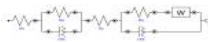
			CPE N = 0.98972 Y0 W = 0,00000842 Mho
--	--	--	--

Table 9 shows that on the 14th day of testing, differences in the shapes of the curves and equivalent circuits were observed, indicating changes in the charge transfer mechanisms in each type of soil used as the electrolyte medium. The polarization resistance ( $R_p$ ) value reflects the resistance of the electrolyte medium to electrochemical reactions, with Pakis Beach Karawang Sand exhibiting the lowest  $R_p$  value, indicating its more corrosive nature compared to the Department Metallurgical and Materials Engineering soil and the Natural Forest Universitas Indonesia's soil.

The Warburg impedance ( $Y_0$ ) value represents the ion diffusion resistance, where Pakis Beach Karawang Sand shows high diffusion resistance, thus inhibiting ion movement. In contrast, the Department Metallurgical and Materials Engineering soil displays lower diffusion resistance, allowing corrosive ions to move more easily and thereby accelerating the corrosion rate. The highest constant phase element (CPE)  $Y_0$  values were also found in the Pakis Beach Karawang Sand, indicating greater charge storage capacity of the electrode and a higher degree of heterogeneity and irregularity in current distribution, which facilitates diffusion processes.

Overall, the results show that the capacitive behavior of the system approaches ideal conditions. The corrosion resistance of carbon steel is the lowest when buried in Pakis Beach Karawang Sand, followed by the Department Metallurgical and Materials Engineering soil, while the Natural Forest Universitas Indonesia's soil provides the best corrosion resistance, in accordance with the electrolyte characteristics of each soil type.

**Table 10.** Day 21 EIS Testing Data and Results

Soil Type	Electrochemical-fit Plot	Equivalent Circuit Model	EIS Data Values
Department Metallurgical and Materials Engineering soil			Chi-square ( $\chi^2$ ) = 0.13673  FIT 1 $R_s$ = 3.750 ohm $R_p$ = 166,29 ohm CPE $Y_0$ = -36.791 mF CPE N = 0.98111  FIT 2 $R_s$ = 3.610 ohm $R_p$ = 956,80 ohm CPE $Y_0$ = 12.689 mF CPE N = 0.99231 $Y_0 W$ = 1,3 Mho

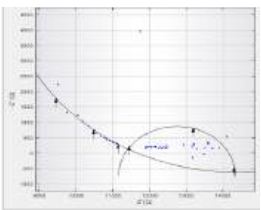
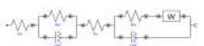
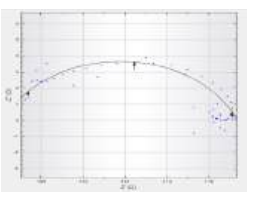

Natural forest Universitas In- donesia's soil			<p>Chi-square (<math>\chi^2</math>) = 0.26339</p> <p>FIT 1</p> <p><math>R_s = 4.820 \text{ ohm}</math></p> <p><math>R_p = 6.820,00 \text{ ohm}</math></p> <p><math>CPE Y_0 = 582.270 \text{ mF}</math></p> <p><math>CPE N = 0.99420</math></p> <p>FIT 2</p> <p><math>R_s = 11.330 \text{ ohm}</math></p> <p><math>R_p = 2.820,11 \text{ ohm}</math></p> <p><math>CPE Y_0 = 104.570 \text{ mF}</math></p> <p><math>CPE N = 0.99479</math></p> <p><math>Y_0 W = 7,8 \text{ Mho}</math></p>
Pakis Beach Karawang Sand			<p>Chi-square (<math>\chi^2</math>) = 0.026067</p> <p>FIT 1</p> <p><math>R_s = 106,190 \text{ ohm}</math></p> <p><math>R_p = 11,16 \text{ ohm}</math></p> <p><math>CPE Y_0 = 5.588 \text{ mF}</math></p> <p><math>CPE N = 0.99547</math></p>

Table 10 shows differences in the mechanisms of charge transfer and electrochemical reactions on the 21st day of testing, as indicated by changes in the curve shapes and the equivalent circuits for different types of soil used as the electrolyte medium. The polarization resistance ( $R_p$ ) value indicates the resistance to electrochemical reactions, where Pakis Beach Karawang Sand exhibits the lowest  $R_p$  value, making it the most corrosive medium. Meanwhile, the Department Metallurgical and Materials Engineering soil shows a decrease in  $R_p$  on day 21, rendering it more corrosive than the Natural Forest Universitas Indonesia's soil.

The Warburg impedance  $Y_0$  value indicates that the Natural Forest Universitas Indonesia's soil has higher diffusion resistance, meaning that ions experience greater resistance to movement. The constant phase element (CPE)  $Y_0$  value reflects the electrode's charge storage capacity, with Pakis Beach Karawang Sand showing the highest CPE magnitude, indicating a greater charge storage capability compared to the Natural Forest Universitas Indonesia's soil. Meanwhile, the CPE  $n$  value suggests that the capacitive behavior of the system remains close to an ideal capacitor.

On the 21st day, the EIS and linear polarization method results show a similar trend: carbon steel embedded in Pakis Beach Karawang Sand has the lowest resistance, while carbon steel in the Natural Forest Universitas Indonesia's soil demonstrates the

highest resistance. These findings are consistent with the resistivity and moisture content characteristics of each soil type.

### 3.3 Comparison of Carbon Steel Corrosion Resistance Research Data

**Table 11.** Comparison of Carbon Steel Corrosion Resistance Research Data

Soil Name	pH	Moisture Content (%)	Resistivity ( $\Omega\cdot\text{cm}$ )	Corrosion Rate (mpy)	icorr ( $\mu\text{A}/\text{m}^2$ )	Polarization Resistance ( $\Omega$ )
Department Metallurgical and Materials Engineering soil	6,6	65	4.577,17	20,52	0,45	956,80
Natural forest Universitas Indonesia's soil	5,9	51	21.772,70	16,89	0,11	2.820,11
Pakis Beach Karawang Sand	5,2	87	59,03	42,57	4,12	11,16

Table 11 shows the comparison of the three evaluation methods used as parameters of corrosion resistance of steel in the soil, namely corrosion rate, current density, and polarization resistance. The relationship between the moisture content and the resistivity value of the three soil variations shows the same trend: as the moisture content increases, the soil resistivity value also increases.

The results of the three evaluation methods show the same overall trend, namely that Pakis Beach Karawang Sand acts as a more corrosive electrolyte medium compared to the Department Metallurgical and Materials Engineering soil or the Natural Forest Universitas Indonesia's soil. This is evidenced by Pakis Beach Karawang Sand having the highest corrosion rate of 42.57 mpy, the highest current density (icorr) of 4.12  $\mu\text{A}/\text{m}^2$ , the lowest polarization resistance of 11.16  $\Omega$ , and the lowest resistivity of 59.03  $\Omega\cdot\text{cm}$  with 87% moisture content.

Meanwhile, the Natural Forest Universitas Indonesia's soil provided better corrosion resistance results across all three evaluation methods. Carbon steel buried in the Natural Forest Universitas Indonesia's soil exhibited the lowest corrosion rate of 16.89 mpy, indicating less mass loss compared to the other two soil variations. The Department Metallurgical and Materials Engineering soil showed the lowest current density value at 0.11  $\mu\text{A}/\text{m}^2$ , suggesting that the amount of current able to pass through the soil was much less than in the other two soil variations. This finding is further supported by its high polarization resistance value of 2,820.11  $\Omega$ . The polarization

resistance value reflects the soil's ability to resist electrical conduction when in contact with the carbon steel surface area. The polarization resistance and resistivity values for the Natural Forest Universitas Indonesia's soil show a consistently higher trend compared to the other two soil variations, indicating a smaller likelihood of corrosion.

**Acknowledgments:** The comments and suggestions from all the editors and reviewers are very much appreciated.

**Conflicts of Interest:** The authors declare no conflict of interest.

## References

1. AB&I Testing, "MAOP," AB&I Testing. [Online]. Available: <https://www.abitesting.com/maop>. [Accessed: Dec. 14, 2024].
2. AB&I Testing, "Accurate determination of the maximum allowable operating pressure (MAOP) of oil and gas pipelines," AB&I Testing. [Online]. Available: <https://www.abitesting.com/accurate-determination-of-the-maximum-allowable-operating-pressure-maop-of-oil-and-gas-pipelines>. [Accessed: Dec. 14, 2024].
3. D. A. Wibowo and A. Ghofur, "Pengaruh Kadar Salinitas Air Terhadap Laju Korosi Baja St 60," *Jtam Rotary*, 2021, vol. 3, no. 2, pp. 145–158, doi: 10.20527/jtam\_rotary.v3i2.4136.
4. A. Solehudin, E. Permana, and H. Salam, "Determination of Soil Corrosion Potential for Gas Pipeline Cathodic Protection System Planning," *Journal of Physics: Conference Series*, 2022, vol. 2243, no. 1, p. 012070. doi: 10.1088/1742-6596/2243/1/012070.
5. F. A. Nuñez Pérez, "Analisis Elektrokimia dari Ketahanan Korosi Baja Annealed Berlapis Mangan: Studi Chronoamperometrik dan Voltametrik," *AppliedChem*, 2024, vol. 4, no. 4, hal. 367–383. doi: 10.3390/appliedchem4040023
6. I. P. Okokpujie, E. S. Odudu, T. M. Azeez, A. O. Onokwai, F. O. Ahmadu, dan A. O. M. Adeoye, "Studi Perilaku Material Baja Karbon Tinggi dalam Media Pengerjaan Panas dan Dingin: Tinjauan," *E3S Web of Conferences*, 2023, vol. 430, hal. 01210. doi: 10.1051/e3sconf/202343001210.
7. N. Chaubey, Savita, A. Qurashi, D.S. Chauhan, M.A. Qurashi, *Frontiers and advances in green and sustainable inhibitors for corrosion applications: a critical review*, *J. Mol. Liq.* 321 (2021), 114385, <https://doi.org/10.1016/j.molliq.2020.114385>.
8. I. P. Okokpujie, E. S. Odudu, T. M. Azeez, A. O. Onokwai, F. O. Ahmadu, dan A. O. M. Adeoye, "Studi Perilaku Material Baja Karbon Tinggi dalam Media Pengerjaan Panas dan Dingin: Tinjauan," *E3S Web of Conferences*, 2023, vol. 430, hal. 01210. doi: 10.1051/e3sconf/202343001210.
9. SSPC: The Society for Protective Coatings, *SSPC-VIS 2: Standard Method of Evaluating Degree of Rusting on Painted Steel Surfaces*, 2008. [Online]. Available: <https://store.ampp.org/sspc-vis-2>. [Accessed: Dec. 28, 2024].
10. BorTec Group, "Carbon Steel," *BorTec Group Glossary*, [Online]. Available: <https://bortec-group.com/glossary/carbon-steel/>. [Accessed: 21-Dec-2024].
11. S.Sundjono dan S. Saefudin, "Pengaruh Temperatur dan pH Air Sadah Kalsium Sulfat terhadap Korosi pada Baja Karbon," *Metalurgi*, 2018., vol. 29, no. 1, hal. 41–50. doi: 10.14203/metalurgi.v29i1.270.
12. H. K. Anggoro, *Analisis Korosi pada Tanah dengan Variasi Kelembaban Menggunakan Baja Karbon*, Tesis, Institut Teknologi Sepuluh Nopember, Surabaya, Indonesia, 2018. Tersedia: [https://repository.its.ac.id/63323/1/1112201016-Master\\_Theses.pdf](https://repository.its.ac.id/63323/1/1112201016-Master_Theses.pdf), diakses: 13 Des. 2024.



13. N. Subekti, "Pengaruh Tegangan: Tinjauan Literatur," Skripsi/Tesis, Universitas Indonesia, 2019. Tersedia: <https://lib.ui.ac.id/file?file=digital%2F131653-T+27598-Pengaruh+tegangan-Tinjauan+literatur.pdf>, diakses: 13 Des. 2024.
14. P. Parjono, Y. Mekiuw, dan K. Wahi, "Evaluasi pH dan Aluminium (Al<sup>3+</sup>) dalam Tanah di Kampung Erambu Distrik Sota Kabupaten Merauke," MAEF-J, 2018, vol. 4, no. 2, pp. 77–82, Apr. <https://ejournal.unmus.ac.id/index.php/ae/index>.
15. C. E. Sanders et al., "Restoration of soil microbial communities across a chronosequence of timber harvesting in temperate forest soils," PLoS One, 2022, vol. 17, no. 2, e0263456, doi: 10.1371/journal.pone.0263456.
16. A. Shahid et al., "Effect of different soil amendments on soil buffering capacity," PLoS One, 2022, vol. 17, no. 2, e0263456, doi: 10.1371/journal.pone.0263456.
17. "Soil pH," Soil Quality Knowledge Base, diakses: 13 Des. 2024. Tersedia: <https://soilqualityknowledgebase.org.au/soil-ph/>.

Article

# Analysis of the Effect of RIB Width and Channel Depth Design Modifications on CFD-Based Parallel Type Bipolar Plates for the Application of Proton Exchange Membrane Fuel Cell Stack Singles

Mochammad Tendi Noer Ramadhan<sup>1,\*</sup>, Amar Banu Mukhlisin<sup>2</sup>, Belyamin<sup>3</sup>, Radhi Maladzi<sup>3</sup>, Abdul Azis Abdillah<sup>4</sup>

<sup>1</sup> Applied Master of Manufacturing Technology Engineering, Mechanical Engineering, Jakarta State Polytechnic

<sup>2</sup> Applied Bachelor of Manufacturing Technology Engineering, Mechanical Engineering, Jakarta State Polytechnic

<sup>3</sup> Mechanical Engineering, Jakarta State Polytechnic

<sup>4</sup> The School of Engineering, mechanical engineering department. University of Birmingham

\* Correspondence: mohammadtendinoerramadhan.tm23@stu.pnj.ac.id

**Citation:** Ramadhan, M. T. N. Mukhlisin, A. B., Benyamin, Maladzi. R., Abdillah, A. A. (2025). Analysis of the Effect of RIB Width and Channel Depth Design Modifications on CFD-Based Parallel Type Bipolar Plates for the Application of Proton Exchange Membrane Fuel Cell Stack Singles. Recent in Engineering Science and Technology, 3(02), 35–49. Retrieved from <https://www.mbi-journals.com/index.php/riestech/article/view/107>

Academic Editor: Vika Rizkia

Received: 20 April 2025

Accepted: 29 April 2025

Published: 30 April 2025

**Publisher's Note:** MBI stays neutral with regard to jurisdictional claims in published maps and institutional affiliations.



**Copyright:** © 2025 by the authors. Licensee MBI, Jakarta, Indonesia. This article is an open access article distributed under MBI license (<https://mbi-journals.com/licenses/by/4.0/>).

**Abstract:** The use of large amounts of fossil fuels can pollute the air with significant amounts of carbon monoxide. Proton Exchange Membrane Fuel Cell (PEMFC) is an attractive alternative because it is able to generate high current with low working temperature, fast start-up time, no pollution, and good durability. In PEMFC systems, bipolar plates are one of the main and important components. This component facilitates the reactants to flow through the designed channel. This study aims to modify the parallel-type flow field design on the bipolar plate using CFD simulation in ANSYS, in order to improve the performance of PEMFC. While flowing through the bipolar plate, the reactants diffuse through the gas diffusion layer, thus connecting with the catalyst layer to generate protons and electrons in the anode and water and heat in the cathode through chemical reactions. The results of the study show that the variation of rib width and channel depth has a significant effect on the pressure distribution and hydrogen flow distribution. These findings can contribute to the improvement of flow distribution efficiency and pressure reduction.

**Keywords:** PEMFC; Bipolar Plate; Rib Width; Channel Depth; Computation Fluid Dynamics (CFD)

## 1. Introduction

Fuel cells, especially Proton Exchange Membrane Fuel Cells (PEMFC), are increasing in popularity in line with the global challenge of reducing greenhouse gas emissions and dependence on fossil fuels. PEMFCs offer an efficient and environmentally friendly energy solution, with great potential for integration into a wide range of applications, from transportation to large-scale energy storage. The technology is capable of generating electricity at high efficiency, even under flexible operating conditions, making it an attractive option for a clean energy future. Furthermore, in the context of the accelerating global energy transition, development and innovation in fuel cell design and optimization are

critical to ensure that the technology can achieve better performance, lower costs, and larger scale production[1].

PEMFC can convert chemical energy from hydrogen into electricity with high efficiency and low environmental impact. PEMFCs can be used for a variety of purposes, such as vehicle power sources, portable power, and backup generators. In addition, they have many advantages, such as long-term stability, high energy density, and low operating temperature. Although the cost of fuel cells challenges commercialization, research continues to improve the efficiency, durability, and cost of the membranes. This makes PEMFCs a promising source of clean energy in the future[2].

Bipolar plates must have certain characteristics, such as good mechanical strength, corrosion resistance, and high electrical conductivity. Graphite, metals, such as stainless steel and titanium, and composites consisting of polymers and conductive fillers, such as carbon black or graphite, are very commonly used. The specific application and environment in which the PEMFC is used greatly influence the choice of materials[3].

Computational Fluid Dynamics (CFD) is a technique used to simulate fluid flow numerically. By replacing differential equations with numbers, CFD allows for the analysis of complex systems and aids in the visualization of fluid behavior and interactions with solid boundaries. This technique has been used in many fields, such as determining channel rates, architecture, turbines, and automotive design, and will continue to evolve as technology advances[4].

The journal written by Agyekum et al. (2022) PEMFC is updated with a focus on performance improvement, material characterization, and publication growth. Efforts are made to increase the voltage generated and reduce the weight of the cell through innovative designs of flow plates, membranes, and catalysts. In addition, research focuses on the development of membranes with improved ionic conductivity and thermal stability, and has recorded significant growth in PEMFC research publications with an average annual growth rate of 19.35% since 2000, indicating increasing interest in the application of this technology to reduce carbon footprints in various industrial sectors[5].

## 2. Materials and Experiment Methods

Type of experimental research with the aim of finding correlations between variables. Using the Computer Fluid Dynamics (CFD) approach by simulating parameters through ANSYS software to obtain optimal results from parameter simulations on ANSYS software and direct field trials. The quantitative research method is research based on the philosophy of positivism, which is used to research natural object conditions (as opposed to experiments) where this research is a key instrument, data sampling is carried out purposively and snowball, data collection techniques with triangulation (combination, data analysis is inductive/qualitative)[6].

The object of this study is the bipolar plate in the PEMFC system, the bipolar plate is one of the main and important components. However, the parallel groove pattern has a

disadvantage, namely producing water droplets and the serpentine groove pattern with four channels has been proven to improve cell performance and reduce the occurrence of water droplets. The width and height of the channel affect the performance of the PEMFC. Water discharge increases as the channel height decreases, but cell performance also decreases. Cell performance decreases as the channel width increases because lower gas velocities result in less water discharge. This shows better cell performance in smaller channel cross-sectional areas, because it has a higher gas velocity[7].

The sampling method is carried out through CFD simulations carried out 9 times from 9 alternative designs. Then, it will be analyzed based on pressure drop and velocity and one of the most optimal designs will be obtained. In this study uses secondary data. Secondary data is data that has been collected for purposes other than solving the problem being faced from literature, articles, journals, and websites related to the research subject. Statistical analysis is used in this technique to analyze the data and identify relationships between variables. In the case of flow field design in PEMFC, statistical analysis can be used to evaluate the impact of flow line design modifications on the performance of the material. This includes the impact on pressure, flow, and temperature[8].

This study uses a Simulation Method with modeling and algorithms to predict system performance and analyze the impact of design modifications on PEMFC performance. Simulation can be used to evaluate the impact of design modifications on the flow path, pressure, and temperature of the PEMFC. This study uses a CFD approach to simulate hydrogen flow performance. CFD simulations are carried out using ANSYS software. The ANSYS software used in this study is ANSYS 2021 R2. Before performing the simulation, there are several settings for adjustment. Here are the steps to perform a CFD simulation:

1. Run the ANSYS software, namely Workbench 2021 R2.
2. In the Toolbox, double click on Fluid Flow (Fluent).
3. In the Fluid Flow (Fluent) table, there are Geometry, Mesh, Setup, Solution, and Results.
4. Geometry:
  - Right-click on Geometry and select Import Geometry.
  - Then, browse and select the PFF modification design to be simulated (p1-p9).
5. Mesh:
  - Right-click on Mesh and select Edit
  - In the Detail of "Mesh" section Defaults, change the Element Order to Program Controlled and the Element Size to 0.1 mm. The changes of both elements are to determine the accuracy and efficiency of the numerical simulation.
  - In the Quality section, change the Mesh Metric to Skewness which aims to evaluate the quality of the mesh. This metric is very 27 important because the quality of the mesh greatly affects the accuracy and stability of the numerical solution in CFD simulations.
  - On the Mesh Tab, select Face Meshing
  - Select Mesh type then select Inflation and enter the boundary effect as follows

- Layer thickness 0.01
- Max layer
- Expansion ratio 10: 1.2
- Then create a name for each part such as inlet, walls, and electrode
- Go to Setup
- In the Fluent software settings (Fluent Launcher), change the Solver Processes value to 2 and click Start. These settings affect the performance of the ongoing simulation.
- In the Fluent software Setup section, there are several settings, namely:
  - Models
  - Energy (On)
  - Species Transport (On)
- Boundary condition:
  - Inlet velocity 10 m/s
- Initialization
- Run Calculation

Analysis of the influence of parameters such as rib width and channel depth is very important to optimize the design of parallel flow fields in PEMFCs. Minitab is a statistical program that can be used to analyze data and measure how certain parameters affect fuel cell performance. In this study 28, two Channel Width and Channel Depth were used in the 3×3 factorial design method. Each factor has three levels with different values. Therefore, it can be classified as a variable that is not affected by these factors. The following table shows the 3×3 factorial design method:

**Table 1.** Factorial Design of 3x3 Rib Width and Channel Depth

	0.6	0.8	1
1.1	1.1 and 0.6 (p1)	1.1 and 0.8 (p1)	1.1 and 1 (p1)
1.3	1.3 and 0.6 (p2)	1.3 and 0.8 (p2)	1.3 and 1 (p2)
1.5	1.5 and 0.6 (p2)	1.5 and 0.8 (p2)	1.5 and 1 (p2)

### 3. Results and Discussion

Subheadings may be used to divide this section. It should provide a concise and precise description of the experimental results, their interpretation, and possible experimental conclusions. The authors should discuss the findings and how they can be interpreted considering previous research and the working hypotheses. The findings and implications should be discussed in the broadest possible context. Future research directions may be highlighted as well.

### 3.1. Design Results p1-p9

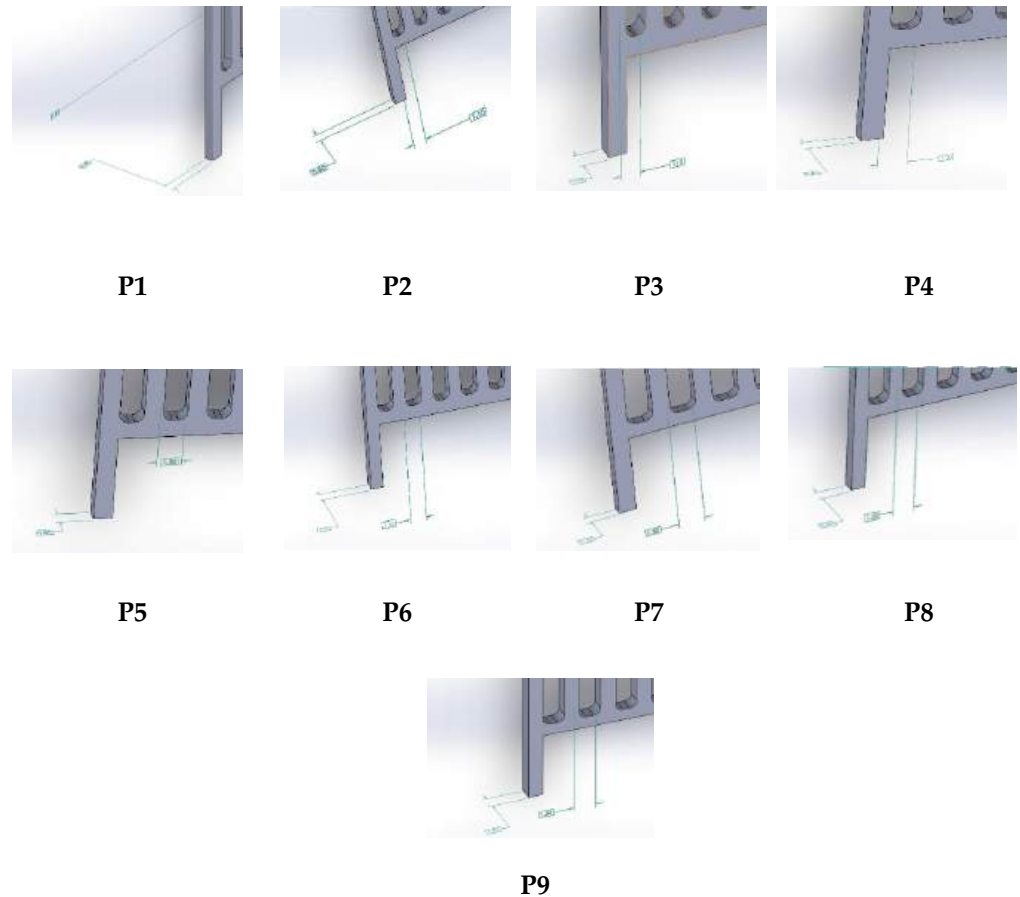


**Figure 1.** Result of Design P1-P9

Based on Figure 1, the design shown is the result of the application of the 3×3 factorial design method, resulting in 9 combinations or 9 alternative designs by varying the Rib Width and Channel Depth. By setting the Channel Width to 1mm, but the length of the channel from the inlet to the outlet varies. This difference is caused by the variation in the rib width in each design. This variation provides an opportunity to evaluate the performance of each design under different conditions, so that the most optimal design can be selected for the desired application.

Rib width and channel depth greatly affect the pressure drop and flow velocity in Proton Exchange Membrane Fuel Cell (PEMFC) design. Increasing rib width reduces the flow cross-sectional area, causing increased local flow velocity and pressure drop due to higher wall friction. Conversely, increasing channel depth enlarges the space for flow, which reduces flow resistance and lowers pressure drop.

**Table 2.** Alternative Design Parameters.

<b>Type</b>	<b>Rib Width (mm)</b>	<b>Channel Depth (mm)</b>	<b>Channel Width (mm)</b>	<b>Fillet Radius (mm)</b>
P1	1.1	0.6	1	0.5
P2	1.1	0.8	1	0.5
P3	1.1	1	1	0.5
P4	1.3	0.6	1	0.5
P5	1.3	0.8	1	0.5
P6	1.3	1	1	0.5
P7	1.5	0.6	1	0.5
P8	1.5	0.8	1	0.5
P9	1.5	1	1	0.5

But can reduce the flow velocity due to a more even flow distribution. Overall, the right combination of rib width and channel depth is very important to optimize PEMFC performance, because both directly affect the flow distribution and system efficiency[9].

### 3.1.1. Pressure Drop Calculation

Will be compared with the simulation process in ANSYS software, which will automatically calculate the pressure drop value generated in the geometry model that has been entered. The fluent module will be used for simulation to evaluate the fluid flow that occurs. In the calculation process, reference values are needed as a basis for normal conditions that are entered manually. Reference values include gravity of 9.81 m/s<sup>2</sup>, pressure of 1 atm, fluid viscosity of 0.8411 (hydrogen gas), and operating temperature of 300K. This process is carried out with 200 iterations until convergent results are obtained. There are a number of data. There are several research variable data that will be used as parameters in calculations with different geometry models as shown in Table 2 The parameters used consist of 3 variations of channel depth and 3 rib width, and this simulation is performed 9 times according to the existing parameters. The researchers used the serpentine line channel type to change 3 different depths and channel lengths[10]. This study uses the parallel channel type because, according to Spiegel's research (2008), the serpentine channel type has a greater pressure drop compared to the parallel flow type[11]. The simulation results will be validated manually by performing theoretical calculations to obtain a pressure drop value that is close to the theory or with a small error rate.

### 3.2. Simulation and Analysis Results

The simulation results were created using ANSYS 2021 R2 software. This simulation aims to evaluate the design performance in terms of flow distribution and pressure drop. The results obtained will be analyzed and compared with other alternative designs to assess the effectiveness of the changes made.

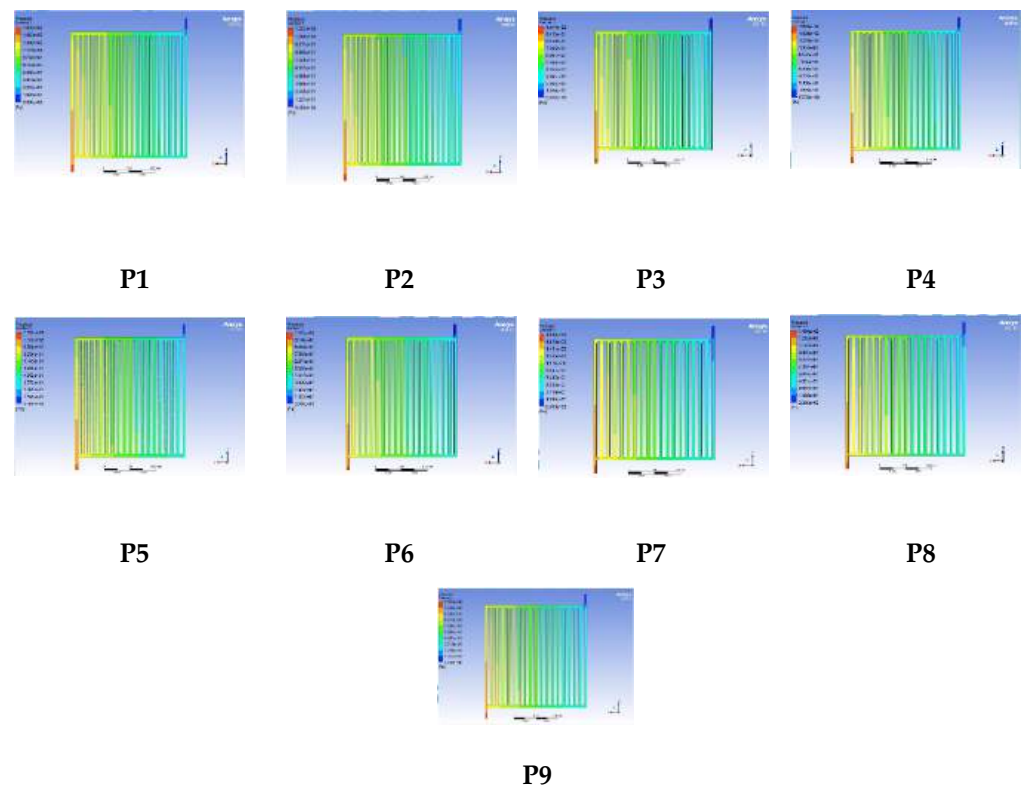


**Figure 2.** Pressure drop simulation result P1-P9

From the simulation data provided, it can be seen that when the Rib Width increases, the pressure drop also increases. This is especially in the comparison between Rib Width 1.1 mm and 1.5 mm for the same Channel Depth:

- At Channel Depth 0.6mm: Increasing Rib Width from 1.1 mm to 1.5 mm causes an increase in pressure drop from 162 Pa to 186 Pa.
- At Channel Depth 1.0 mm: Increasing Rib Width from 1.1 mm to 1.5 mm increases the pressure drop from 102 Pa to 117 Pa. Increasing Rib Width reduces the effective flow area within the channel, which increases the resistance to fluid flow. With a smaller area, the flow becomes more obstructed, thus causing an increase in pressure drop. However, this can also lead to a more even flow distribution along the channel, although with the penalty of increased pressure drop.
- At Rib Width 1.1mm: Increasing Channel Depth from 0.6 mm to 1.0 mm reduces pressure drop from 162 Pa to 102 Pa.
- At Rib Width 1.5mm: Increasing Channel Depth from 0.6 mm to 1.0 mm reduces pressure drop from 186 Pa to 117 Pa.

As channel depth increases, the volume of the flow chamber increases, which reduces the resistance to flow. This results in a decrease in pressure drop because the fluid can flow more easily through the deeper channel.



### 3.2.1. Plot Pressure Factorial Results and Analysis

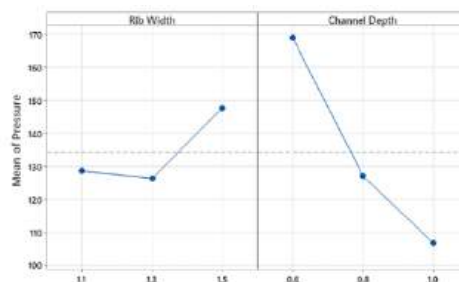


**Figure 3.** Factorial Plot Pressure

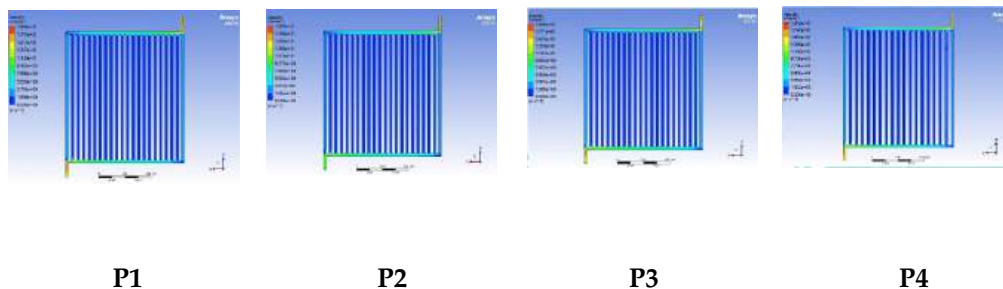
Based on Figure 3 these results show that the difference in Rib Width and Channel Depth factors will greatly affect the pressure drop. At 1.1mm Rib Width the pressure drop rate is relatively low and stable, and for 1.3mm there is a slight decrease in pressure drop compared to 1.1 mm, but it is almost the same. While the Rib Width is 1.5mm Results in a significant increase in pressure drop.

Increased rib width from 1.1 mm to 1.5 mm leads to increased pressure drop. This is due to the decrease in effective flow area when the rib width is larger, increasing fluid flow resistance and cause an increase in pressure drop. At 0.6mm Channel Depth Indicates pressure drop highest, and at 0.8mm there is a significant drop in pressure. Meanwhile, at 1mm the lowest pressure drop can be seen.

The larger the channel depth, the smaller the pressure drop produced. This can be explained by the increased flow volume that allows the fluid to flow more freely, reduce the resistance and pressure required to move the flow through the channel. The conclusion of the plot is that the 1.1 mm and 1.3 mm rib widths produce a lower and more stable pressure drop compared to the 1.5 mm rib width. and Increase channel depth from 0.6 mm to 1.0 mm significantly reduce pressure drop.

### 3.3. Simulation and Velocity Analysis Results

Flow rate distribution is an important parameter in bipolar plate performance analysis in PEMFC. A high flow rate can ensure that the reactants are distributed efficiently to the entire surface of the electrode, increasing the effectiveness of the reaction electrochemical. The results of the simulation using ANSYS show hydrogen flow velocity profile in a parallel flow channel has been modified.



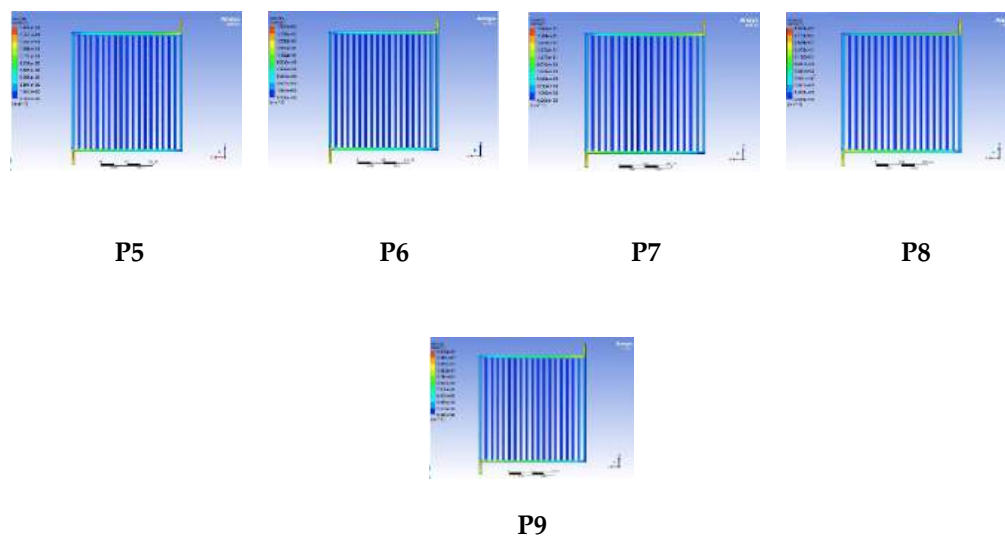


**Figure 4.** Velocity simulation result P1-P9

From the data provided, we can analyze how the Rib changes Width and Channel Depth affect the flow rate within the channel.

#### 1. Effect of Rib Width

At a Rib Width of 1.1mm and a Channel Depth of 0.6mm, the flow speed is 18.9 m/s while at Channel Depth 1mm the flow speed is increased to 19.6 m/s. While at a Rib Width of 1.3mm with Channel Depth 0.6mm flow rate is 19.4 m/s and at Channel Depth 1mm flow speed increased to 19.9 m/s. And at a Rib Width of 1.5mm with a Channel Depth of 0.6mm of flow speed is 19.6 m/s, while with a Channel Depth of 1mm speed The flow increased again to 19.8 m/s. From the simulation data, it shows an increase in ribs width, there is an increase in the flow rate. The following occurs due to the fact that larger rib widths tend to narrow effective area within the channel, which results in increased speed flow to maintain a constant mass flow. However, the change in The flow rate was not very significant between the different rib width variations, suggesting that the rib width had a limited influence at the flow rate in this design.

#### 2. Influence of Channel Depth

At a Rib Width of 1.1mm, an increase in Channel Depth from 0.6 mm to 1.0 mm led to an increase in flow speed from 18.9 m/s to 19.6 m/s produces 0.7 m/s difference increase and achieves a percentage an increase of 3.7%.

Based on the results of the data, Increased channel depth generally increase the flow speed, mainly due to the increase in Channel depth reduces flow resistance. More flow speed high is required to maintain a steady flow of fluid inside deeper channels. Optimal combination of rib width and channel The depth that provides the highest flow speed is found at the rib width 1.3 mm and Channel Depth 1.0 mm, with a flow speed of 19.9 m/s. This indicates that in this design, the channel depth increase has a more significant influence on the flow speed compared to the increased rib width. So that conclusions can be drawn The effect of increasing Channel Depth is more effective in increasing speed flow

compared to Rib Width and Design with a Channel Depth that is larger and larger Rib width can provide excellent performance optimal in terms of flow speed, which is important for efficiency gas transportation in PEMFC.

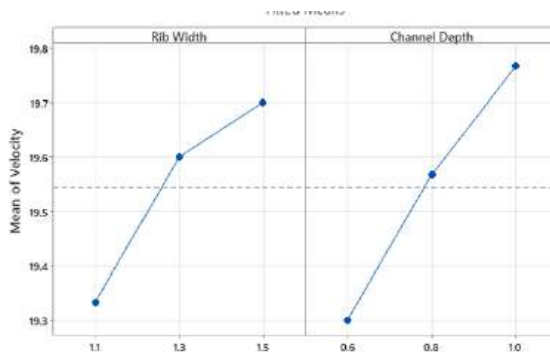


**Figure 5.** Factorial Plot Pressure

Based on Figure 5 the factorial results of the plot shows when the width of the rib increases from 1.1 mm to 1.3 mm, there is a significant increase in flow velocity. However, when the rib width increases from 1.3 mm to 1.5 mm, the increase in velocity becomes more moderate. This shows that increasing the rib width up to 1.3 mm can effectively increase the flow velocity, but further increases have a smaller impact. Meanwhile, the influence of Channel Depth from the graph shows that increasing the channel depth from 0.6 mm to 1.0 mm causes a significant increase in flow velocity. Larger channel depths (from 0.6 mm to 1.0 mm) tend to provide wider flow paths, thereby increasing the flow velocity. Increasing the rib width from 1.1 mm to 1.5 mm shows that the flow velocity increases, but not as much as the influence of channel depth. Larger rib widths reduce the flow path area, which tends to increase velocity, but the impact is not significant after a certain point. On the other hand, increasing the channel depth from 0.6 mm to 1.0 mm causes a greater increase in flow velocity, because the deeper channel volume allows more fluid to flow with lower resistance. The combination of the two shows that channel depth has a dominant effect in increasing flow velocity compared to rib width.

### 3.4. Results of Analysis of Variance (ANOVA)

**Table 3.** Information of Factor.

Factor	Type	Levels	Value
Rib Width (mm)	Fixed	3	1.1 ; 1.3 ; 1.5
Channel Depth (mm)	Fixed	3	0.6 ; 0.8 ; 1

Based on Table 3 shows information about the factors that used for analysis, particularly on experiments involving variations in Rib Width and Channel Depth in the design of parallel flow areas. This information includes two factors, each with three different levels of value. The value is a fixed value if it is categorized as a value remain.

### 3.4.1 ANOVA based on Pressure

**Table 4.** Analysis of Variance by Pressure.

Sources	DF	Adj SS	Adj MS	F-Value	P-Value
Rib Width (mm)	2	821.56	410.78	46.80	0.002
Channel Depth (mm)	2	6062.89	3031.44	345.35	0.000
Error	4	35.11	8.78		
Total	8	6919.56			

The very small P-Value (0.002), far below the significance level of 0.05, indicates that rib width has no significant impact on pressure response, as shown by the ANOVA results shown in Table 4. The F-Value of 46.80 indicates that variations in Rib Width are a contributing component but with no significant effect on the simulated system pressure changes. In addition, Channel Depth has a more significant effect on pressure; has a P-Value of 0.000, which indicates a high level of statistical significance, the F-Value of 356.02 indicates that Channel Depth has a more significant effect on pressure.

**Table 5.** Summary Model by Pressure.

S	R-sq	R-sq (adj)	R-sq (pred)
2.96273	99.49%	98.99%	97.43%

Based on the model summary results in Table 5, this model has proven to be very good at explaining data variations, with an R-sq value reaching 99.49% and an R-sq(adj) of 98.99%. This means that almost all variations in the pressure response can be explained by a model involving channel depth and rib width as factors. In addition, the R-sq(pred) value of 97.43% shows that this model is very effective in predicting pressure for new data. The S value of 2.96273, which is the residual standard deviation, shows that the difference between the observed and predicted values by the model is very small, so the prediction accuracy of this model is very high.

### 3.4.2 ANOVA based on Velocity

**Table 6.** Analysis of Variance.

Sources	DF	Adj SS	Adj MS	F-Value	P-Value
Rib Width (mm)	2	0.2156	0.10778	3.66	0.0125
Channel Depth (mm)	2	0.3289	0.16444	5.58	0.070
Error	4	0.1178	0.02944		
Total	8	0.6622			

Based on the ANOVA results in Table 6, it can be seen that Rib Width has a significant effect on the flow velocity response. This is evidenced by the very small P-Value (0.000), far below the significance limit of 0.05. The F-Value of 3.66 confirms that variation in Rib Width is the main factor that significantly affects the velocity changes in the simulated system. In addition, rib width also has a significant impact on flow velocity, with a P-Value of 0.000, indicating a high level of statistical significance. Although its influence is not as large as the channel width, the F-Value of 356.02 indicates that rib width still provides an important contribution to flow velocity variations.

**Table 7.** Summary Model by Velocity.

S	R-sq	R-sq (adj)	R-sq (pred)
0.171594	82.21%	64.43%	9.6%

Summary Model in Table 7 shows that this model has a very good performance in explaining data variation, with an R-sq value of 82.21% and an R-sq(adj) of 64.43%. This means that almost all variations in speed can be explained by the model that considers rib width and channel depth as factors. However, the R-sq(pred) value of 9.6% indicates that this model is less accurate in predicting speed for new data. In addition, the S value of 0.171594, which is the residual standard deviation, indicates that the difference between the observed value and the predicted value by the model is very small, indicating that the model's prediction is very accurate.

## 3. Conclusions

Based on the variation of rib width and channel depth in the design of parallel bipolar plates in PEMFC, it has a significant effect on the pressure drop  $\epsilon$  (pressure drop) and flow velocity. From this, it can be concluded that:

- Modifications to rib width and channel depth significantly affect hydrogen flow and pressure drop in PEMFC, but channel depth has a greater effect on pressure and velocity compared to rib width. In the development of fuel cell systems for

electric vehicles, modification of rib width and channel depth can be optimized to improve hydrogen flow efficiency. In energy storage applications, as well as in industrial applications requiring high power, modification of the bipolar plate design with deeper channel depth can reduce the pressure required for hydrogen flow.

- b. From the simulation results, the design with a rib width of 1.3 mm and a channel depth of 1 (p6) mm provides the best balance between high flow velocity (19.9 m/s) and low pressure drop (101 Pa), so it can be considered as the most optimal design for single stack PEMFC applications. The bipolar plate design with 1.3 mm rib width and 1 mm channel depth is ideal for applications requiring a balance between high flow rates and low pressure drop, making it an ideal solution for a wide range of fuel cell applications in the automotive, commercial and heavy equipment industries.
- c. The relationship between pressure and channel depth in a Proton Exchange Membrane Fuel Cell (PEMFC) can be summarized as follows is Inverse Relationship, As the channel depth increases, the pressure drop across the channel decreases. This is because a deeper channel provides a larger volume for the fluid to flow through, which reduces flow resistance so increasing the channel depth generally leads to a decrease in pressure drop, facilitating better fluid dynamics within the fuel cell system. And The effect of increasing Channel Depth is more effective in increasing speed flow compared to Rib Width and Design with a Channel Depth that is larger and larger Rib width can provide excellent performance optimal in terms of flow speed, So which is important for efficiency gas transportation in PEMFC.

## References

1. M. M. Tellez-Cruz, J. Escorihuela, O. Solorza-Feria, and V. Compañ, "Proton exchange membrane fuel cells (Pemfcs): Advances and challenges," *Polymers (Basel)*, vol. 13, no. 18, pp. 1–54, 2021, doi: 10.3390/polym13183064.
2. M. Sauermoser, N. Kizilova, B. G. Pollet, and S. Kjelstrup, "Flow Field Patterns for Proton Exchange Membrane Fuel Cells," *Front. Energy Res.*, vol. 8, no. February, pp. 1–20, 2020, doi: 10.3389/fenrg.2020.00013.
3. A. Tang, L. Crisci, L. Bonville, and J. Jankovic, "An overview of bipolar plates in proton exchange membrane fuel cells," *J. Renew. Sustain. Energy*, vol. 13, no. 2, 2021, doi: 10.1063/5.0031447.
4. M. M. Bhatti, M. Marin, A. Zeeshan, and S. I. Abdelsalam, "Editorial: Recent Trends in Computational Fluid Dynamics," *Front. Phys.*, vol. 8, no. October, pp. 1–4, 2020, doi: 10.3389/fphy.2020.593111.
5. E. B. Agyekum, J. D. Ampah, T. Wilberforce, S. Afrane, and C. Nutakor, *Research Progress, Trends, and Current State of Development on PEMFC-New Insights from a Bibliometric Analysis and Characteristics of Two Decades of Research Output*, vol. 12, no. 11, 2022. doi: 10.3390/membranes12111103.
6. S. P. D. K. A. S. H. M. A. Ciq. M. J. M. P. Ph.D. Ummul Aiman, M. P. Z. F. Suryadin Hasda, M. P. I. N. T. S. K. M.Kes. Masita, and M. P. M. K. N. A. M.Pd. Meilida Eka Sari, *Metodologi Penelitian Kuantitatif*. 2022.
7. A. Pengaruh, L. Saluran, P. Pelat, B. P. Terhadap, and J. T. Mesin, *Politeknik negeri jakarta*. 2024.

8. Y. Wang, K. S. Chen, J. Mishler, S. C. Cho, and X. C. Adroher, “A review of polymer electrolyte membrane fuel cells: Technology, applications, and needs on fundamental research,” *Appl. Energy*, vol. 88, no. 4, pp. 981–1007, 2011, doi: 10.1016/j.apenergy.2010.09.030.
9. S. Mo *et al.*, *Recent Advances on PEM Fuel Cells: From Key Materials to Membrane Electrode Assembly*, vol. 6, no. 1. Springer Nature Singapore, 2023. doi: 10.1007/s41918-023-00190-w.
10. P. D. I. Torino, L. Magistrale, P. Misul, and D. Anna, “Corso di Laurea Magistrale in Automotive Engineering,” 2022.
11. J. F. Wendt, *Computational Fluid Dynamics: An Introduction*. 2009.

Article

# Mobile Ad-Hoc Network (MANET) Method: Some Trends and Open Issues

Dwi Wijonarko<sup>1</sup>, Samsul Arifin<sup>2,\*</sup>, Muhammad Faisal<sup>2</sup>, Muhammad Nabil Pratama<sup>2</sup>, Okta Nindita Priambodo<sup>3</sup>, Edwin Setiawan Nugraha<sup>4</sup>

- <sup>1</sup> Department of Information Technology, Faculty of Computer Science, University of Jember, Jember, East Java, Indonesia
  - <sup>2</sup> Department of Data Science, Faculty of Engineering and Design, Institut Teknologi Sains Bandung; Bekasi, West Java, Indonesia
  - <sup>3</sup> Department of Palm Oil Processing Technology, Vocational Faculty, Institut Teknologi Sains Bandung, Bekasi, West Java, Indonesia
  - <sup>4</sup> Study Program of Actuarial Science, School of Business, President University, West Java, Indonesia
- \* Correspondence: samsul.arifin@itsb.ac.id

**Abstract:** This study analyzes the latest developments and trends in the field of Mobile Ad-Hoc Networks (MANET) through a bibliometric approach using a metadata dataset from publications taken from Scopus between 2021 and 2024. By utilizing VOSviewer to visualize the data, the study identified key keywords that dominated the MANET literature, such as "security", "routing protocols", "mobility", and "5G". The visualization results show several important clusters, including topics related to network security, vehicle networks (VANET), and the application of advanced technologies such as machine learning in network management. Despite the decline in the number of publications in 2023 and 2024, collaboration between authors continues to show a strong trend. The research also highlights various challenges that are still open problems, such as the development of efficient routing protocols, improving network security, and managing resources in a dynamic MANET environment. In addition to the VOSviewer analysis, further exploration was carried out using the built-in visualization tools from the Scopus web platform to enrich the interpretation of emerging topics and research connections. This was followed by a deeper conceptual mapping using Scopus AI, which provided a visual breakdown of interconnected themes such as security issues, routing protocols, and different network types like VANET and FANET. To complement and validate the findings, the study also incorporated evidence-based summaries retrieved from Consensus.app, offering additional insights from AI-driven scientific consensus. This multi-platform approach enhances the reliability of the analysis and provides a more comprehensive view of current and future research directions in the MANET domain.

**Citation:** Wijonarko, D., Arifin, S., Faisal, M., Pratama, M. N., Priambodo, O. N., Nugraha, E. S. (2025). Mobile Ad-Hoc Network (MANET) Method: Some Trends and Open Issues. *Recent in Engineering Science and Technology*, 3(02), 49–74. Retrieved from <https://www.mbi-journals.com/index.php/riestech/article/view/108>

Academic Editor: Vika Rizkia

Received: 22 April 2025

Accepted: 29 April 2025

Published: 30 April 2025

**Publisher's Note:** MBI stays neutral with regard to jurisdictional claims in published maps and institutional affiliations.



**Copyright:** © 2025 by the authors. Licensee MBI, Jakarta, Indonesia. This article is an open access article distributed under MBI license (<https://mbi-journals.com/licenses/by/4.0/>).

**Keywords:** Bibliometrics; MANET; Scopus; Vosviewer; Visualization

## 1. Introduction

This study discusses the latest developments of the Mobile Ad-Hoc Network (MANET) method through bibliometric analysis using metadata datasets from Scopus in the period 2021 to 2024. MANET is a dynamic, self-contained, wireless network that does not require fixed infrastructure, making it an essential solution for communication in situations such as disasters, military, and rural environments. As technology develops, the methods used in MANET continue to undergo innovation to improve network performance, security,



and communication efficiency. In this study, bibliometric analysis techniques were applied to map research trends and scientific developments in the field of MANET. The dataset collected from Scopus includes scientific publications from relevant journals, conferences, and other papers. The analysis process was carried out using VOSviewer software to visualize the relationship between keywords, collaboration between researchers, and publication patterns over the past four years. This analysis is expected to provide a comprehensive overview of current research focuses and identify areas of rapid growth [1], [2], [3].

The results of this bibliometric analysis show a significant increase in research related to routing protocols, network security, energy efficiency, and the application of MANET in IoT (Internet of Things) environments. Visualization with VOSviewer allows the identification of dominant research clusters as well as demonstrating global collaboration between institutions and researchers in this field. In addition, trends in technological developments such as integration with 5G networks and the implementation of artificial intelligence (AI) for network optimization are also in the main spotlight. This research also identifies several challenges that are still faced in the development of MANET, such as data security issues, network stability in dynamic conditions, and limited device resources. Through this analysis, recommendations for future research were prepared, including the exploration of hybrid routing methods, improved security using cutting-edge cryptography techniques, and the integration of MANET with future network technologies [4], [5], [6]. Figure 1 below contains an illustration of the Concept of MANET.



**Figure 1.** Concept of MANET

As such, the study makes an important contribution to researchers, technology developers, and policymakers in understanding MANET's developments and challenges. The results of this bibliometric analysis can be a strategic guide to direct MANET research

and development to be more effective in responding to the evolving needs of wireless communication in this digital era [7], [8], [9].

## 2. Methodology

The dataset used in this study was obtained from Scopus, one of the largest databases of abstracts and citations for academic literature covering a wide range of disciplines, including science, technology, medicine, social sciences, arts, and humanities. This dataset includes metadata of publications related to the Mobile Ad-Hoc Network (MANET) published between 2021 and 2024, with information such as document title, author, author affiliation, year of publication, number of citations, keywords, and cited references. The data collection process is carried out using the query: TITLE-ABS-KEY ( mobile AND ad-hoc AND network ) AND ( LIMIT-TO ( PUBYEAR , 2021 ) OR LIMIT-TO ( PUBYEAR , 2022 ) OR LIMIT-TO ( PUBYEAR , 2023 ) OR LIMIT-TO ( PUBYEAR , 2024 ) ), which ensures the results include a study of mobile networks that can form dynamic and self-sufficient connections without fixed infrastructure. Restrictions based on the year of publication (2021-2024) make the results more relevant to the latest research, covering the latest technological developments, challenges, and innovations related to MANET. This dataset is then downloaded in CSV format for easy further analysis [10], [11], [12].

The query is designed to filter out the latest publications relevant to the Mobile Ad-Hoc Network (MANET) in the period 2021 to 2024. After conducting a search, 4,685 documents were obtained which included journal articles, conference papers, and scientific reviews. The data is then exported in CSV format, which includes important information such as title, abstract, author, institution, keyword, and year of publication. The initial step of analysis is carried out by utilizing the standard visualization features provided by the Scopus web platform. This visualization includes the distribution of publications by year, document type, country of origin of the researcher, and the most frequently used keywords. Scopus' built-in visualization feature provides an early overview of research trends, the dominance of certain topics, and the geographic distribution of scientific contributions in the field of MANET. These results serve as a basis to understand the general research pattern before conducting a more in-depth analysis [13], [14], [15].

Furthermore, bibliometric analysis continued using the VOSviewer software to obtain more detailed and interactive visualization. The CSV data obtained from Scopus is imported into VOSviewer, and the mapping process is done based on keywords, citations, and author collaboration. This technique allows the identification of interrelated research clusters, relationships between topics, and the evolution of research trends in the period analyzed. Visualization with VOSviewer includes network visualization, overlay visualization, and density visualization to provide comprehensive insights. In the analysis using VOSviewer, various parameters are selected to ensure accurate and informative visualization results. One of them is determining the minimum number of keyword occurrences to filter out significant terms. In addition, co-occurrence analysis is used to see

how often two keywords appear together in a publication, so that the pattern of relationships between concepts can be clearly seen. Visualization of collaboration between researchers and institutions was also carried out to understand the dynamics of global co-operation in the field of MANET [16], [17], [18].

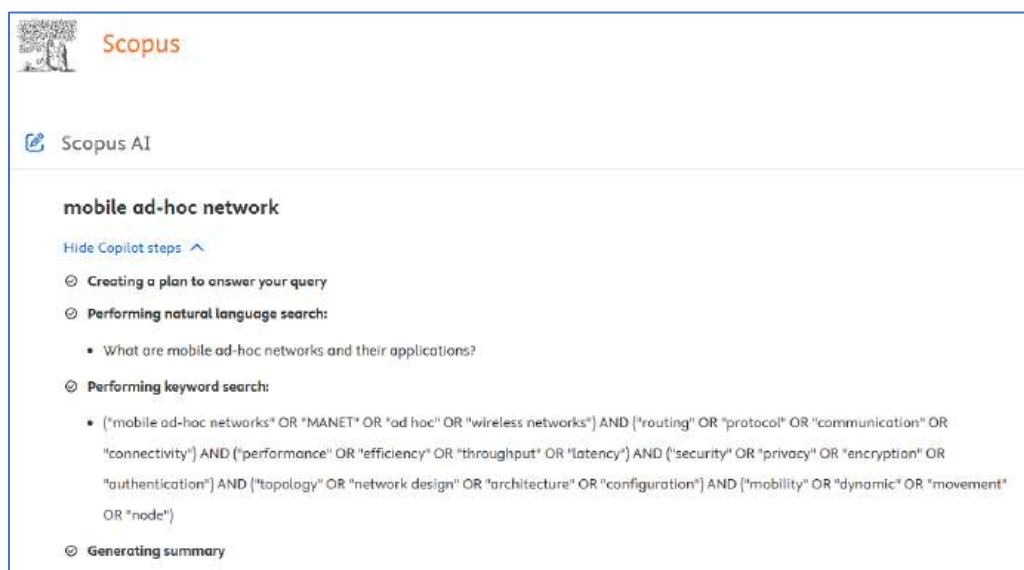


Figure 2. Copilot steps in Scopus-AI

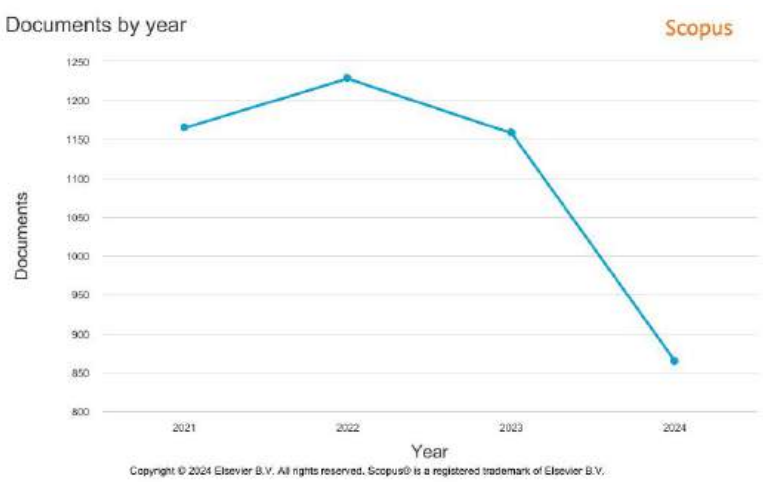
After processing the dataset obtained from the Scopus database using VOSviewer to identify key themes and research clusters, further analysis was conducted by examining the built-in visualizations available on the Scopus web platform. This was followed by an exploration using Scopus AI to generate a concept map highlighting the interconnections between core topics such as security issues, routing protocols, and types of networks within the Mobile Ad-Hoc Networks (MANETs) research domain. To enrich the analysis and gain broader insight, the findings were also cross-validated and expanded using results from Consensus.app, which provided AI-driven evidence-based summaries from scientific literature [19]. The results of this methodology provide an in-depth understanding of the development of MANET research over the past four years. The resulting visualization shows key topics, emerging research trends, and networks of collaboration between researchers. With a combination of preliminary analysis from Scopus and advanced mapping using VOSviewer, this study was able to provide a comprehensive picture that can be used as a basis for further studies or future MANET technology development policies [20], [21], [22]. Figure 2 contains information on Copilot steps in Scopus-AI.

### 3. Results and Discussion

Applications in MANET bibliometric analysis include various types of analysis, such as co-authorship analysis to look at author collaboration networks, co-occurrence analysis to identify trends in research topics, and citation analysis to understand the influence of certain publications in MANET's field. In terms of counting methods, fractional counting is more suitable to get a proportional picture of the contributions of each author or institution, while full counting can be used to focus on the total number of collaborations or appearances. By using authors, organizations, and keywords as units of analysis, it is possible to obtain comprehensive insights into the parties involved in the MANET research, the origin of the institution, and the main topics being researched [23], [24].

Table 1 contains a list of some of the built-in visualizations available in Scopus Web, designed to help users analyze and understand research data effectively. These visualizations include a variety of tools such as publication trend graphs that illustrate the growth of research over time, a map of collaboration between countries or institutions, as well as a graph of author networks that show relationships between collaborators. In addition, there is a keyword analysis feature to identify key research topics, as well as citation charts to assess the influence of a particular publication. With this visualization, Scopus Web makes it easier for researchers to dig important insights from bibliometric data [25], [26], [27].

Table 1. Some built-in visualizations from Scopus Web

Component	Visualization										
Scopus Analyze Year	 <table border="1"><caption>Documents by year</caption><thead><tr><th>Year</th><th>Documents</th></tr></thead><tbody><tr><td>2021</td><td>1170</td></tr><tr><td>2022</td><td>1230</td></tr><tr><td>2023</td><td>1160</td></tr><tr><td>2024</td><td>870</td></tr></tbody></table>	Year	Documents	2021	1170	2022	1230	2023	1160	2024	870
Year	Documents										
2021	1170										
2022	1230										
2023	1160										
2024	870										

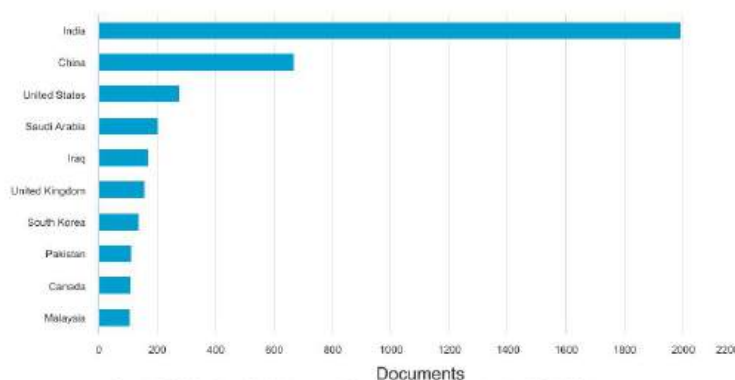
Scopus Analyze Source	<div><div>Documents per year by source</div><div>Compare the document counts for up to 10 sources. Compare sources and view CiteScore, SJR, and SNIP data.</div><div><table><tr><th>Source</th><th>2021</th><th>2022</th><th>2023</th><th>2024</th></tr><tr><td>Lecture Notes in Networks And Systems</td><td>28</td><td>28</td><td>48</td><td>48</td></tr><tr><td>Wireless Personal Communications</td><td>42</td><td>45</td><td>20</td><td>20</td></tr><tr><td>IEEE Access</td><td>34</td><td>30</td><td>28</td><td>25</td></tr><tr><td>Lecture Notes in Electrical Engineering</td><td>19</td><td>31</td><td>16</td><td>4</td></tr><tr><td>IEEE Transactions On Vehicular Technology</td><td>15</td><td>8</td><td>13</td><td>20</td></tr><tr><td>IEEE Access</td><td>15</td><td>8</td><td>13</td><td>20</td></tr></table></div><div>Copyright © 2024 Elsevier B.V. All rights reserved. Scopus® is a registered trademark of Elsevier B.V.</div></div>	Source	2021	2022	2023	2024	Lecture Notes in Networks And Systems	28	28	48	48	Wireless Personal Communications	42	45	20	20	IEEE Access	34	30	28	25	Lecture Notes in Electrical Engineering	19	31	16	4	IEEE Transactions On Vehicular Technology	15	8	13	20	IEEE Access	15	8	13	20
Source	2021	2022	2023	2024																																
Lecture Notes in Networks And Systems	28	28	48	48																																
Wireless Personal Communications	42	45	20	20																																
IEEE Access	34	30	28	25																																
Lecture Notes in Electrical Engineering	19	31	16	4																																
IEEE Transactions On Vehicular Technology	15	8	13	20																																
IEEE Access	15	8	13	20																																
Scopus Analyze Author	<div><div>Documents by author</div><div>Compare the document counts for up to 15 authors.</div><div><table><tr><th>Author</th><th>Documents</th></tr><tr><td>Rajaram, A.</td><td>20</td></tr><tr><td>Murase, T.</td><td>15</td></tr><tr><td>Qay, V.K.</td><td>14</td></tr><tr><td>Singh, R.</td><td>13</td></tr><tr><td>Venkatesubramanian, S.</td><td>13</td></tr><tr><td>An, B.</td><td>10</td></tr><tr><td>Azer, M.A.</td><td>10</td></tr><tr><td>Jubak, M.A.</td><td>10</td></tr><tr><td>Liht, D.M.</td><td>10</td></tr><tr><td>Pandey, P.</td><td>10</td></tr></table></div><div>Copyright © 2024 Elsevier B.V. All rights reserved. Scopus® is a registered trademark of Elsevier B.V.</div></div>	Author	Documents	Rajaram, A.	20	Murase, T.	15	Qay, V.K.	14	Singh, R.	13	Venkatesubramanian, S.	13	An, B.	10	Azer, M.A.	10	Jubak, M.A.	10	Liht, D.M.	10	Pandey, P.	10													
Author	Documents																																			
Rajaram, A.	20																																			
Murase, T.	15																																			
Qay, V.K.	14																																			
Singh, R.	13																																			
Venkatesubramanian, S.	13																																			
An, B.	10																																			
Azer, M.A.	10																																			
Jubak, M.A.	10																																			
Liht, D.M.	10																																			
Pandey, P.	10																																			
Scopus Analyze Affiliation	<div><div>Documents by affiliation</div><div>Compare the document counts for up to 15 affiliations.</div><div><table><tr><th>Affiliation</th><th>Documents</th></tr><tr><td>K.L. Deemed to be University</td><td>85</td></tr><tr><td>SRM Institute of Science and Technology</td><td>70</td></tr><tr><td>Savithe School of Engineering</td><td>60</td></tr><tr><td>Savithe Institute of Medical and Tech...</td><td>58</td></tr><tr><td>Parimalar Engineering College</td><td>48</td></tr><tr><td>Anna University</td><td>45</td></tr><tr><td>Vel Tech Rangarajan Dr.Sagunthala RA...</td><td>38</td></tr><tr><td>Chitkara University, Punjab</td><td>38</td></tr><tr><td>Chandigarh University</td><td>35</td></tr><tr><td>Bathubama Institute of Science and Te...</td><td>35</td></tr></table></div><div>Copyright © 2024 Elsevier B.V. All rights reserved. Scopus® is a registered trademark of Elsevier B.V.</div></div>	Affiliation	Documents	K.L. Deemed to be University	85	SRM Institute of Science and Technology	70	Savithe School of Engineering	60	Savithe Institute of Medical and Tech...	58	Parimalar Engineering College	48	Anna University	45	Vel Tech Rangarajan Dr.Sagunthala RA...	38	Chitkara University, Punjab	38	Chandigarh University	35	Bathubama Institute of Science and Te...	35													
Affiliation	Documents																																			
K.L. Deemed to be University	85																																			
SRM Institute of Science and Technology	70																																			
Savithe School of Engineering	60																																			
Savithe Institute of Medical and Tech...	58																																			
Parimalar Engineering College	48																																			
Anna University	45																																			
Vel Tech Rangarajan Dr.Sagunthala RA...	38																																			
Chitkara University, Punjab	38																																			
Chandigarh University	35																																			
Bathubama Institute of Science and Te...	35																																			

Scopus An-  
alyze Coun-  
try

## Documents by country or territory

Scopus

Compare the document counts for up to 15 countries/territories.

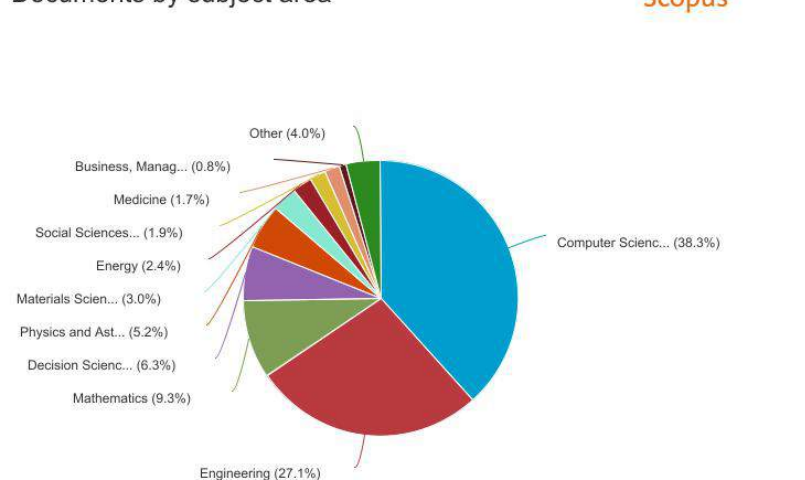


Copyright © 2024 Elsevier B.V. All rights reserved. Scopus® is a registered trademark of Elsevier B.V.

Scopus An-  
alyze Sub-  
ject

## Documents by subject area

Scopus



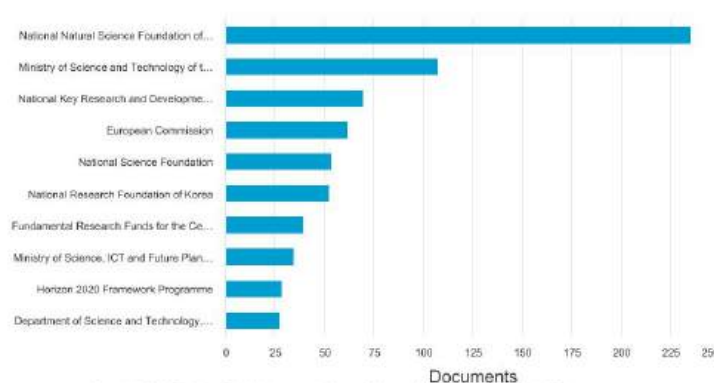
Copyright © 2024 Elsevier B.V. All rights reserved. Scopus® is a registered trademark of Elsevier B.V.

Scopus An-  
alyze Fund-  
ing Sponsor

## Documents by funding sponsor

Scopus

Compare the document counts for up to 15 funding sponsors.



Copyright © 2024 Elsevier B.V. All rights reserved. Scopus® is a registered trademark of Elsevier B.V.

Here are the steps to use VOSviewer: first, set up and enter the dataset to be analyzed into VOSviewer. Next, select the appropriate type of analysis, such as co-authorship, co-occurrence, citation, or bibliographic coupling. After that, determine the counting method, whether to use full counting or fractional counting, depending on the purpose of the analysis. Then, select the relevant unit of analysis, such as authors, organizations, or keywords. Once all the parameters are defined, run the analysis to get the visualization results in the form of a network map or other graph. Details of each step and the results of the visualization can be seen in some of Figure 3 below [28], [29].

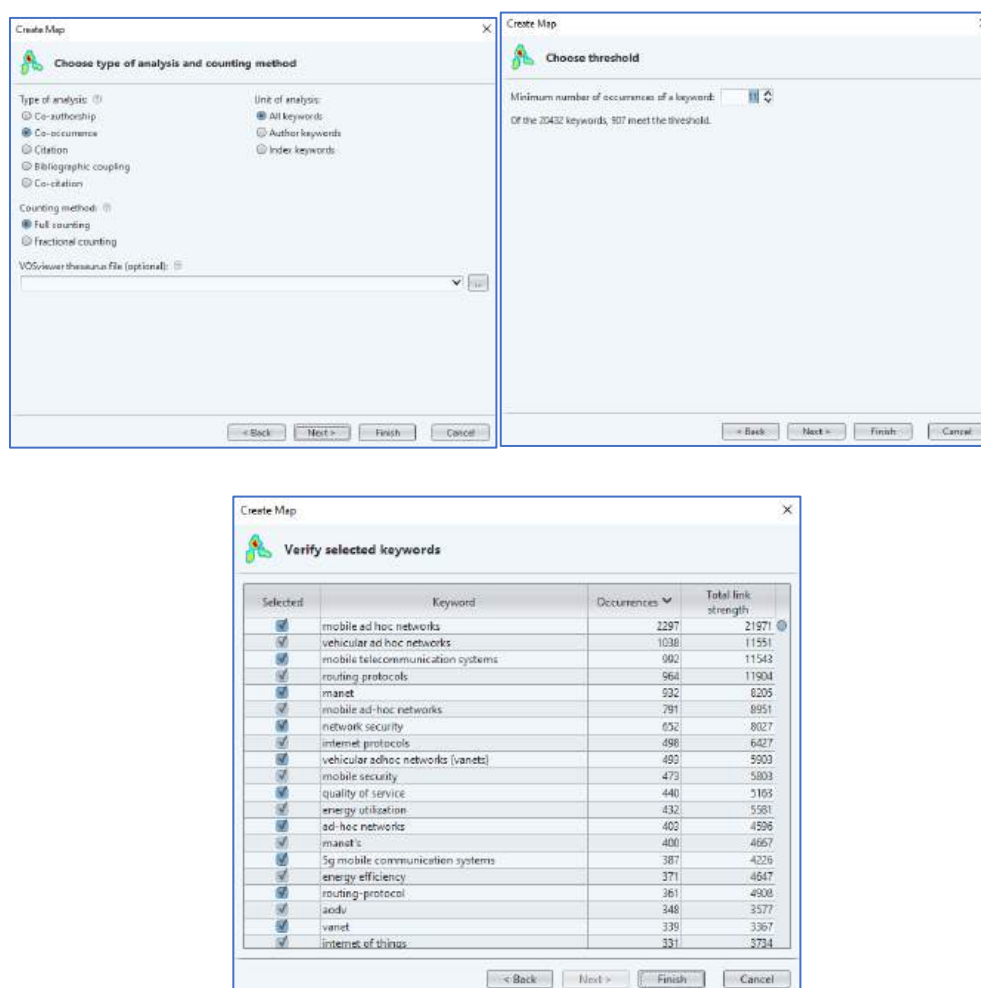


**Figure 3.** Steps to use Visviewer

Here are all the results of the visualization generated using the VOSviewer software, which displays the network of relationships between keywords based on several analyses of relevant studies. This visualization consists of multiple clusters identified through color differences, with each cluster representing an interrelated group of research topics or themes. The size of the circle describes the level of frequency of a keyword in the data, while the connecting lines and proximity between the circles reflect the co-emergence



relationship between keywords. These visualizations provide a comprehensive overview of the structure, trends, and key focuses within the research area, facilitating analysis of specific areas of study and identifying potential collaborations or further exploration of topics [30], [31].

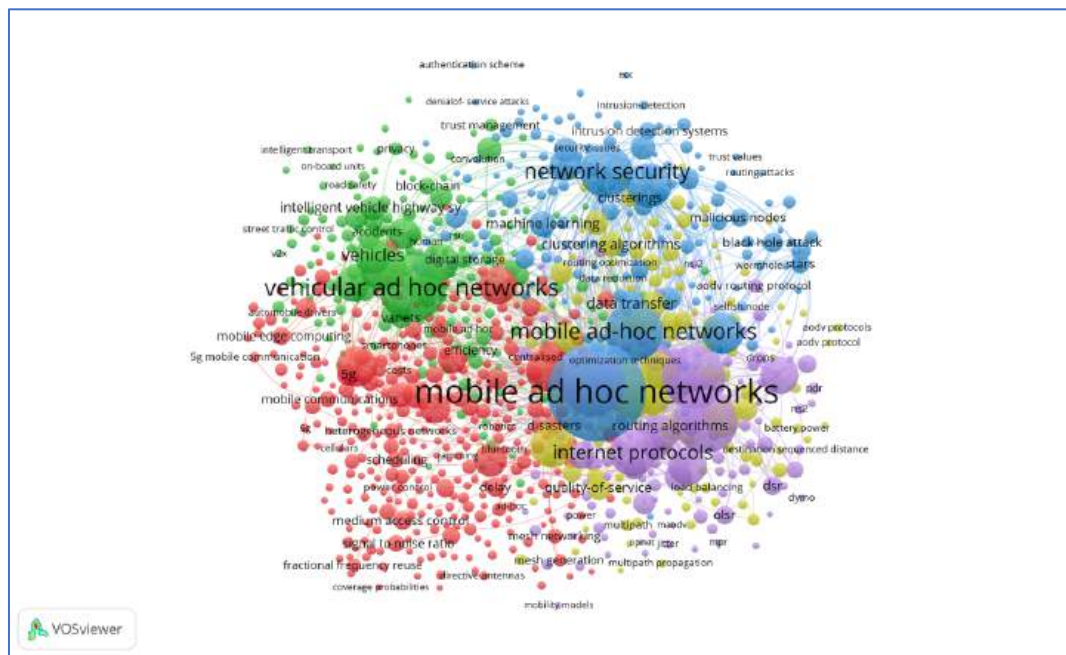


**Figure 4.** Visualization of Co-occurrence - All Keywords

The VOSviewer visualization in Figure 4 illustrates a bibliometric network map of research topics centered around “mobile ad hoc networks” (MANETs). Each node represents a keyword or term from scientific literature, where the size of the node indicates its frequency, and the lines between them reflect co-occurrence relationships. The term “mobile ad hoc networks” is positioned at the center, suggesting it is the primary focus across the dataset. Terms in proximity and connected by stronger links indicate more frequent joint appearances in the literature. The map is divided into color-coded clusters, each representing thematically related subfields within the broader research domain. The red cluster primarily focuses on vehicular communications and mobility-centric technologies, including “vehicular ad hoc networks,” “5G,” “mobile edge computing,” and “intelligent transport.” This reflects an increasing interest in integrating MANETs into intelligent transportation systems and modern mobile communication frameworks. The green cluster complements this by emphasizing applications related to smart highways, vehicle safety, and on-board units, signifying an alignment between MANET research and the development of intelligent vehicle ecosystems. Meanwhile, the blue and yellow clusters emphasize technical and security aspects of MANETs. The blue cluster covers “network



security,” “intrusion detection,” “trust management,” and “machine learning,” indicating active research addressing vulnerabilities in mobile networks. The yellow and purple clusters center on routing and optimization, with terms like “routing algorithms,” “ad hoc on-demand distance vector,” and “load balancing,” which highlight the ongoing exploration of efficient data transmission methods. Collectively, this visualization reveals the diverse and interdisciplinary nature of MANET research, spanning from communication protocols and vehicular applications to cybersecurity and optimization techniques [7], [32].

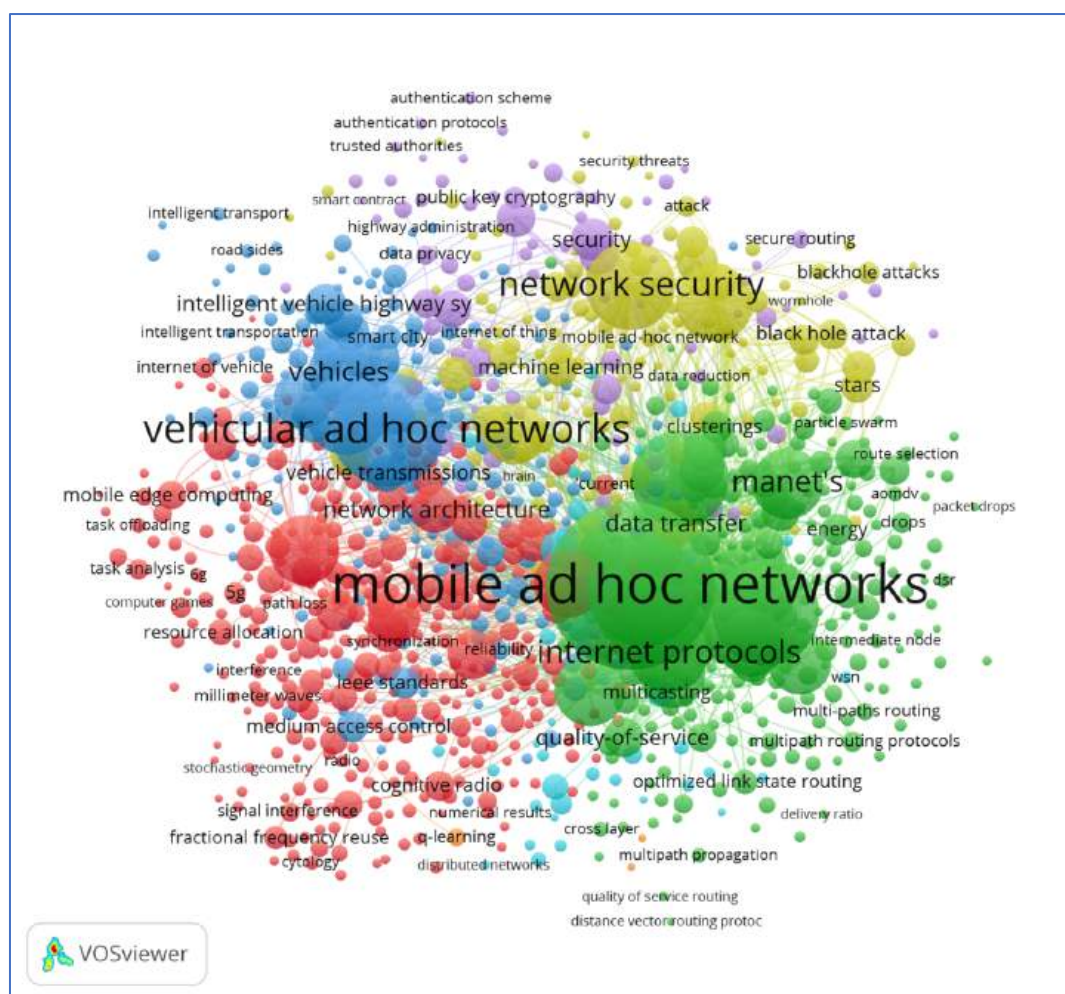


**Figure 5.** Visualization of Co-occurrence - index keywords

Figure 5. display a map of the keyword network in the research related to Mobile Ad-Hoc Networks (MANET) based on the publication dataset from 2021 to 2024. The keywords "mobile ad hoc networks" and "vehicular ad hoc networks" emerged as the main centers of the research, with large sizes indicating a high frequency of occurrence. The different colors indicate various research clusters, such as green clusters that focus on

internet protocols, data transfer, and routing protocols, as well as red clusters that highlight topics such as 5G, medium access control, and resource allocation. The blue cluster highlights the concepts of vehicular networks, intelligent transportation systems, and intelligent vehicle highway systems, while the purple cluster emphasizes aspects of network security and public key cryptography. The connecting lines between keywords indicate the degree of interconnectedness or co-occurrence, reflecting how these concepts are often researched together. This visualization provides in-depth insights into MANET's research focus and trends, as well as potential collaboration areas and ongoing challenges [16], [33].

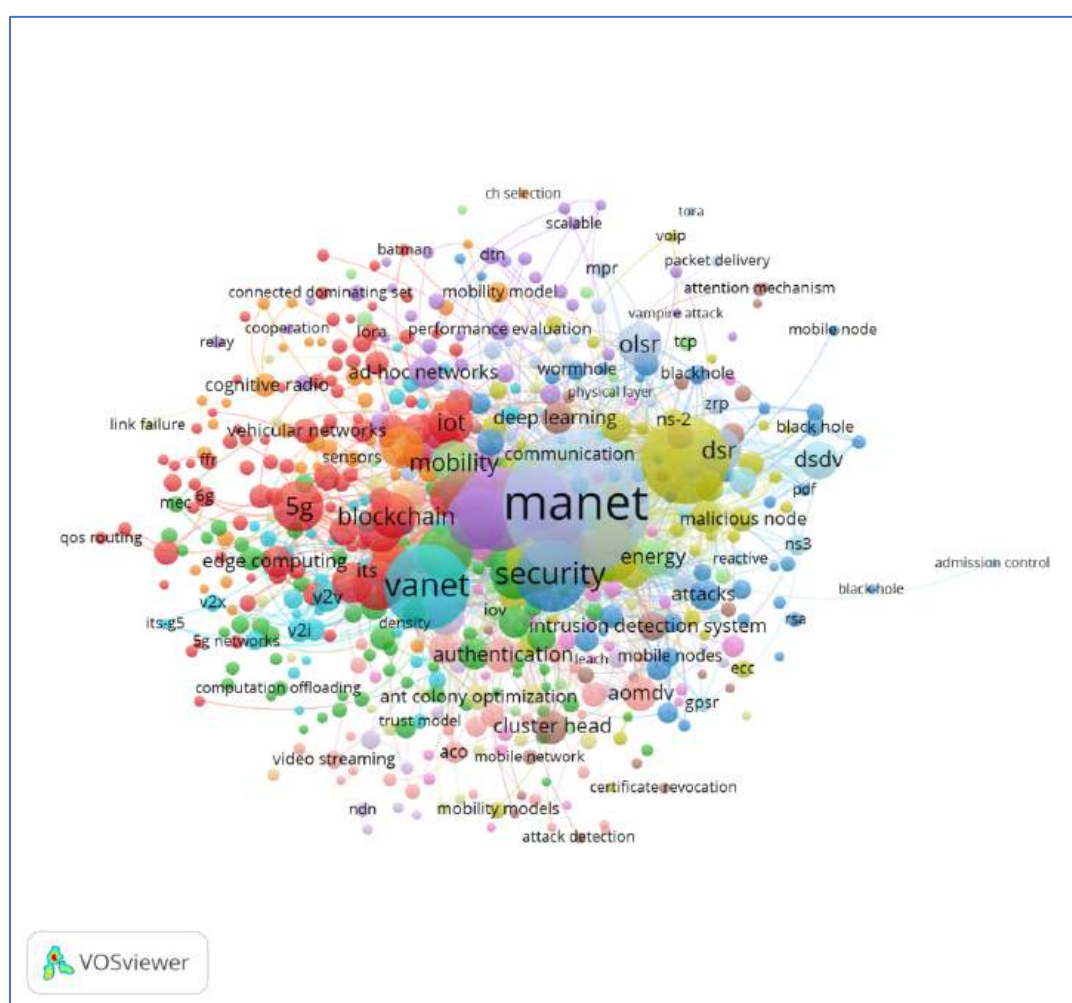


**Figure 6.** Visualization of Co-occurrence - Author Keyword

Figure 6. shows a bibliometric network map related to Mobile Ad-Hoc Network (MANET) research based on the most frequently published keywords between 2021 and 2024. Each point represents a keyword, where the size of the point describes the frequency with which it appears in the dataset. Key keywords such as "manet", "security", "vanet", and "mobility" emerged dominantly, indicating the research focus on aspects of security,

vehicle networks (VANET), and node movement within MANET. The different colors represent interrelated research clusters; for example, the red cluster shows the relationship between 5G technology, edge computing, and vehicular networks, while the green cluster is related to security and intrusion detection. The connecting lines between keywords describe the degree of co-occurrence, indicating concepts that are often researched together. These visualizations help understand research trends, emerging topics, and potential areas of collaboration in MANET studies [34], [35].

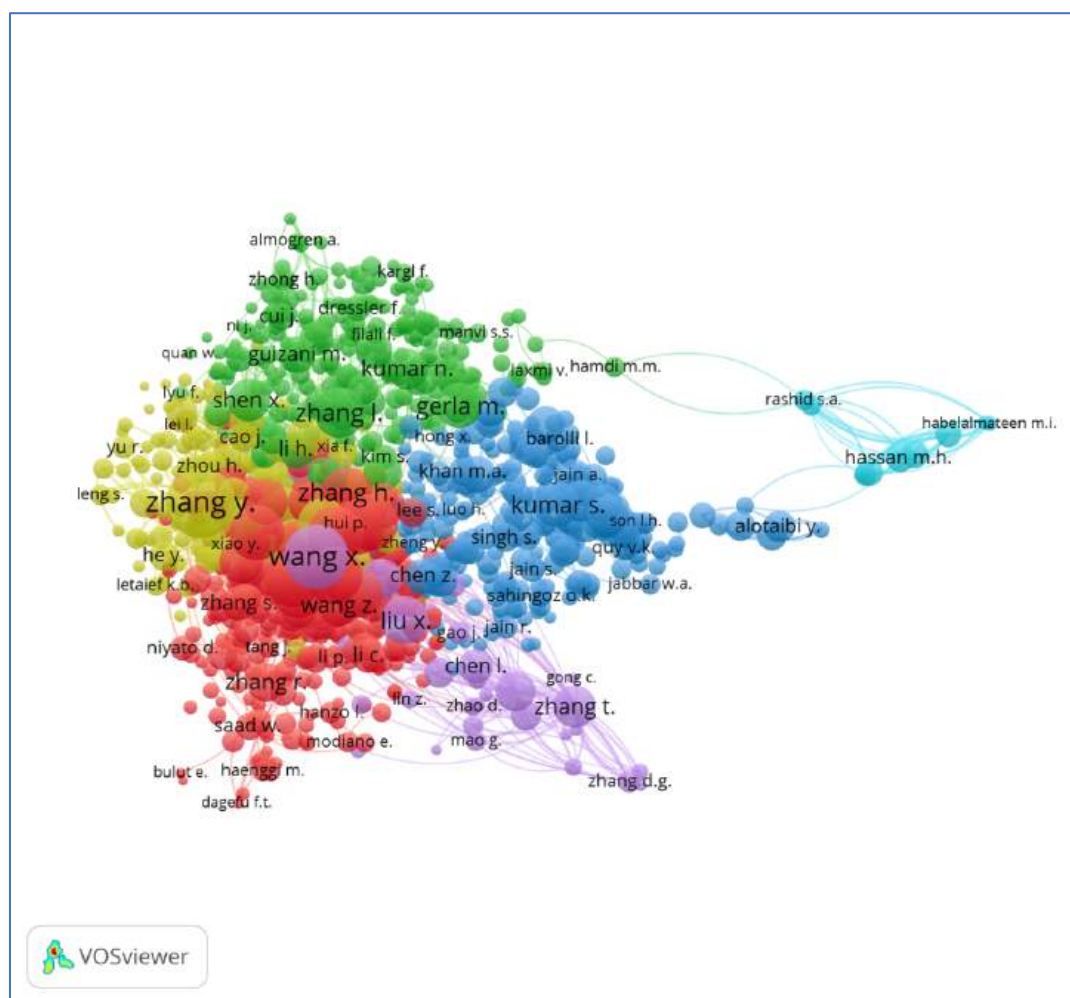


**Figure 7.** Visualization of Cocitation - Author

The VOSviewer visualization in Figure 7 represents a co-authorship network, where each node corresponds to an author involved in research related to a particular academic domain, likely mobile ad hoc networks based on context. The size of each node reflects the number of publications or the author's prominence, while the lines (or links) denote collaborative relationships between authors. The visualization is grouped into different colored clusters, each representing a group of closely connected authors who frequently collaborate. Central figures such as "Wang," "Zhang Y.," "Zhang H.," and "Kumar S."

indicate prolific contributors with widespread collaborations across multiple clusters. The spatial arrangement reveals collaboration patterns within the research community. The dense clustering in the left portion of the map suggests strong intra-group collaboration among authors, especially within the red, yellow, and green clusters. These clusters are tightly packed, showing intensive co-authorship, possibly from research institutions or regional collaborations. In contrast, the blue cluster, especially on the right-hand side with names like “Hassan M.H.” and “Habelalmateen M.I.,” appears more peripheral and loosely connected, suggesting either emerging authors or groups working in relative isolation or within niche topics. Overall, this visualization highlights the structure of scientific collaboration and the key players driving research in the domain [24], [36].

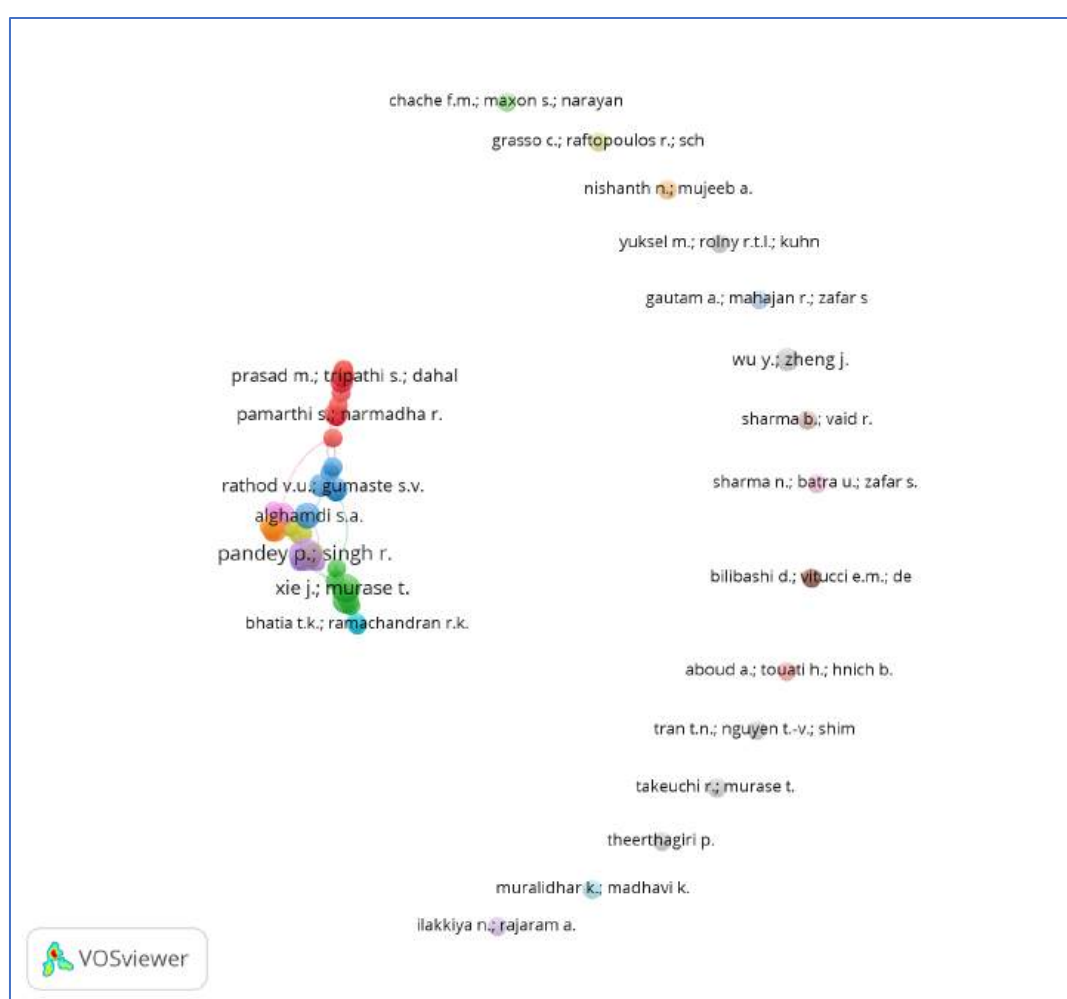


**Figure 8.** Visualization of Bibliographic Coupling - Author

Figure 8 describes a bibliographic network based on couplings between authors using VOSviewer. In this graph, groups of authors are grouped based on their degree of similarity or bibliographic relationship, which is indicated by the color and proximity of the positions between the nodes. Authors such as Pandey P., Singh R., and Murase T. appear

to be in a dense group, suggesting a strong bibliographic connection. Meanwhile, some authors such as Chache F.M., Maxon S., and Narayan are more detached, reflecting weaker relationships or different specializations. The size of the text indicates the author's contribution or involvement in the network being analyzed [37], [38].

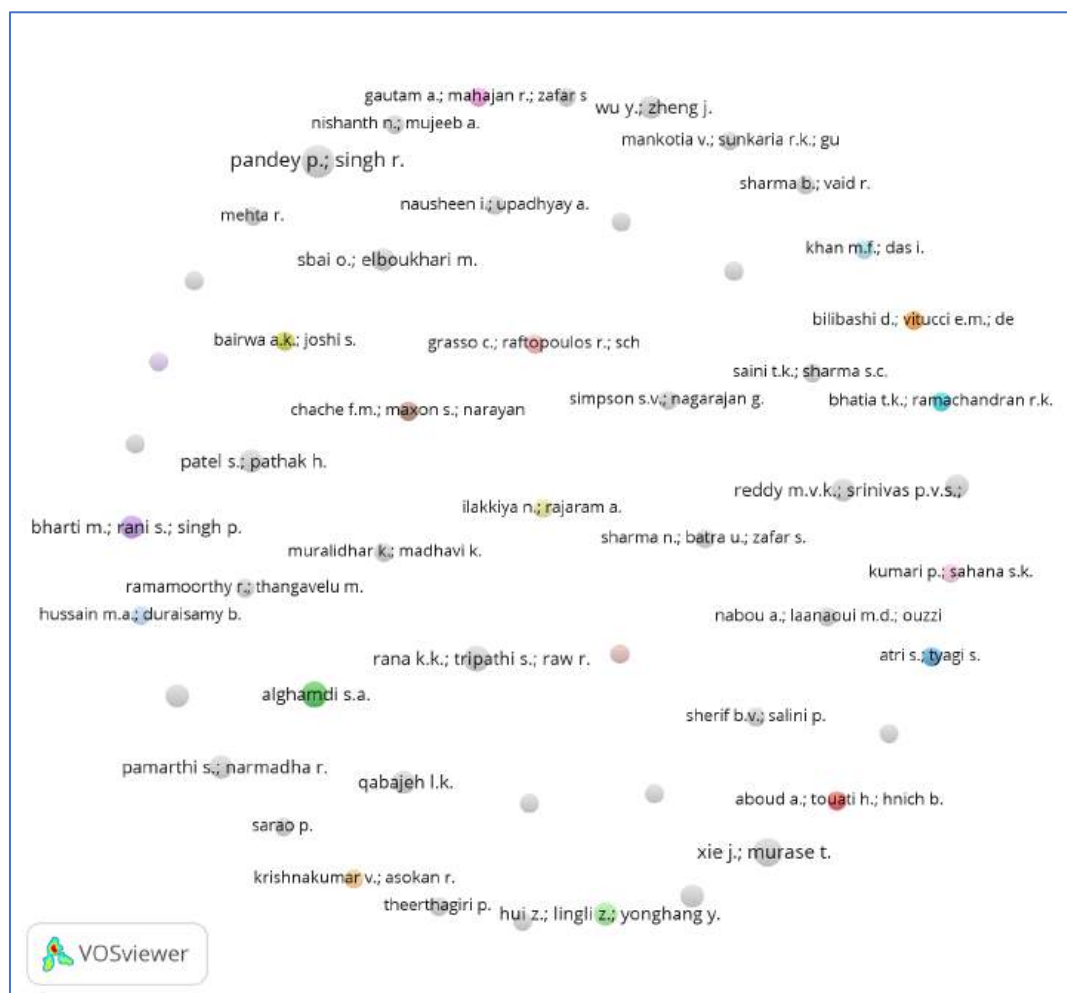


**Figure 9.** Visualization of Citation - Author

The VOSviewer visualization illustrates a co-authorship network characterized by sparse collaboration among researchers. Each node represents an individual author, while the distance and connectivity (or lack thereof) between nodes highlight the extent of their collaborative efforts. Unlike the previous dense networks, this visualization shows minimal interconnectedness, with most authors appearing as isolated or loosely associated entities. The relatively small node sizes and limited clustering indicate that these researchers are either early in their publication journey or are contributing independently without forming strong collaborative ties. A few minor clusters are visible, such as around authors like "Pandey P." and "Singh R.," who show some degree of co-authorship, but overall, the network lacks central figures or dominant collaborative groups. The scattered nature of the visualization implies that the topic under analysis



might be relatively new or niche, leading to fragmented contributions from various isolated researchers. Additionally, the low density suggests opportunities for increased collaboration and network formation in the future, especially if the field continues to grow and attract interdisciplinary research [39], [40].



**Figure 10.** Visualization of Country

Figure 10 is a network map that displays relationships between countries using VOSviewer software. In this visualization, countries such as India, Israel, and the Czech Republic are seen to be in one closely interconnected group, indicated by their stacks in a circle. Meanwhile, countries such as Palestine, Trinidad and Tobago, and Croatia are separate, showing weaker ties or a lack of connection with the main group. The size and position of the text on this map reflect the level of involvement or connection of the country in the network being analyzed [41], [42]. Here's the comparison table of MANET routing protocols based on performance metrics and bibliometric impact (citations, trends, etc.).

**Table 2.** MANET routing protocols based on performance metrics and bibliometric impact

Routing Protocol	Type	Technical Performance	Citation Count / Trend (2021–2024)	Strengths	Weaknesses
<b>AODV</b> (Ad hoc On-Demand Distance Vector)	Reactive (On-Demand)	Low latency on active routes, energy-efficient	Very frequently cited (stable high trend)	Routes are created only when needed, saving bandwidth	Initial delay in route discovery
<b>DSR</b> (Dynamic Source Routing)	Reactive	Good for small networks; routing information carried in packet headers	Declining trend; still cited for high-density networks	No need for routing tables, highly adaptive	Header overhead increases in large networks
<b>DSDV</b> (Destination-Sequenced Distance-Vector)	Proactive (Table-driven)	Regular routing table updates; good stability	Less cited compared to AODV/DSR	Routes always available without initial delay	High control overhead even in low traffic
<b>ZLR</b> (Zone-based Location Routing)	Hybrid (Proactive + Reactive)	Optimized routing by dividing network into zones	Emerging trend; currently fewer citations	Efficient for large-scale MANETs	High implementation complexity
<b>SPSR</b> (Secure Path Selection Routing)	Proactive (Security-focused)	Emphasizes secure routing; tolerant to attacks	Emerging (trend rising but minor)	Secure against route manipulation attacks	Cryptographic processing overhead
<b>ARIADNE</b>	Secure Reactive	End-to-end authentication using symmetric keys	Moderate; often referenced in security research	Protects against various routing attacks	Requires accurate time synchronization
<b>SAODV</b> (Secure AODV)	Secure Reactive	Strengthens AODV against attacks (with digital signatures)	Rising trend in security-related studies	Resilient to black-hole/wormhole attacks	Digital signature adds computational load
<b>MOSAODV</b> (Modified SAODV)	Enhanced Secure Routing	Optimization of SAODV; faster packet delivery	Very recent topic, few citations yet (niche area)	Minimizes delay and overhead	More complex than standard SAODV

This study provides a detailed bibliometric overview of research trends in the field of Mobile Ad-Hoc Networks (MANET) from 2021 to 2024. Using data visualization tools

such as VOSviewer and Scopus, key aspects of MANET research were identified, including the most frequently occurring keywords, the most active authors, and the country's leading contributions to the field. Table 3 highlights the dominant research topics and technological focuses, such as security, mobility, and integration with emerging technologies like 5G. Table 4 presents the authors with the highest collaboration and publication activity, showcasing key figures who are driving advancements in MANET studies. Meanwhile, Table 5 illustrates the geographical distribution of research efforts, emphasizing the countries that have made significant contributions to MANET development. Together, these tables offer a comprehensive snapshot of the global research landscape surrounding MANETs [38], [42], [43].

**Table 3.** Top 10 Keywords in MANET Research (2021–2024)

Rank	Keyword	Frequency Level
1	mobile ad hoc networks	Very High
2	security	High
3	vehicular ad hoc networks (VANET)	High
4	mobility	High
5	5G	Medium-High
6	network security	Medium-High
7	intrusion detection	Medium
8	routing algorithms	Medium
9	load balancing	Medium
10	edge computing	Medium



**Table 4.** Top 10 Authors by Publication or Collaboration

Rank	Author Name	Collaboration/Citation Notes
1	Wang	Very Active
2	Zhang Y.	Very Active
3	Zhang H.	Very Active
4	Kumar S.	Active
5	Hassan M.H.	Moderately Active
6	Habelalmateen M.I.	Moderately Active
7	Pandey P.	Active
8	Singh R.	Active
9	Murase T.	Active
10	Chache F.M.	Moderately Involved

**Table 5.** Top 10 Countries by Research Involvement

Rank	Country	Notes
1	India	Highly Dominant
2	Israel	Dominant
3	Czech Republic	Dominant
4	Palestine	Moderate
5	Trinidad and Tobago	Moderate
6	Croatia	Moderate

Rank	Country	Notes
7	China	Highly Contributing
8	United States (USA)	Highly Contributing
9	Malaysia	Fairly Contributing
10	Pakistan	Fairly Contributing

Additional studies from consensus.app are as follows [44]. Mobile Ad Hoc Networks (MANETs) are decentralized, self-organized wireless networks where devices communicate without relying on fixed infrastructure. Their dynamic topology presents unique challenges in network configuration, routing, and security. Traditional methods like DHCP are unsuitable due to the distributed nature of MANETs, prompting the development of novel approaches such as extended IPv6 stateless autoconfiguration and binary split methods for IP allocation. These strategies address issues like network partitioning and merging. Routing is equally complex, with protocols like DSDV (proactive), DSR and AODV (reactive), and secure versions such as SAODV and ARIANDE being designed to adapt to frequent topological changes. Among them, DSR performs well in high-density networks, while ARIANDE shows strength in securing communication [45], [46].

Security and Quality of Service (QoS) are critical concerns in MANETs. Their open nature makes them vulnerable to attacks like blackholes, leading to the development of enhanced protocols such as MOSAODV, which strengthens AODV by improving packet delivery with minimal delay and overhead. Other innovative solutions include cellular automata for node authentication and secure transmission. On the QoS front, ensuring stable performance is difficult without centralized control, making admission control essential to manage bandwidth and session allocation. Techniques like HELLO packet advertisements and channel state differentiation have been proposed for better resource estimation. Simulation tools play a key role in testing these solutions—while NS-3 supports heterogeneous MANET environments, newer platforms incorporating SDN devices are helping researchers explore even broader scenarios. As MANETs continue to evolve, ongoing research is essential to develop robust, adaptive, and secure communication protocols for increasingly mobile and decentralized environments [47], [48].

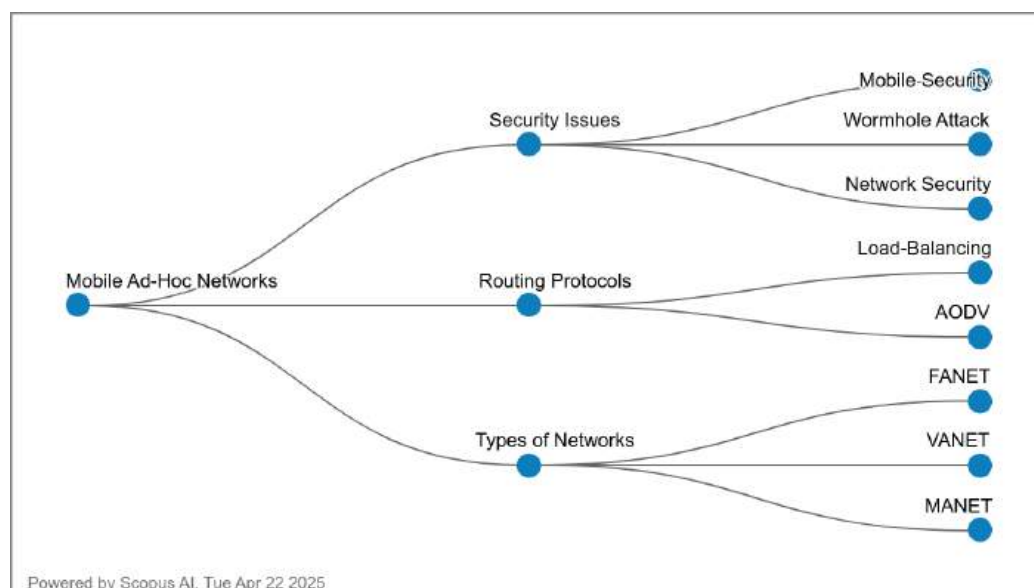


**Figure 11.** Concept map from Scopus AI [49]

The results of the study from Scopus-AI are as follows [50]. A Mobile Ad-Hoc Network (MANET) is a decentralized, self-configuring wireless network that operates without fixed infrastructure or centralized administration. Key characteristics of MANETs include dynamic topology due to node mobility, multi-hop communication where nodes relay data for one another, and support for heterogeneous devices such as laptops, smartphones, and sensors. These networks are especially useful in scenarios like emergency and disaster response, military operations, and civilian applications such as mobile classrooms and personal networking. Routing protocols commonly used in MANETs include AODV, DSR, DSDV, ZLR, and SPSR, each offering different strategies to manage communication in dynamic environments [51], [52]. Despite their flexibility and wide range of applications, MANETs face significant challenges, particularly in terms of security and technical constraints. Their open architecture and rapidly changing topology make them vulnerable to various attacks and complicated the maintenance of secure routes. Additionally, limited resources such as battery life and processing power pose operational challenges. Solutions to these issues include multi-fence security frameworks, cluster-based security schemes, and multi-path routing techniques aimed at improving data confidentiality and reliability. Overall, MANETs present a robust networking solution in infrastructure-less settings, but ongoing research is necessary to address their routing, security, and scalability issues [53], [54].

The diagram generated by Scopus AI in Figure 11 presents a conceptual map of research themes related to Mobile Ad-Hoc Networks (MANETs). It categorizes the main areas of scholarly focus into three major branches: Security Issues, Routing Protocols, and Types of Networks. Under "Security Issues," key topics include Mobile Security, Wormhole Attack, and Network Security, indicating an emphasis on the vulnerabilities and

threats faced by MANETs and the need for robust protective measures. This branch reflects ongoing research into safeguarding data transmission and preventing malicious activities within the network [55]. The "Routing Protocols" section highlights specific strategies for managing data flow in MANETs, such as AODV (Ad hoc On-Demand Distance Vector) and concepts like Load-Balancing, which are essential for efficient and reliable communication. The "Types of Networks" branch further classifies ad-hoc networks into subtypes like FANET (Flying Ad Hoc Networks), VANET (Vehicular Ad Hoc Networks), and MANET, suggesting diversification in the application of ad-hoc network models based on mobility environments (air, land, etc.). Overall, this visualization helps illustrate the multidimensional research landscape surrounding MANETs, encompassing both technical and security challenges as well as application-specific developments [46], [56].

## Conclusion

The conclusions of this bibliometric analysis show that research on Mobile Ad-Hoc Networks (MANET) fluctuated in the period 2021 to 2024, with a significant decrease in the number of publications from 2022 to 2024. Despite the decline in the number of publications, the topics covered remain relevant and include technical, security, and application aspects of MANET in various fields. The visualization generated through VOSviewer shows the dominance of keywords such as "MANET", "security", "vanet", and "mobility", indicating a major focus on the development of security solutions, vehicle connectivity, and dynamic movement within the network. The clustering seen in the keyword network map illustrates the interconnectedness between various topics, such as 5G, edge computing, and vehicle networks, as well as security aspects such as intrusion detection and attack detection. The authors' collaborative analysis shows that there is a strong interaction between different groups of scientists who focus their research on the latest technological innovations and the challenges faced in the implementation of MANET. Overall, despite the decline in the number of publications from 2022 to 2024, the study still highlights key trends in MANET research involving the development of more efficient routing protocols, the implementation of machine learning, and improvements in service quality and network security. The collaboration between authors identified in the collaboration visualization shows that there is significant synergy between researchers from different institutions around the world, which accelerates progress in this field. By leveraging VOSviewer for bibliometric mapping, the study provides deeper insights into current research developments, dominating topics, and areas that require further attention, especially in the face of complex technical and security challenges in real-world MANET applications. To strengthen the paper's conceptual contribution, we have identified several underexplored areas in MANET research, such as the development of AI-driven hybrid routing protocols and blockchain-based security mechanisms. Additionally, we propose a new conceptual framework classifying MANET research into three

major domains: routing optimization, resource management, and network security enhancement. This framework aims to map current research focuses and highlight new directions for future technological innovations in MANETs.

Although research on Mobile Ad-Hoc Networks (MANET) continues to grow, there are still some open problems that need to be addressed to advance this field. One of the key challenges is improving the efficiency and scalability of routing protocols in dynamic and resource-constrained network conditions. In addition, security issues, such as protection against blackhole, wormholes, and sybil attacks, are still major issues that hinder the implementation of MANET in the real world, especially in critical applications such as vehicle communications or the Internet of Things (IoT). The use of new technologies such as machine learning and 5G offers potential solutions, but the integration and application of these technologies in highly dynamic networks and without fixed infrastructure still requires further research. On the other hand, the management of resources, such as energy and bandwidth, as well as the implementation of more efficient network management in high-density environments, are also issues that need more attention in future research.

## References

1. M. Bima, R. Baharsyah, Leman, S. A. Roni, and Hanifadinna, "Analisis Publikasi Ilmiah mengenai Prestasi Belajar Siswa melalui Pendekatan Bibliometrik dan Teknologi," *J. VOKASI Teknol. Ind.*, vol. 6, no. 2, pp. 1–14, 2024.
2. B. Sharan *et al.*, "AI-based intelligent mobility in vehicular ad hoc networks," in *Intelligent Networks: Techniques, and Applications*, School of Engineering and Sciences, Department of Computer Science and Engineering, SRM University-AP, Amaravati, Andhra Pradesh, India: CRC Press, 2024, pp. 18–41. doi: 10.1201/9781003541363-2.
3. S. F. M. Hussain and S. M. H. S. S. Fathima, "Federated Learning-Assisted Coati Deep Learning-Based Model for Intrusion Detection in MANET," *Int. J. Comput. Intell. Syst.*, vol. 17, no. 1, 2024, doi: 10.1007/s44196-024-00590-w.
4. Suwarno, N. P. P. Murnaka, S. Arifin\*, M. M. M. Manurung, and B. Siregar, "A Bibliometric Study of 3D Printing's Educational Applications," *J. VOKASI Teknol. Ind.*, vol. 6, no. 1, pp. 12–29, 2024.
5. G. K. Ahirwar, R. Agarwal, and A. Pandey, "A competent CCHFMO with AMDH for QoS improvisation and efficient route protection in MANET," *Concurr. Comput. Pract. Exp.*, vol. 36, no. 27, 2024, doi: 10.1002/cpe.8272.
6. A. GhorbanniaDelavar and Z. Jormand, "FMORT: The Meta-Heuristic routing method by integrating index parameters to optimize energy consumption and real execution time using FANET," *Comput. Networks*, vol. 255, 2024, doi: 10.1016/j.comnet.2024.110869.
7. U. Sutrisno *et al.*, "Trends, Contributions and Prospects: Bibliometric Analysis of ANOVA Research in 2022-2023," *Indones. J. Appl. Math. Stat.*, vol. 1, no. 1, pp. 27–38, 2024.
8. J. V Ananthi, P. S. H. Jose, and M. Nesasudha, "An efficient optimization approach with mobility management for enhanced QoS and secure communication in flying adhoc networks," *Comput. Electr. Eng.*, vol. 120, 2024, doi: 10.1016/j.compeleceng.2024.109665.

9. D. S. Bhatti, S. Saleem, A. Imran, H. J. Kim, K.-I. Kim, and K.-C. Lee, "Detection and isolation of wormhole nodes in wireless ad hoc networks based on post-wormhole actions," *Sci. Rep.*, vol. 14, no. 1, 2024, doi: 10.1038/s41598-024-53938-9.
10. S. Arifin, M. M. Manurung, S. Jonathan, M. Effendi, and P. W. Prasetyo, "Trend Analysis of the ARIMA Method: A Survey of Scholarly Works," *Recent Eng. Sci. Technol.*, vol. 2, no. 03, pp. 1–14, 2024.
11. L. Rui, L. Zhao, Z. Guo, Z. Wang, X. Qiu, and S. Guo, "Mobile ad hoc network access authentication mechanism based on rotation election and two-factor aggregation," *Comput. Networks*, vol. 254, 2024, doi: 10.1016/j.comnet.2024.110826.
12. D. N. Melati *et al.*, "A comparative evaluation of landslide susceptibility mapping using machine learning-based methods in Bogor area of Indonesia".
13. S. Arifin *et al.*, "Long Short-Term Memory (LSTM): Trends and Future Research Potential," *Int. J. Emerg. Technol. Adv. Eng.*, vol. 13, no. 5, pp. 24–35, 2023.
14. R. Rousseau, L. Egghe, and R. Guns, *Becoming metric-wise: A bibliometric guide for researchers*. Chandos Publishing, 2018.
15. L. Bornmann, P. Atkinson, S. Delamont, A. Cernat, J. W. Sakshaug, and R. A. Williams, *Bibliometric Indicators*. in Measurement methods. SAGE Publications Limited, 2020. [Online]. Available: [https://books.google.co.id/books?id=\\_m1ZzwEACAAJ](https://books.google.co.id/books?id=_m1ZzwEACAAJ)
16. S. Arifin *et al.*, "Prospects and Possibilities for Future Research of Fuzzy C-Means (FCM)," *Int. J. Intell. Syst. Appl. Eng.*, vol. 11, no. 2, pp. 741–751, 2023.
17. J. I. Gorraiz, R. Repiso, N. De Bellis, and G. Deiner, *Best Practices in Bibliometrics & Bibliometric Services*. in Frontiers Research Topics. Frontiers Media SA, 2022. [Online]. Available: <https://books.google.co.id/books?id=qfBXEAAQBAJ>
18. S. Arifin *et al.*, "Graph Coloring Program of Exam Scheduling Modeling Based on Bitwise Coloring Algorithm Using Python," 2022, doi: 10.3844/jcssp.2022.26.32.
19. A. S. Nargunam and M. P. Sebastian, "Cluster based security scheme for mobile ad hoc networks," in *IEEE International Conference on Wireless and Mobile Computing, Networking and Communications 2006, WiMob 2006*, Department of Computer Science and Engineering, N.I College of Engineering, Thuckalay, Tamil Nadu, India, 2006, pp. 391–396. doi: 10.1109/WIMOB.2006.1696379.
20. K. Pushpalatha, P. Sherubha, S. P. Sasirekha, and D. Kumar Anguraj, "A constructive delay-aware model for opportunistic routing protocol in MANET," *Expert Syst. Appl.*, vol. 255, 2024, doi: 10.1016/j.eswa.2024.124527.
21. N. J. van Eck and L. Waltman, *Vosviewer: A Computer Program for Bibliometric Mapping*. SSRN, 2010. [Online]. Available: <https://books.google.co.id/books?id=kmDmzgEACAAJ>
22. R. Todeschini and A. Baccini, *Handbook of Bibliometric Indicators: Quantitative Tools for Studying and Evaluating Research*. Wiley, 2016. [Online]. Available: <https://books.google.co.id/books?id=7BuACgAAQBAJ>
23. R. Zhang, D. Zou, and G. Cheng, "A review of chatbot-assisted learning: pedagogical approaches, implementations, factors leading to effectiveness, theories, and future directions," *Interact. Learn. Environ.*, 2023, doi: 10.1080/10494820.2023.2202704.
24. I. Assagaf, A. Sukandi, A. A. Abdillah, and S. Arifin, "Machine Predictive Maintenance by

- Using Support Vector Machines," *J. Recent Eng. Sci. Technol.*, vol. 1, no. 1, pp. 1–5, 2023.
25. A. Ahmi, *Bibliometric Analysis for Beginners: A starter guide to begin with a bibliometric study using Scopus dataset and tools such as Microsoft Excel, Harzing's Publish or Perish and VOSviewer software* in Pre-print Edition. 2021. [Online]. Available: <https://books.google.co.id/books?id=kZ9BEAAQBAJ>
  26. J. V. Arteaga, M. L. Gravini-Donado, and L. D. Z. Riva, "Digital Technologies for Heritage Teaching: Trend Analysis in New Realities," *Int. J. Emerg. Technol. Learn.*, vol. 16, no. 21, pp. 132–148, 2021, doi: 10.3991/ijet.v16i21.25149.
  27. S. Tarigan, N. P. Murnaka, and S. Arifin, "Development of teaching material in mathematics 'Sapta Maino Education' on topics of plane geometry," in *AIP Conference Proceedings*, American Institute of Physics Inc., 2021. doi: 10.1063/5.0041650.
  28. N. Mohammad, R. Ahmad, A. Kurniawan, and M. Y. P. Mohd Yusof, "Applications of contemporary artificial intelligence technology in forensic odontology as primary forensic identifier: A scoping review," *Front. Artif. Intell.*, vol. 5, 2022, doi: 10.3389/frai.2022.1049584.
  29. S. Arifin *et al.*, "Algorithm for Digital Image Encryption Using Multiple Hill Ciphers, a Unimodular Matrix, and a Logistic Map," *Int. J. Intell. Syst. Appl. Eng.*, vol. 11, no. 6, pp. 311–324, 2023.
  30. Z. M. Arshad, M. N. A. Azman, O. Kenzhaliyev, and F. R. Kassimov, "Educational Enhancement Through Augmented Reality Simulation: A Bibliometric Analysis," *Int. J. Adv. Comput. Sci. Appl.*, vol. 15, no. 7, pp. 706–714, 2024, doi: 10.14569/IJACSA.2024.0150769.
  31. S. Arifin, K. Tan, A. T. Ariani, S. Rosdiana, and M. N. Abdullah, "The Audio Encryption Approach uses a Unimodular Matrix and a Logistic Function," *Int. J. Emerg. Technol. Adv. Eng.*, vol. 13, no. 4, pp. 71–81, 2023.
  32. A. Karmaoui, S. El Jaafari, H. Chaachouay, and L. Hajji, "A bibliometric review of geospatial analyses and artificial intelligence literature in agriculture," *GeoJournal*, 2023, doi: 10.1007/s10708-023-10859-w.
  33. F. Jia, D. Sun, and C.-K. Looi, "Artificial Intelligence in Science Education (2013–2023): Research Trends in Ten Years," *J. Sci. Educ. Technol.*, 2023, doi: 10.1007/s10956-023-10077-6.
  34. R. Gil, J. Virgili-Gomà, J.-M. López-Gil, and R. García, "Deepfakes: evolution and trends," *Soft Comput.*, vol. 27, no. 16, pp. 11295–11318, 2023, doi: 10.1007/s00500-023-08605-y.
  35. S. Arifin *et al.*, "Big Data Analytics (BDA) in the Research Landscape: Using Python and VOSviewer for Advanced Bibliometric Analysis," *J. Comput. Sci.*, vol. 21, no. 2, 2025, doi: 10.3844/jcssp.2025.347.362.
  36. S. Chakim, "Bibliometric Analysis: Symbolic Power Publication Trends in Scopus. com," 2022.
  37. K. Diéguez-Santana and H. González-Díaz, "Machine learning in antibacterial discovery and development: A bibliometric and network analysis of research hotspots and trends," *Comput. Biol. Med.*, vol. 155, 2023, doi: 10.1016/j.compbimed.2023.106638.
  38. A. A. Abdillah, Azwardi, S. Permana, I. Susanto, F. Zainuri, and S. Arifin, "Performance Evaluation Of Linear Discriminant Analysis And Support Vector Machines To Classify Cesarean Section," *Eastern-European J. Enterp. Technol.*, vol. 5, no. 2–113, pp. 37–43, 2021, doi: 10.15587/1729-4061.2021.242798.
  39. H. Monson, J. Demaine, L. Banfield, and T. Felfeli, "Three-year trends in literature on artificial

- intelligence in ophthalmology and vision sciences: a protocol for bibliometric analysis," *BMJ Heal. Care Informatics*, vol. 29, no. 1, 2022, doi: 10.1136/bmjhci-2022-100594.
40. D. Sousa, S. Sargento, and M. Luís, "A Simulation Environment for Software Defined Wireless Networks with Legacy Devices," *Proc. 18th ACM Int. Symp. QoS Secur. Wirel. Mob. Networks*, 2022, doi: 10.1145/3551661.3561369.
  41. B. K. Prahani, I. A. Rizki, B. Jatmiko, N. Suprpto, and T. Amelia, "Artificial Intelligence in Education Research During the Last Ten Years: A Review and Bibliometric Study," *Int. J. Emerg. Technol. Learn.*, vol. 17, no. 8, pp. 169–188, 2022, doi: 10.3991/ijet.v17i08.29833.
  42. M. A. Ibrahim *et al.*, "AN EXPLAINABLE AI MODEL TO HATE SPEECH DETECTION ON INDONESIAN TWITTER," *CommIT (Communication Inf. Technol. J.)*, vol. 16, no. 2, 2022.
  43. S. Tarigan, N. P. Murnaka, and S. Arifin, "Development of teaching material in mathematics 'Sapta Maino Education' on topics of plane geometry," in *AIP Conference Proceedings*, American Institute of Physics Inc., Apr. 2021, p. 020003. doi: 10.1063/5.0041650.
  44. M. Mohsin and R. Prakash, "ASSIGNMENT IN A MOBILE AD HOC NETWORK," 2002, [Online]. Available: <https://consensus.app/papers/assignment-in-a-mobile-ad-hoc-network-mohsin-prakash/f0ef06fd4c2753efb19d4c252a0be74a/>
  45. Y. Khasa, "Performance Evaluation of Routing Protocols in MANET," 2016, [Online]. Available: <https://consensus.app/papers/performance-evaluation-of-routing-protocols-in-manet-khasa/b9d6518a3c3f5604a860490cfbca99a1/>
  46. F. Aina, S. Yousef, and O. Osanaiye, "Bandwidth Estimation for Admission Control in MANET: Review and Conceptual MANET Admission Control Framework," *Proc. Futur. Technol. Conf. 2018*, 2018, doi: 10.1007/978-3-030-02683-7\_46.
  47. H. N. Saha, "A Novel Approach for Attacks Mitigation in Mobile Ad Hoc Networks Using Cellular Automatas," *Int. J. Ad Hoc, Sens. Ubiquitous Comput.*, vol. 3, pp. 33–48, 2012, doi: 10.5121/ijasuc.2012.3204.
  48. D. Ron and E. Negrus, "AD HOC Networks for the Autonomous Car," *IOP Conf. Ser. Mater. Sci. Eng.*, vol. 252, 2017, doi: 10.1088/1757-899X/252/1/012094.
  49. K. J. Abhilash and K. S. Shivaprakasha, "Secure Routing Protocol for MANET: A Survey," in *Lecture Notes in Electrical Engineering*, K. S., K. M., and S. K.S., Eds., Department E & CE, Bahubali College of Engineering, Shravanabelagola, India: Springer, 2020, pp. 263–277. doi: 10.1007/978-981-15-0626-0\_22.
  50. S. Al Ajrawi and B. Tran, "Mobile wireless ad-hoc network routing protocols comparison for real-time military application," *Spat. Inf. Res.*, vol. 32, no. 1, pp. 119–129, 2024, doi: 10.1007/s41324-023-00535-z.
  51. A. Singhal, V. Jha, S. Virmani, and P. Jain, "Towards the study of a living mobile backbone: VANET," in *2018 4th International Conference on Computing Communication and Automation, ICCCA 2018*, Faculty of Engineering Technology, Manav Rachna International Institute of Research Studies, Faridabad Accendere Knowledge Management Services, New Delhi, India: Institute of Electrical and Electronics Engineers Inc., 2018. doi: 10.1109/CCAA.2018.8777573.
  52. J. Hoebeke, I. Moerman, B. Dhoedt, and P. Demeester, "An overview of mobile ad hoc networks: Applications and challenges," *J. Commun. Netw.*, vol. 3, no. 3, pp. 60–66, 2004.
  53. B. Ul Islam Khan, R. F. Olanrewaju, F. Anwar, A. R. Najeeb, and M. Yaacob, "A survey on



- MANETs: Architecture, evolution, applications, security issues and solutions," *Indones. J. Electr. Eng. Comput. Sci.*, vol. 12, no. 2, pp. 832–842, 2018, doi: 10.11591/ijeecs.v12.i2.pp832-842.
54. P. Prabhakaran and M. Saravanan, "Efficient packet transmission using path selection in MANET-SPSR & ZLR," *Inf.*, vol. 17, no. 9B, pp. 4649–4659, 2014.
55. P. Lavanya, V. S. K. Reddy, and A. M. Prasad, "Research and survey on multicast routing protocols for MANETs," in *Proceedings of the 2017 2nd IEEE International Conference on Electrical, Computer and Communication Technologies, ICECCT 2017*, Department of E. C. E., SNIST, Hyderabad, India: Institute of Electrical and Electronics Engineers Inc., 2017. doi: 10.1109/ICECCT.2017.8117929.
56. B. Pribadi, S. Rosdiana, and S. Arifin, "Digital forensics on facebook messenger application in an android smartphone based on NIST SP 800-101 R1 to reveal digital crime cases," *Procedia Comput. Sci.*, vol. 216, no. 10.1016, 2023.

Article

# Feasibility Study on One Shot Vapor Compression Systems for Gas Storage Applications Using R-32 in Residential Air Conditioning

Anisa Ramadhani<sup>1,\*</sup>, Haolia Rahman<sup>1</sup>, Fauzan<sup>2</sup>, Paulus Sukusno<sup>1</sup>

<sup>1</sup> Applied Master of Manufacturing Technology Engineering, Mechanical Engineering, Jakarta State Polytechnic, Indonesia

<sup>2</sup> Department of Mechanical Engineering, Kookmin University, Seoul, South Korea

\* Correspondence: anisaramadhanic@gmail.com

**Abstract:** This study investigates the technical feasibility and environmental sustainability of R-32 refrigerant in one-shot vapor compression gas storage medium in residential air conditioning systems. R-32 stands out for its low global warming potential (GWP 675), zero ozone depletion potential, and higher energy efficiency compared to traditional refrigerants such as R-410A, making it a leading choice for eco-friendly HVAC applications. The research highlights that, while R-32 enables improved heat transfer and reduced refrigerant charge, its elevated discharge temperatures-reaching up to 30°C-pose operational challenges that demand advanced compressor innovations, such as liquid injection, to ensure system reliability and longevity. Experimental results from cold storage scenarios demonstrate that R-32 systems can achieve evaporator temperatures between 28°C and 31°C under hybrid energy conditions, indicating adaptability to typical residential cooling requirements. The findings underscore the importance of integrating robust data logging and compressor technology advancements to fully leverage R-32's benefits while addressing its thermodynamic challenges. Overall, the study supports R-32 as a technically viable and sustainable solution for modern residential air conditioning, provided that system design prioritizes both performance monitoring and compressor reliability.

**Keywords:** R-32; HVAC; Energy Storage System

**Citation:** Ramadhani, A., Rahman, H., Fauzan, Sukusno, P. (2025). Feasibility Study on One Shot Vapor Compression Systems for Gas Storage Applications Using R-32 in Residential Air Conditioning. *Recent in Engineering Science and Technology*, 3(02), 75–82. Retrieved from <https://www.mbi-journals.com/index.php/riestech/article/view/105>

Academic Editor: Iwan Susanto

Received: 18 April 2025

Accepted: 2 Mei 2025

Published: 3 Mei 2025

**Publisher's Note:** MBI stays neutral with regard to jurisdictional claims in published maps and institutional affiliations.



**Copyright:** © 2025 by the authors. Licensee MBI, Jakarta, Indonesia. This article is an open access article distributed under MBI license (<https://mbi-journals.com/licenses/by/4.0/>).

## 1. Introduction

Difluoromethane (CH<sub>2</sub>F<sub>2</sub>), commonly known as Refrigerant R-32, is a modern refrigerant increasingly used in cooling and HVAC systems due to its superior energy efficiency and lower environmental impact compared to older refrigerants such as R-410A and R-22.[1].

The research aims to demonstrate the feasibility of an air conditioning system using refrigerant type R-32 by deactivating the compressor element. Generally, the compressor is a vital component in an air conditioning system and is often the most frequently damaged part due to its critical role in reliable operation [2]. Using R-32 refrigerant, which is known for its high latent heat and excellent heat transfer capabilities [3], can improve cooling efficiency and reduce energy consumption compared to older refrigerants. R-32

also has a lower global warming potential and zero ozone depletion potential, making it environmentally friendlier than refrigerants like R-410A or R-22[4].

Since the compressor is responsible for compressing and circulating the refrigerant to maintain the cooling cycle, disabling it challenges the conventional operation of the AC system. This study explores whether the system can maintain acceptable performance without the compressor active, leveraging the efficient thermodynamic properties of R-32. In summary, the research investigates the innovative approach of operating an R-32-based air conditioning system without compressor activation, which could potentially reduce mechanical failures and energy consumption [5], given the compressor's usual role as the most failure-prone and energy-intensive component in AC systems [6]

## 2. Materials and Experiment Methods

The method used in this research consists of observation and experimentation. The experimental setup includes one storage tank, a  $\frac{3}{4}$  PK air conditioning unit with indoor and outdoor elements, manual valves, and pressure gauges to measure pressure. To record temperature data when the compressor is not operating, a MAX6675 sensor is employed as the measuring indicator, connected to a 1.25-meter Type K thermocouple as the measurement medium [7]. The temperature data is displayed via serial monitor on Arduino IDE software version 2.2.1.

This approach allows precise monitoring of temperature changes in the system during compressor inactivity, enabling analysis of system performance under these conditions. The combination of pressure measurement and temperature sensing provides comprehensive data to evaluate the feasibility of operating an R-32 refrigerant air conditioning system without compressor activation.

## 3. Results and Discussion

This study analyzes the system's condition using two methods:

- **Conventional Method**  
Operating the air conditioning system normally with the compressor active to compress and circulate the refrigerant, as in a standard AC setup.
- **Compressor-Off Method**  
Deactivating the compressor and utilizing the refrigerant stored in a storage tank, which contains compressed Freon accumulated during the system's normal operation.

Temperature changes within the air conditioning system are recorded at 5-second intervals to monitor and compare the performance between these two operational modes.

This dual-method approach allows for a comprehensive evaluation of the system's behavior both under typical compressor-driven conditions and during compressor

inactivity, providing insights into the feasibility of maintaining cooling performance using stored refrigerant alone.

### 3.1. Materials Use

These materials and instruments enabled direct observation of the refrigeration system's condition under two operational methods: the conventional compressor-driven method and the compressor-off method utilizing stored refrigerant in the tank.

- Compressor
- Condenser
- Evaporator

Mechanical refrigerations part lists look such as:

- Gas storage
- Pressure gauge
- Valve
- Pipe
- Tee and Nepple

### 3.2. Data Record Method

Using the MAX6675 sensor in combination with an Arduino Uno board and a Type K thermocouple [8], the temperature measurement system operates as follows based on research setup below:

---

MAX6675 Sensor	The MAX6675 module interfaces with the Arduino Uno via SPI communication, requiring three main signal connections: Serial Clock (SCK), Chip Select (CS), and Serial Out (SO). Typical pin connections are SCK to Arduino pin 8, CS to pin 9, and SO to pin 10, along with power (3.3V or 5V) and ground connections.[9]
Type K thermocouple	Connected to the MAX6675, measures temperature by generating a voltage proportional to the temperature difference, which the MAX6675 converts into a digital temperature reading
Arduino Uno	The Arduino Uno reads the digital temperature data from the MAX6675 module using a dedicated library (such as the Adafruit MAX6675 library), which simplifies communication and data retrieval. Temperature data is sampled at regular intervals (e.g., every 5 seconds as in this research) and transmitted to the Arduino IDE serial monitor for real-time monitoring and recording

---

### 3.2.1 Data Record Code for Serial Reading

```
#include <Thermocouple.h>
#include <MAX6675_Thermocouple.h>

#define SCK_PIN 8
#define CS_PIN 9
#define SO_PIN 10

Thermocouple* thermocouple;

// the setup function runs once when you press reset or power the board
void setup() {
    Serial.begin(9600);

    thermocouple = new MAX6675_Thermocouple(SCK_PIN, CS_PIN, SO_PIN);
}

// the loop function runs over and over again forever
void loop() {
    // Reads temperature
    const double celsius = thermocouple->readCelsius();
    const double kelvin = thermocouple->readKelvin();
    const double fahrenheit = thermocouple->readFahrenheit();

    // Output of information
    Serial.print("Temperature: ");
    Serial.print(celsius);
    Serial.print(" C, ");
    Serial.print(kelvin);
    Serial.print(" K, ");
    Serial.print(fahrenheit);
    Serial.println(" F");

    delay(500); // optionally, only to delay the output of information in the example.
}
```

### 3.3 Schemes

Operate the AC system normally with the compressor active. Record temperature and pressure data at 5-second intervals throughout the testing period to establish base-line system performance.

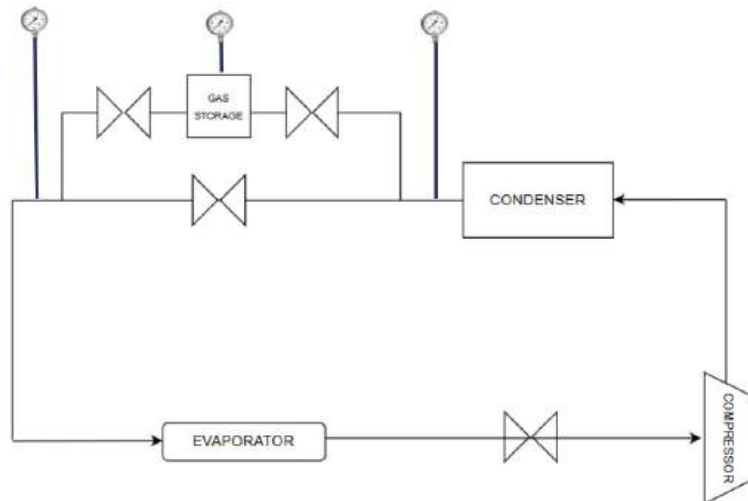


**Figure 1.** Ilustrasion of First Method

In this scheme, the refrigerant system operates according to its intended function. However, an additional component is introduced: a storage tank. Normally, the refrigerant flows directly from the condenser to the evaporator, but in this setup, a portion of the refrigerant is routed through the storage tank. This allows the refrigerant to be utilized during the switching to the second method, where the compressor is inactive.

**Table 1.** This is a table of 5 second data collect from first method

No.	Time	Temperature °C
1	10.30	23,5
2	10.31	24
3	10.32	23,75
4	10.33	23,50
5	10.34	23,75

The data presented in Table 1 were recorded at 5-second intervals as the average of the experiments, with the air conditioning temperature set to 20°C.

**Table 2.** This is a table of 5 second data collect from second method

No.	Time	Temperature °C
1	10.48	28,25
2	10.49	28,25
3	10.50	28,5
4	10.51	30,25

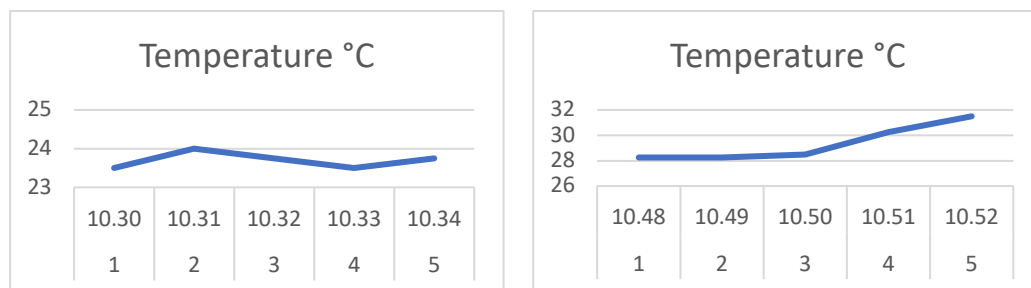


Figure 1 : With active compressor

Figure 2 : Using freon from storage tank

5	10.52	31,5
---	-------	------

Table 2 was recorded 5 second as same with table 1, the data shown that without using the compressor, the temperature cannot be stabilized.

The data shown in Figure 2, which corresponds to the scheme without the compressor as the main component, indicate that the temperature remains stable only during the first 2 seconds. After this initial period, the temperature continuously rises significantly.

In contrast, with the method using the compressor, the data show stable temperatures maintained below 24 degrees Celsius.

#### 4. Conclusions

This study investigated the performance of an air conditioning system using R-32 refrigerant under two operational methods: with the compressor active and without using compressor (the compressor deactivated while utilizing stored refrigerant in a storage tank). The experimental data shows that when the compressor was turned off, the system was unable to maintain a stable temperature, with temperature rising significantly after an initial short period of stability. Conversely, when the compressor are were operated, the system maintained a stable temperature below 24°C, indicating effective cooling performance.

These results confirm the critical role of the compressor in sustaining the refrigeration cycle and ensuring consistent cooling. While the concept of using stored refrigerant without compressor activity presents an interesting approach, it proved insufficient to maintain desired temperature stability in this study. Therefore, the compressor remains an essential component for reliable and efficient air conditioning operation.

Future research could explore alternative methods to enhance cooling performance without continuous compressor operation, potentially improving energy efficiency and reducing mechanical wear[10], [11].

## References

1. M. Mohanraj and J. D. A. P. Abraham, "Environment friendly refrigerant options for automobile air conditioners: a review," Jan. 01, 2022, *Springer Science and Business Media B.V.* doi: 10.1007/s10973-020-10286-w.
2. M. E. Kahn, "The climate change adaptation literature," *Rev Environ Econ Policy*, vol. 10, no. 1, pp. 166–178, Dec. 2016, doi: 10.1093/reep/rev023.
3. B. Goetzler, J. Young, M. Umland, M. Butrico, and C. Torrado, "Cool Refrigerant Developments for a Warming World: Low GWP HVAC Refrigerant Regulations and Technologies in US and Global Markets," 2024.
4. J. Liu, Y. Liu, C. Liu, L. Xin, and W. Yu, "Experimental and Theoretical Study on Thermal Stability of Mixture R1234ze(E)/R32 in Organic Rankine Cycle," *Journal of Thermal Science*, vol. 32, no. 4, pp. 1595–1613, Jul. 2023, doi: 10.1007/s11630-023-1790-2.
5. A. E. Stagrum, E. Andenæs, T. Kvande, and J. Lohne, "Climate change adaptation measures for buildings-A scoping review," *Sustainability (Switzerland)*, vol. 12, no. 5, Mar. 2020, doi: 10.3390/su12051721.
6. S. Zhang *et al.*, "Study on the temperature distribution of motor and inverter in an electric scroll compressor for vehicle air conditioning under refrigeration conditions," *International Journal of Refrigeration*, vol. 154, pp. 111–124, Oct. 2023, doi: 10.1016/J.IJREFRIG.2023.05.012.
7. S. Hadiati, A. Pramuda, and M. Matsun, "Musschenbroek Learning Media with Arduino Based with Relay and Max6675 Sensor to Increase HOTS and Creativity," *Jurnal Penelitian Pendidikan IPA*, vol. 9, no. 3, pp. 1006–1011, Mar. 2023, doi: 10.29303/jppipa.v9i3.2634.
8. S. P. Nalavade, A. D. Patange, C. L. Prabhune, S. S. Mulik, and M. S. Shewale, "Development of 12 channel temperature acquisition system for heat exchanger using MAX6675 and Arduino interface," in *Lecture Notes in Mechanical Engineering*, Pleiades journals, 2019, pp. 119–125. doi: 10.1007/978-981-13-2697-4\_13.
9. J. Rekayasa Material, M. dan Energi, K. Umurani, A. Rudi Nasution, and Ms. Zufri, "Design And Implementation Of Temperature Measuring Device Using Max6675 And Thermocouple On Wet Cooling Tower," vol. 7, no. 2, pp. 335–342, 2024, doi: 10.30596/rmme.v7i2.19801.
10. M. Mohanraj and J. D. A. P. Abraham, "Environment friendly refrigerant options for automobile air conditioners: a review," Jan. 01, 2022, *Springer Science and Business Media B.V.* doi: 10.1007/s10973-020-10286-w.
11. S. Zou, Q. Zhang, C. Yue, J. Wang, and S. Du, "Study on the performance and free cooling potential of a R32 loop thermosyphon system used in data center," *Energy Build*, vol. 256, p. 111682, Feb. 2022, doi: 10.1016/J.ENBUILD.2021.111682.





PT. Mencerdaskan  
Bangsa Indonesia

PT MENCERDASKAN BANGSA INDONESIA  
(MBI), 4th Floor Gedung STC Senayan Room  
31-34, Jl. Asia Afrika Pintu IX, Jakarta 10270,  
Indonesia.